

UNITED STATES DEPARTMENT OF THE INTERIOR
GEOLOGICAL SURVEY

GROUNDWATER EXPLORATION WITH SCHLUMBERGER SOUNDINGS
NEAR JEAN, NEVADA

By

Adel A.R. Zohdy

Open-File Report 88-291

1988

This report is preliminary and has not been
reviewed for conformity with the U.S.
Geological Survey editorial standards.
Any use of trade names is for descriptive
purposes only and does not constitute
endorsement by the USGS.

GROUNDWATER EXPLORATION WITH SCHLUMBERGER SOUNDINGS NEAR JEAN, NEVADA

By Adel A.R. Zohdy

INTRODUCTION

In November 1986 and in March and June, 1987, the U.S. Geological Survey, in cooperation with the Las Vegas Valley Water District, made a direct current resistivity survey in Ivanpah Valley near Jean, Nevada. The very small town of Jean lies approximately 25 miles (40 Km) south-southwest of Las Vegas, Nevada, on U.S. Interstate 15. The survey consisted of thirty six Schlumberger soundings. Figure 1 shows the location of the sounding stations and most of the wells in the area. The Schlumberger sounding technique and other geophysical methods, as applied in groundwater exploration, are described by Zohdy and others (1974).

The purpose of the resistivity survey was twofold: (1) to study the subsurface electrical resistivity of valley fill and its relation to the groundwater quality distribution, and (2) to explore the potential of groundwater in the carbonate aquifer in the Paleozoic limestone, at the base of the Bird Spring Range, in the northern part of the valley.

BACKGROUND AND DRILL HOLE INFORMATION

In September 1981, the Desert Research Institute, Reno, Nevada, conducted a groundwater exploration program by drilling several test wells to locate a source of fresh groundwater for the Southern Nevada Correctional Center which is located about one half mile east of Jean (Mifflin, 1982). A preexisting well near Jean yields water of unacceptable quality with TDS (total dissolved solids) of about 1700 mg/l (milligram per liter). The State of Nevada standard for potable water calls for a maximum TDS of 1000 mg/l. A reversed osmosis process was used to remove the dissolved solids from the water of the Jean well. Initial costs in the mid 1970's were about \$65,000 per year, these costs increased to more than \$400,000 per year by 1981 (Mifflin, 1982). This dramatic increase in cost was one good reason to initiate the drilling program to find a new source of fresh water.

The Desert Research Institute program started by drilling two wells (wells A and B) in the Jean Lake Valley (east of Jean and south of Jean Dry Lake). These two wells (see figure 1 for location) encountered groundwater of marginal to unacceptable quality (950 to 1100 mg/l) and penetrated volcanic rocks (andesite and basalt) at depths of 535 feet and 243 feet, respectively. The plan to drill two additional

wells (wells C and D) in the Jean Lake Valley, east of Jean, was abandoned in favor of drilling other wells west of Jean. Wells E, F and G were drilled, about one mile apart, along the road to the town of Goodsprings, with test well E closest to Jean and test well G farthest from Jean (see figure 1). These wells were subsequently renamed as follows: G became A3-1, F became A3-2, and E became A3-3, with A3-1 being farthest from Jean. In this report I will use the original names: E, F, and G, for brevity. Test well G was drilled first then E and then F.

Test well E yielded water of very good quality (about 420 to 500 mg/l, TDS). Surprisingly, however, wells F and G which are west-northwest of well E, and therefore farther away from Jean (see figure 1), yield water of lesser quality with TDS of about 780 mg/l and 845 mg/l, respectively. I calculated these TDS values from the chemical analysis tables (Mifflin, 1982, appendix D). Higher TDS values were initially estimated by converting electrical conductivity from water samples to TDS (Mifflin, 1982, figure 10).

A production well was drilled at 123 feet from test well E, and at present it supplies the needed potable water, at the rate of about 225 gpm (gallons per minute), to the correctional institution. Four additional test wells (A3-6, A3-8, A3-9, and A3-11) were drilled at distances of about one quarter to about three quarters of a mile from the production well (see figure 1). Test wells A3-4, A3-5, A3-7, and A3-10, were planned but not drilled.

Figure 2 shows a bar graph summarizing the TDS values for the various wells in the Jean area. The location of the wells in figure 2 is determined from their projection on the road from Jean to Goodsprings. It should be noted that the estimated TDS values (from the electrical conductivity measurements from water samples) for wells F and G are alarmingly close to the maximum limit of 1000 mg/l allowed by the Nevada standard; whereas the calculated TDS values (from chemical analysis) show that these two wells are well within the acceptable limit but still not as good as well E. The multiple horizontal markers on the columns for test wells A3-11, E, A3-8, and A3-6, show calculated TDS values from water samples obtained at different depths (see Mifflin's report, 1982, for exact depths).

Samples from well A3-11, about one half to three quarters of a mile west-southwest of the production well, yielded water of good quality, ranging from 475 to 681 mg/l, TDS (see figure 2). The water quality in well A3-11 improved to a TDS of 475 mg/l at a depth of 785 feet. Samples from the other 3 test wells showed higher quantities of TDS (see figure 2). Well A3-6 yielded water in the range from 890 to 1030 mg/l, well A3-8 yielded water in the range from 660 to 775 mg/l, and well A3-9 yielded water in the range from 770 to 800

mg/l. In 1987, following the resistivity survey, water samples were taken from test wells A3-8 and A3-11 and their electrical conductivity in micromhos/cm was measured (Terry Katzer, Las Vegas Valley Water District, oral communication). These two wells are the only remaining test wells that have not been plugged or destroyed. The two electrical conductivity measurements from wells A3-8 and A3-11 were in good agreement with the earlier measurements, and were also in good agreement with the interpretation of the electrical sounding data. The 1982 measurements of the electrical conductivity and TDS in test wells F and G are not what one would expect on the basis of the interpretation of the resistivity sounding data (as discussed later in this report). Unfortunately, new data from test wells F and G could not be obtained.

NEW WELL

In September 1987, following the resistivity survey, a new test well was drilled one half mile west of well A3-11 and west of sounding 29 (see figure 1 for location). The purpose of the new well was to test the water quality for a newly built commercial development in Jean. Preliminary results indicate that the water table is at 550 feet, and that the water quality at a depth of approximately 650 feet is about 500 mg/l (TDS) with an electrical conductivity of about 750 micromhos/cm or about 13 ohm-m (Kay Brothers, Las Vegas Valley Water District, oral communication). The well was drilled to a total depth of 1280 feet (390 m) and did not penetrate limestone basement. The water quality improved with depth (Terry Katzer, Las Vegas Valley Water District, oral communication). A sample taken from a depth of approximately 1250 feet contained TDS of 400 mg/l with an electrical conductivity of 670 micromhos/cm or about 15 ohm-m. These encouraging preliminary results are in very good agreement with the interpretations of sounding 29 to the east and sounding 8 to the north.

RESISTIVITY SURVEY

Thirty six Schlumberger soundings were made along six profiles. The data were collected in three short field trips (3 to 5 days each). Two of the field trips were made in connection with other field trips, near Las Vegas, to study the carbonate aquifer in the Black Hills and to study the valley fill across the Las Vegas shear zone. There, sixty three Schlumberger soundings were made and their interpretation is the subject of another report. In the Jean area, soundings 1 to 9 were made during the first trip (November 1986), soundings 10 to 20 were made during the second trip (March 1987), and soundings 21 to 36 were made during the third trip (June 1987).

FIELD CONDITIONS

The survey area, to the west of U.S. Interstate 15, is generally characterized by high contact resistance which is caused by lack of moisture and/or clayey materials. The contact resistance at the current electrodes was particularly high (several thousand ohms) along the northern east west dirt road at the foot of the Bird Spring Range (Paleozoic limestone ridges), where soundings 1 to 6 were made (see figure 1). Impressed voltages of 1000 to 1200 volts were necessary to inject only about 15 or 20 milliamperes in the ground. This very high contact resistance limited the maximum current electrode spacing expansions of the first few soundings. Fortunately, after the second day of the survey, heavy rain showers, in the late evening, considerably reduced the contact resistance along that road. The survey was halted for half a day to avoid current leakage problems (Zohdy, 1968). Although the contact resistance was reduced, and the resistivity measurements could be made faster, work progressed much slower than normal, along that road, because of drainage channels that cut across the road at several places which drastically reduced driving speeds during deployment and picking up of the current cables. A power line exists along the very edge of the road, but its poles are not grounded except at two far apart locations. Therefore, the power line did not affect the resistivity measurements by acting as a giant fence with grounded metal posts. Sixty cycle interference was negligible using the proper filters in the equipment.

On the road to Goodsprings, where soundings 7, 8, 9, 16, 17, 18, and 19 were made, there are several metal culverts. These culverts were used advantageously as current electrodes (when present at appropriate electrode spacings that are greater than 1000 feet). The culverts provided excellent electrical contact with the ground, allowed large amounts of current to be injected, and hence resulted in excellent quality measurements for soundings 16, 17, 18, and 19.

A second power line, with grounded poles, runs parallel to the road to Goodsprings, but it is sufficiently displaced from the road that it did not affect the resistivity measurements. This conclusion is supported by the undistorted form of the sounding curves and by the fact that the interpretation of the soundings obtained along the road (such as sounding 7, which is expanded parallel to the grounded power line) does correlate very well with soundings expanded perpendicular to the power line (such as soundings 10 and 15).

Before proceeding with sounding measurements along the road to Goodsprings, I was concerned with the possible detrimental effect of another man made feature: the buried pipe line from the production well to the prison facility near Jean. I made

few measurements very close (within 10 feet) to the buried pipe line and expanded the electrodes parallel to it. The purpose of the measurements was not necessarily to measure the resistivity, but to look for IP (induced polarization) effects on the measured voltages between the potential electrodes. If the pipe line is made of metal, it will produce an IP decay voltage. None was observed. I proceeded with the survey, and did not observe any IP effects nor distortions on the sounding curves that could be caused by a metal pipe line. Subsequently, at a meeting with the Las Vegas Valley Water District personnel I was informed that the pipe line is made of AC (asbestos-concrete).

Few fences with metal posts are present along the roads east of U.S. Interstate 15, but none were sufficiently close to the center of the sounding stations or sufficiently well grounded to seriously affect the resistivity measurements.

DATA COLLECTION

The Schlumberger soundings were made with a field crew composed of 5 people and using three vehicles: an instrument carryall truck and two additional pickup trucks for deploying the current lines. All trucks were equipped with 90 watt FM radios for communication. The two pickup trucks are equipped with precision foot-odometers for measuring current electrode spacings at distances greater than 100 feet. Electrode spacings from 10 to 100 feet were measured with a measuring cloth tape. A 5 kilowatt generator was used for power supply. The potential difference between the potential electrodes was measured on a Honeywell potentiometric chart recorder.

Most soundings (except the first few) were expanded to electrode spacings $AB/2$ (half distance between current electrodes A and B) of 10,000 feet. Although the electrode spacing distances were measured in feet, the electrode spacings and interpreted depths are reported here in meters. Both the apparent resistivities and the interpreted resistivities were computed and are presented here in ohm-meters.

DATA PROCESSING AND INTERPRETATION

The Schlumberger sounding data were interpreted using an automatic interpretation computer program that I developed recently (Zohdy, in press). The program is somewhat analogous to a program that I developed several years ago (Zohdy, 1973 and 1975) except that it is generally faster and it yields a model in which there are no anomalous thin layers of unusually very low or very high resistivities (which are geologically unrealistic). O'Neill's filter coefficients (O'Neill, 1975) are used in the convolution method for the

forward calculation of theoretical sounding curves. The field sounding curves, the corresponding digitized curves, and their interpretations are given in the appendix. Each sounding curve was prepared for interpretation by shifting the various segments upward or downward to form a continuous curve (Zohdy and others, 1973). The last segment on a curve is held fixed in position and the other segments are shifted upward or downward to form the continuous curve. The shifted curve is digitized from right to left and sampled at the rate of six logarithmically equally spaced points per decade. Some sounding curves, such as those of soundings 6 and 13, had to be corrected for winding road effects (Zohdy and Bisdorf, 1982). This correction was made prior to shifting and digitizing the field curves. Titles of interpreted sounding curves that are followed by CR, SM, or EX (see appendix) indicate that the interpreted sounding curve was corrected for winding road effects, smoothed, or extended, respectively.

The automatic interpretation of each sounding curve produces a model in which the interpreted true resistivity varies with depth as a step function. A continuous variation of resistivity with depth curve (Bisdorf and Zohdy, 1979) is derived by drawing, or calculating, a curve that passes through the mid point of each horizontal and vertical line on the step function curve (see figure 3). The continuous curve is smoothly merged at each end with the horizontal lines representing the first and last layer resistivities, respectively. This transformation is made to generate contour maps and cross sections of interpreted true resistivity.

The individual sounding interpretations, including the graphical representations shown in the appendix, were made on an HP 9845/B desk top computer. The location map, the cross sections, the block diagram, and the resistivity at given depth maps were all constructed on an AMIGA 1000 desk top computer, using the commercial paint program Deluxe Paint II (Silva, 1987). The results were printed on a Xerox 4020 ink jet color printer.

RELATION BETWEEN INTERPRETED RESISTIVITIES AND WATER QUALITY IN THE JEAN AREA

True resistivity values derived from the interpretation of direct-current resistivity sounding curves depend on many geophysical and geological factors. Without going into much detail, it is important to remember that the interpreted true resistivities from the sounding data depend on rock lithology, porosity, water quantity, and water quality. Thus, unlike water conductivity measurements, surface resistivity measurements are influenced by porosity and lithology. Furthermore, whereas water quality measurements are based on samples obtained at few given depths, the interpreted

electrical resistivity from the sounding data represents the resistivity of a much larger volume of material of water and rock.

The purpose of this section is to outline the relationship between the interpreted true resistivity contours, shown on the geoelectric maps and cross sections, and the potential for fresh groundwater supply. The following table summarizes this relationship for the Jean area:

Resistivity Values	Probable Lithology and Water Quality
>750 ohm-m	Dry alluvium or limestone.
300-500 ohm m	Alluvium or fractured limestone, with excellent water, if present.
100-200 ohm-m	Limestone with acceptable water or alluvium with good water.
45-100 ohm-m	Alluvium with acceptable water (<1000 mg/l, TDS).
< 45 ohm-m	Alluvium with marginal or unacceptable water quality (>1000 mg/l, TDS).

The above table is not a universal table, it only represents reasonable estimates for the Jean area. Indeed, in many parts of Arizona, New Mexico, and Texas, fresh-water alluvial aquifers have resistivities in the range of 30 to 45 ohm-m (see for example Zohdy, 1969; Zohdy and others, 1969; Zohdy and Jackson, 1973). Yet, the above table shows that layers with less than 45 ohm-m should be interpreted as an aquifer with water of marginal or unacceptable quality. There are at least two explanations for this discrepancy:

(1) In the areas referred to in Arizona, New Mexico and Texas, the salt-water alluvial-aquifers have resistivities of less than 3 ohm-m and contain water with several thousands mg/l of TDS. In the Jean area, however, the unacceptable water in the Jean well has less than 2000 mg/l, TDS, and except for well A3-6, all the other wells (according to the chemical analysis) are within the limit of less than 1000 mg/l (see figure 2). Therefore, the resistivity exploration problem in the Jean area, represents the mapping of a transition from brackish-water to fresh-water, compared to the mapping of a transition from brine to fresh-water in the other areas.

(2) It is possible to reinterpret all the resistivity soundings and to attempt to force the low resistivity layers to have lower resistivity values using the principle of equivalence. Such an interpretation procedure will result in aquifer thicknesses that are smaller than the presently interpreted ones, and consequently the depth to the limestone bedrock will be shallower. This was not done because there are no available electric logs to warrant such a change and the present estimates to the limestone beneath the valley fill are reasonable. Thus, although previous experience indicates that the cutoff resistivity for very poor quality water in alluvial aquifers to be 10 to 15 ohm-m or less, the present investigation in the Jean area indicates that we should assume that layers with interpreted true resistivities of 30 to 45 ohm-m (or less) to contain water of marginal or below standard quality.

GEOELECTRIC SECTIONS

Six geoelectric sections are presented in figures 4, 5, and 6. These sections represent contours of interpreted true resistivities as obtained from the interpretation of the individual soundings. The contour interval is quasi-logarithmic.

The interpreted-resistivity contours, shown on the cross sections and maps, are based on the continuous variation of resistivity with depth models and not on the step-function models given in the appendix. Therefore, depths to certain layer resistivities from the step-function models may not coincide exactly with those shown on the contoured maps and cross sections.

It should be noted that the automatic interpretation of the electrical soundings was made without any constraints added from geologic or hydrologic information from the drill holes. The drill holes shown on some of the geoelectric sections were added after the sections were constructed in order to compare how well the geoelectric predictions correlate with geologic and hydrologic findings.

SECTIONS A-A', B-B', and C-C':

Figure 4 shows three cross sections A-A', B-B', and C-C' and it also shows a location map for easy reference. The following features are seen on all three cross sections: a top layer of variable and generally high resistivities (>200 ohm-m) representing dry alluvium that extends to an average depth of about 150 m, a middle layer of medium to low resistivity (30 to 100 ohm-m) representing water saturated alluvium that extends to an average depth of about 500 m, and a bottom layer of high resistivity (>200 ohm-m) probably

representing Paleozoic limestone.

A buried ridge(s) of high resistivity material (Paleozoic limestone ?) was discovered on all three cross sections. This structure is about 2 kilometers south of Jean and trends northwest. A small outcrop of Paleozoic limestone exists at a distance of about 300 m east of sounding 23. The resistivity high beneath sounding 23, on section C-C', is most likely a buried extension of that outcrop, but whether the ridge beneath sounding 23 is connected with the buried ridge beneath sounding 26 on section B-B' and beneath sounding 15 on section A-A' is not definite.

A low resistivity layer of 30 to 45 ohm-m is shown on all three cross sections. The relatively low value of less than 30 ohm-m was interpreted from the data of sounding 22 (on section C-C') and is assumed to exist beneath Jean by interpolation between soundings 25 and 28 (on section B-B'). This relatively low resistivity layer of 30 to 45 ohm-m correlates well with the below standard water in the aquifer below the Jean area.

The less than 45 ohm-m lens beneath soundings 10, 7, and 15, on cross section A-A', correlates very well with the marginal and near marginal quality water sampled from test holes A3-6 and A3-8, respectively, (see figure 2). For the Jean area, good quality water in the alluvial aquifer is delineated along the three cross sections with the material encompassed between the contours of 70 and 150 ohm-m. The material delineated by the lenses of 30 to 45 ohm-m probably contains marginal or below standard water and therefore should be avoided.

SECTION D-D':

Figure 5 shows cross sections D-D', E-E', and a location map. Cross section D-D' is along the road to the town of Goodsprings and will be discussed here first. Geologic and hydrologic information from the production well and the two test wells F and G is included on the cross section. The bottom 200 ohm-m contour, as on the sections discussed above, is a good marker for the top of the Paleozoic limestone. Test well G, penetrated limestone at a depth of 117 m (385 feet) and bottomed in fractured limestone at a depth of 286 m (939 feet). Test well F, near sounding 8, was drilled in alluvium to a depth of 256 m (840 feet) and did not penetrate limestone. Similarly, the production well (between soundings 7 and 9) and test well A3-8 (near sounding 7) did not penetrate limestone. This geologic information is in excellent agreement with the geoelectrical interpretations.

The shallow high resistivity material (of about 1000 ohm-m) beneath sounding 18, near the left side of section D-D', is interpreted as dry limestone under a thin veneer of alluvium (no surface expression of limestone at sounding 18). By extending the right edge of this resistivity high to the top of the limestone in test well G (where the data from nearby sounding 17 does not yield a definitive interface between alluvium and limestone) we find that the trend for the top of the limestone continues logically to the 200 ohm-m contour beneath sounding 16 and continues, along the 200 ohm-m contour, to the remainder of the section toward sounding 7.

The depth to the water table (228 m) in test well G is in good agreement with the bottom of the high resistivity material beneath sounding 18. Similarly the depth to the water table in test well F, at the production well, and at test well A3-8 are all in good agreement with the interpretation of the sounding data.

The expected water quality distribution along section D-D', according to the interpretation of the electrical soundings, is only in partial agreement with water quality data. The interpretation of the electrical soundings shows a steady increase in the alluvial-aquifer resistivity from right to left (from soundings 7 to 8). This steady increase in alluvial-aquifer resistivity should also indicate a steady improvement in water quality from right to left. In the right side of the section, the interpretation of sounding 7 shows the potential for marginal water quality (< 45 ohm-m layer) which is in good agreement with data from nearby test well A3-8. The fact that the interpreted resistivity for the alluvial-aquifer increases from sounding 7 to sounding 9 (signifying a possible improvement in water quality) is supported by the good water quality produced from the production well which is located between these two soundings. However, the water quality, reported in 1982, from test hole F near sounding 8 and from test well G near sounding 17 do not fully agree with the sounding interpretation results at those locations.

The electrical conductivity of the production well was 600 to 700 micromhos/cm (16.6 to 13.3 ohm-m). According to the geoelectric section this corresponds to an alluvial-aquifer resistivity of 45 to 70 ohm-m. The interpreted aquifer resistivity increases toward sounding 8 and therefore one would expect test well F to yield better quality water than at the production well. Nevertheless, the electrical conductivity of water samples from test well F ranges from 1230 to 1424 micromhos/cm (or 8 to 7 ohm-m). This means that although the water resistivity at test well F is nearly half what it is at the production well, the interpreted aquifer resistivity (according to the sounding interpretation) has doubled. If the water conductivity measurements at test well F are correct then the porosity and clay content at test well

F must be much less than at the production well. This one possible explanation is not unreasonable because well F is located up the alluvial fan where coarser material and less clay is expected to occur. Another possible explanation, however, is that either the electrical conductivity measurements of water samples from test well F were in error or that the water samples were somehow contaminated. Since test well F no longer exists we will never know the correct answer (without drilling a new test well near sounding 8).

The water conductivity at test well G, near sounding 17, is reportedly about 1300 micromhos/cm (or 7.7 ohm m), almost the same as at test well F. Here, the water is in limestone, not in alluvium. The interpreted high resistivity value of about 200 ohm-m is surprisingly high for a limestone saturated with somewhat brackish water. One possible explanation is that the limestone has low porosity and is not as highly fractured as one might expect. Indeed, according to Mifflin (1982, p. 17), the limestone in test well G was encountered at a depth of 385 feet and that the rock "remained tight and essentially unfractured until close to 889 feet where the first fracture permeability occurred". The well was drilled to a total depth of 939 feet and then drilling problems began by losing the lower eight sections of the pipe. Subsequently, the upper part of the well (alluvium) caved in and the well was lost.

Results obtained from test well A3-11 and from the interpretation of sounding 29, which are not included on the above cross section (D-D') but are about one kilometer south of it (see figure 1 for location) are in very good agreement. The aquifer resistivity from the interpretation of sounding 29, is in the 70 to 100 ohm-meter range (with no layers of 45 ohm-m or less) and the quality of water sampled from test well A3-11 is in the 500 to 550 mg/l (TDS) range. Furthermore, the results obtained from the newly drilled well, west of sounding 29 are also in good agreement with the interpretation of sounding 29. These encouraging results lead me to believe that the interpretation of the sounding data near sounding 8 on section D-D' are indicative of good water potential in spite of the earlier analysis of water samples from test well F.

SECTION E-E':

Section E-E', shown in figure 5, extends from sounding 33 in the west to sounding 22 in the east and crosses U.S. Interstate 15 between soundings 34 and 25. Both soundings 22 and 25, east of U.S. Interstate 15, and south of the town of Jean, indicate that the aquifer resistivity is generally less than 45 ohm-m and can be less than 30 ohm-m beneath sounding 22. This is interpreted to indicate the presence of water of below standard quality. To the west of U.S. Interstate 15 the aquifer resistivity is primarily characterized by

resistivities in the range of 70 to 100 ohm-m, which is indicative of an aquifer with potentially good water. The 100 ohm-m zone beneath sounding 32, near the left part of the section, is a particularly attractive target for an exploratory hole to test the water quality.

As in the other cross sections discussed above, the 200 ohm-m contour (near the bottom of section E-E') represents a good marker for the depth to the top of the limestone. A buried ridge is shown beneath sounding 34 and beneath U.S. Interstate 15, this is probably the same buried ridge shown earlier on sections A-A', B-B' and C-C'.

SECTION F-F':

Section F-F', shown in figure 6, is located at the foot of the Bird Spring Range in the northern part of the survey area. The section extends from sounding 18 on the road to the town of Goodsprings, in the west, to sounding 20 east of U.S. Interstate 15, in the east. The high resistivity material (450 to > 1000 ohm-m) beneath soundings 18, 1, 2, 3, 4, and 5 most probably represents dry limestone. The blank area beneath soundings 1, 2, 3, 4, and 5 represents the limited probing depth of those soundings which were made in the early part of the survey. A major electrical discontinuity exists between soundings 5 and 6. It probably represents a major fault that separates Paleozoic limestones in the west from Mesozoic sandstones in the east (Gary Dixon, USGS, oral communication). This electrical discontinuity has no evident surface expression between soundings 5 and 6. Limestone outcrops do exist near sounding 13 but according to the sounding interpretation they must represent a relatively thin layer that does not extend to any great depth. The water quality beneath soundings 6, 13, and 20 should be good.

To the west of sounding 2 and beneath sounding 1, the high resistivity limestone layer thins considerably. A major fault (Gary Dixon, USGS, oral communication) exists in that area. In view of this geologic information and the fact that the 200 and 300 ohm-m resistivity contours approach the earth surface beneath sounding 1, this area represents a good target for a test well to intercept the fault and explore the water potential in the carbonate aquifer. It should be noted however that beneath sounding 2 the highly resistive limestone thickens considerably; therefore, the location of a test hole to intercept the fault, below the water table and at relatively shallow depth, must be carefully selected.

RESISTIVITY MAPS

Four resistivity maps were prepared and are shown in figures 7 through 10. These represent interpreted true resistivity contours at depths of 100 m, 200 m, 300 m, and 400 m, respectively. The contour values are based on a quasi-logarithmically equal interval. The resistivity map at 100 m (330 feet) depth primarily shows the resistivity distribution above the water table.

The 200 m (660 feet) map shows the resistivity distribution near and below the water table. The low resistivity anomaly near the town of Jean is strikingly evident. Accordingly, the area enclosed by the less than 70 ohm-m contour should be avoided and that enclosed by the less than 45 ohm-m contour should definitely be avoided in drilling for a fresh water supply.

The 300 m (approximately 1000 feet) depth map depicts similar information, but in addition, it shows a steep gradient in the resistivity contours between soundings 8 and 16 which may represent a northeast-southwest trending fault in the buried limestone surface. The high resistivity closure about 2 km southwest of Jean represents the buried ridge referred to earlier in the discussion of the cross sections.

The 400 m (1300 feet) depth map primarily shows the prominence of the buried ridge southwest of Jean and what seems to be a general trend of shallower depth to the limestone in the southern part of the survey area. It should be noted that the production well, test well A3-11 and the new well all lie within the > 45 ohm m contour areas on all maps.

BLOCK DIAGRAM

To further illustrate the resistivity interpretation results in the Jean area, an aerial view map (figure 11) and a block diagram (figure 12) were constructed. These two figures primarily represent the new possible ways of presenting resistivity data interpretation using today's available computer graphics technology. The two figures also help add a little humor to the usually dry presentation of scientific results.

SUMMARY AND CONCLUSIONS

The variation of water quality in the Jean area represents a subtle and difficult problem for geophysical exploration. Unlike many other surveys where the water quality changes from fresh water to brine, the Jean area presented a more subtle problem where water quality changes from about 500 mg/l to less than 2000 mg/l with the cutoff being the State of Nevada standard at 1000 mg/l. By correlating the resistivity interpretation with the known geologic and hydrologic information it was possible to arrive at a reasonable conclusion regarding the subtle differences in interpreted resistivity values that distinguish alluvial aquifers with acceptable water quality from those with marginal or unacceptable water quality. It is concluded that in the Jean area, aquifers with an interpreted true resistivity of less than 45 ohm-m contain water of marginal or unacceptable quality whereas those in the 70 to 150 ohm-m range should contain water of acceptable quality. The geoelectric predictions were supported by the drilling of a new test well that yielded water of good quality. Geologic mapping and geophysical interpretations indicate that a test well between soundings 1 and 2 has a high potential for intersecting a fault where significant groundwater flow in fractured limestone rocks may be tapped.

REFERENCES

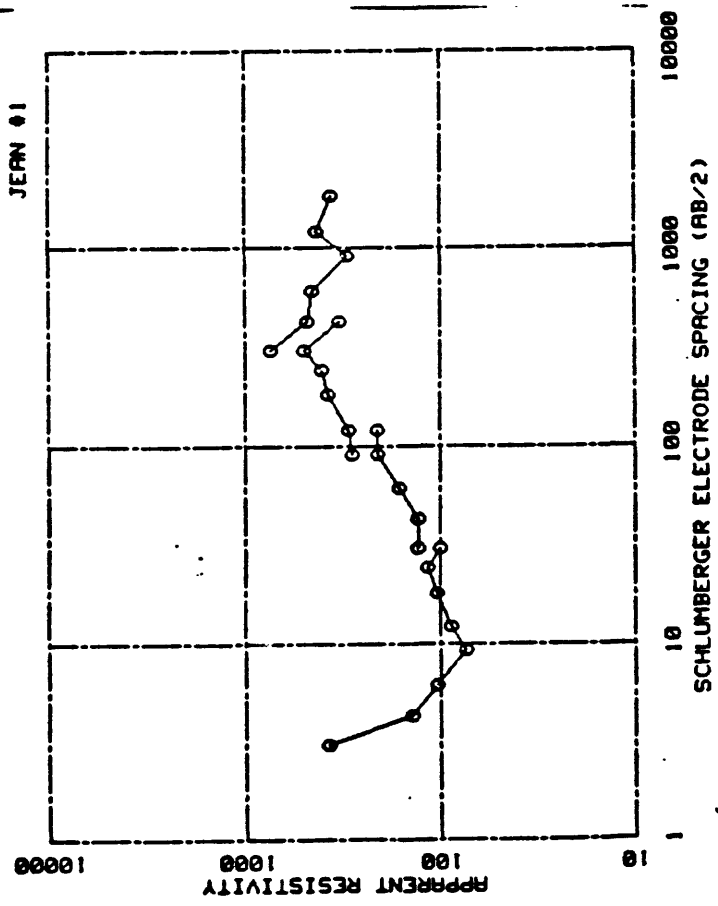
- Bisdorf, R.J. and Zohdy, A.A.R., 1979, Geoelectric investigations with Schlumberger soundings near Brunswick, Georgia: U.S. Geological Survey Open-File Report 79-1551, 125 p.
- Mifflin, M.D., 1982, Exploration and development of a ground-water supply for the southern Nevada correctional center Jean, Nevada: Desert Research Institute, University of Nevada System, Water Resources Center, 43 p. + Appendices.
- O'Neill, D.J., 1975, Improved linear filter coefficients for application in apparent resistivity computations: Bull. Aust. Soc. Explor. Geophys., v. 6, no. 4, pp. 104-109.
- Silva, Daniel, 1987, Deluxe Paint II, Electronic Arts, 1820 Gateway Drive, San Mateo, CA.
- Zohdy, A.A.R., 1968, The effect of current leakage and electrode spacing errors on resistivity measurements, in Geological Survey Research 1968, U.S. Geol. Survey Prof. Paper 600-D, pp. D258-D264.
- , 1969, The use of Schlumberger and equatorial soundings in groundwater investigations near El Paso, Texas: Geophysics, v. 34, no 5, pp. 713-728.
- , 1973, A computer program for the automatic interpretation of Schlumberger sounding curves over horizontally stratified media: Nat. Tech. Inform. Serv., no PB-232 703, 27 p. Springfield, VA.
- , 1975, Automatic interpretation of Schlumberger sounding curves using modified Dar Zarrouk functions: U.S. Geological Survey Bull. 1313-E, 39 p.
- , in press, A new method for the automatic interpretation of Schlumberger and Wenner Sounding curves, 34 text pages + 12 figures (Directors approval 10/26/87).
- Zohdy, A.A.R., Jackson D.B., Mattick R.E. and Peterson, D.L., 1969, Geophysical surveys for ground water at White Sands Missile Range, New Mexico: U.S. Geol. Survey Open-File Report, 31 p.
- Zohdy, A.A.R. and Jackson, D.B., 1973, Recognition of natural brine by electrical soundings near the Salt Fork of the Brazos River, Kent and Stonewall Counties, Texas: U.S. Geological Survey Prof. Paper 809-A, 14 p.
- Zohdy, A.A.R., Anderson, L.A., and Muffler, L.P.J., 1973, Resistivity, self potential, and induced polarization surveys of a vapor dominated geothermal system: Geophysics, v. 38,

no. 6, pp. 1130-1144.

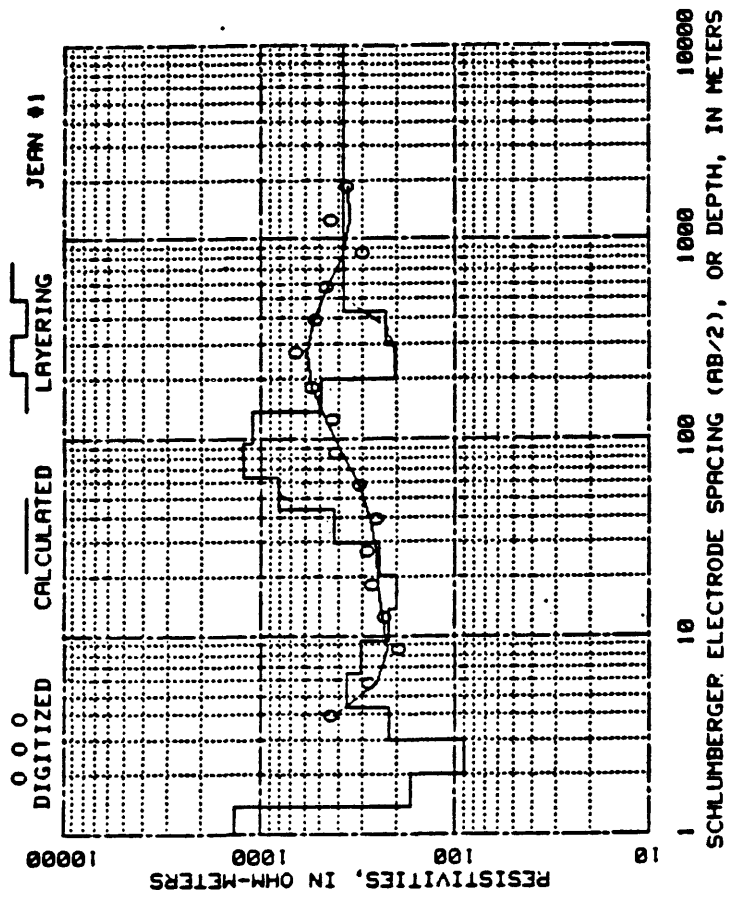
Zohdy, A.A.R., Eaton, G.P. and Mabey, D.R. 1974, Application of surface geophysics to ground-water investigations: Techniques of water-resources investigations of the United States Geological Survey, Book 2, Chapter D1, 116 p.

Zohdy, A.A.R. and Bisdorf, R.J., 1982, Schlumberger soundings in the Medicine Lake area, California: U.S. Geological Survey Open-File Report 82-887, 162 p.

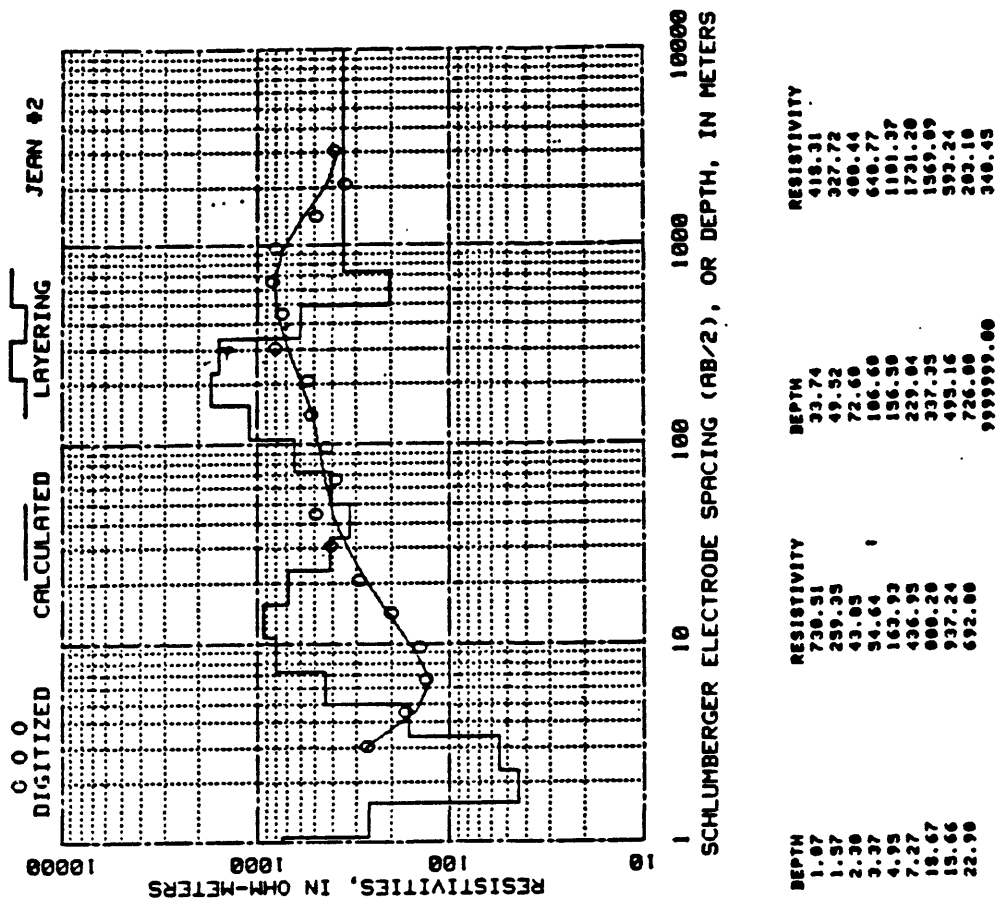
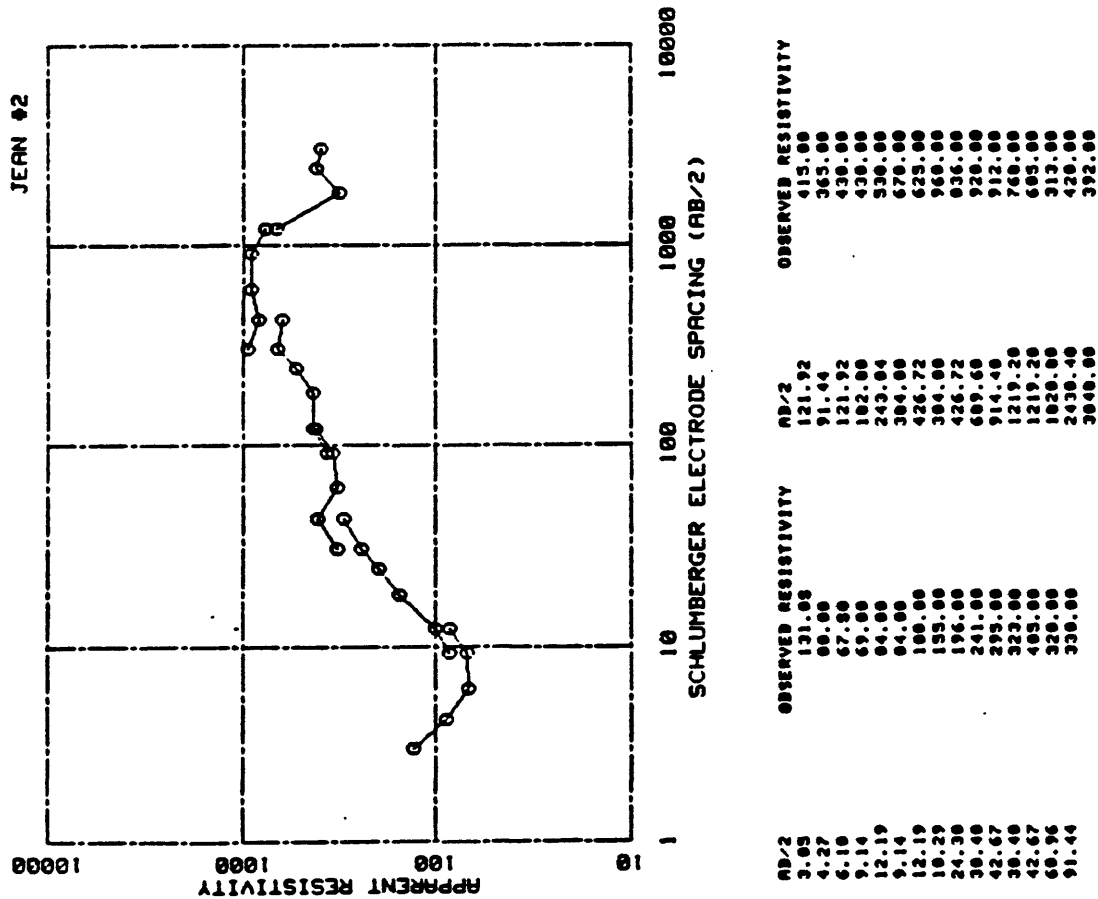
APPENDIX

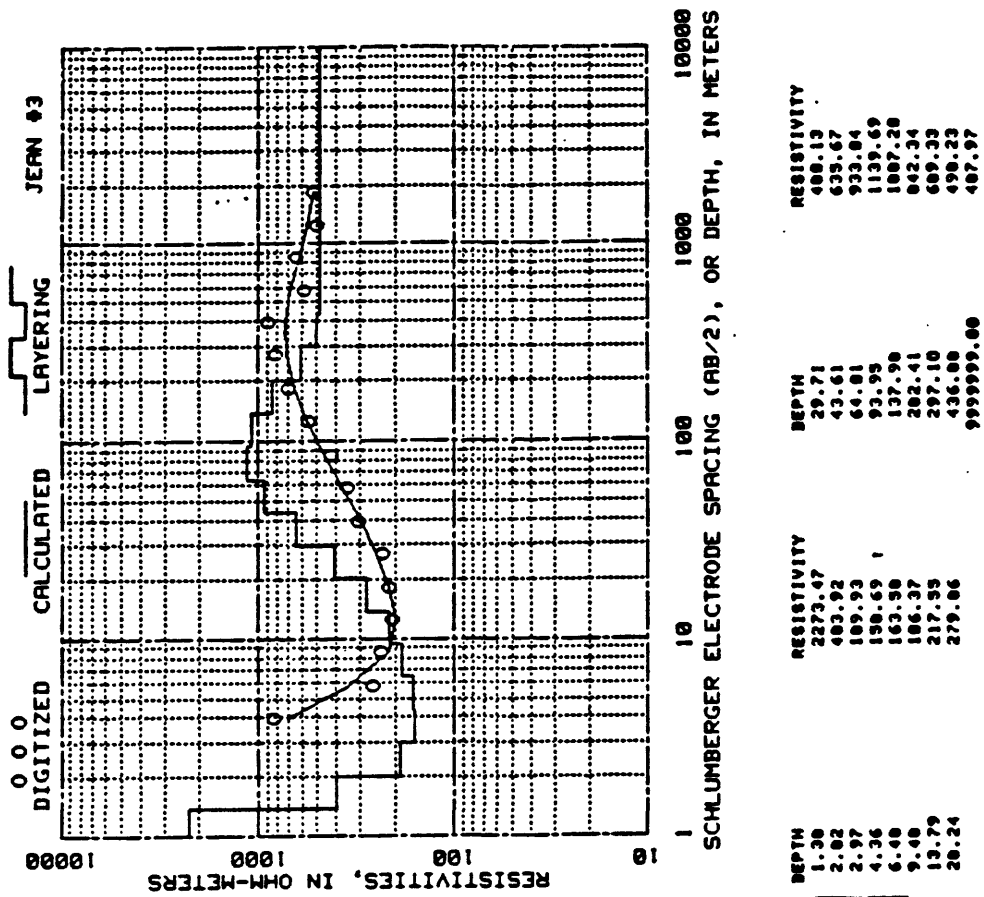
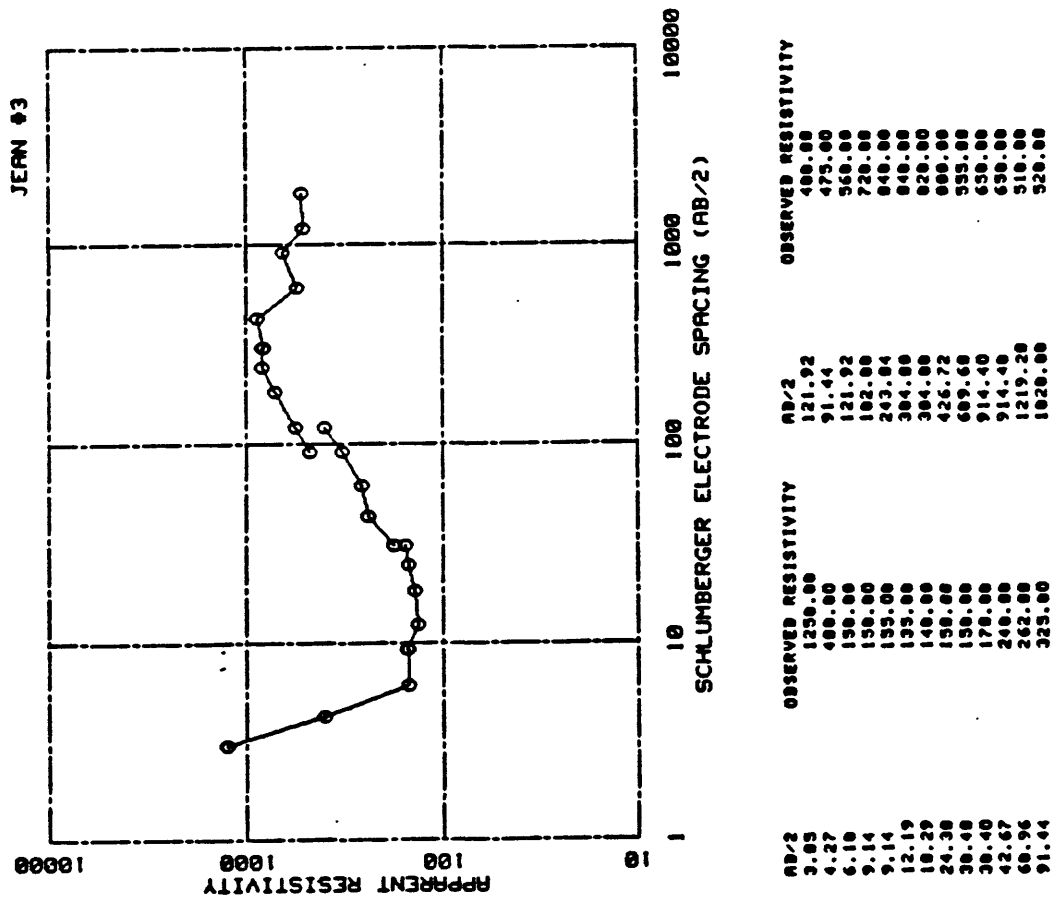


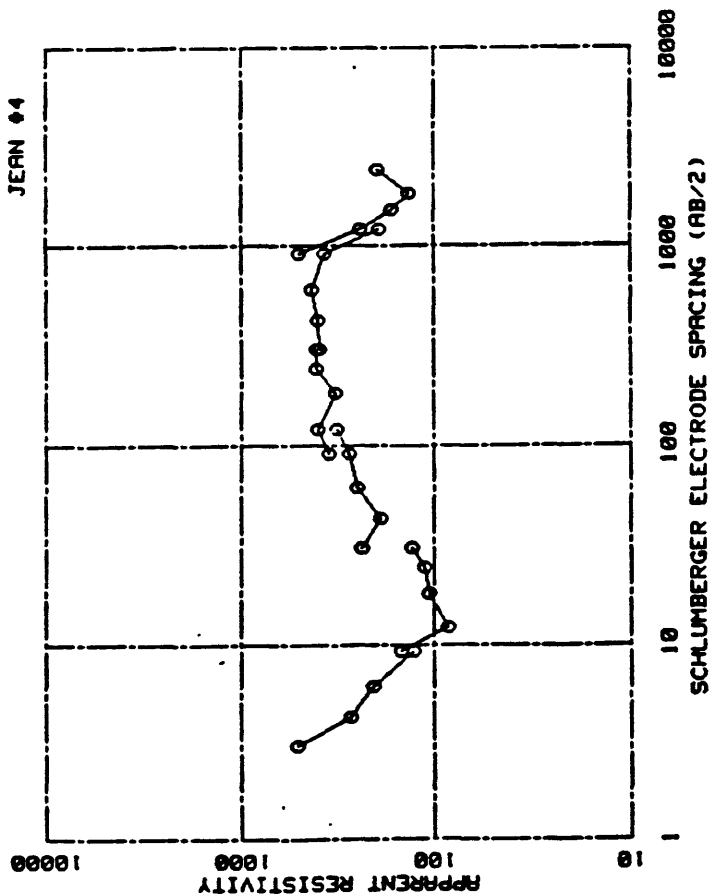
AB/2	OBSERVED RESISTIVITY	AB/2	OBSERVED RESISTIVITY
3.05	300.00	121.92	213.00
4.27	140.00	91.44	205.00
6.16	103.00	121.92	295.00
9.14	74.00	102.00	370.00
12.19	60.00	243.04	410.00
16.29	104.00	304.00	500.00
24.30	115.00	426.72	330.00
36.46	100.00	304.00	750.00
48.67	130.00	426.72	400.00
60.96	131.00	609.60	460.00
91.44	162.00	914.40	300.00
	210.00	1219.20	430.00
		1020.00	363.00



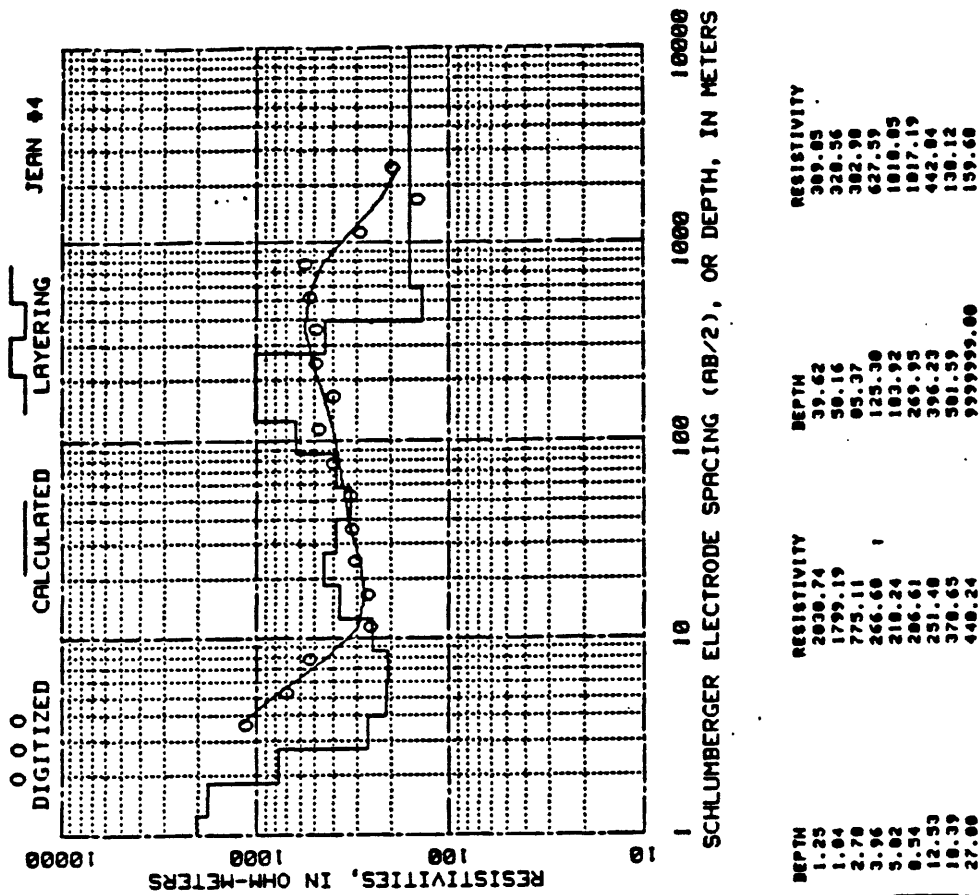
DEPTH	RESISTIVITY	DEPTH	RESISTIVITY
1.30	1356.55	29.71	246.12
2.02	159.06	43.61	425.73
2.97	80.00	64.01	822.73
4.36	210.03	93.95	1247.74
6.40	364.32	137.90	1105.32
9.40	306.06	202.41	493.43
13.79	210.65	297.10	205.10
20.24	199.02	436.00	220.97
		999.9999.00	301.01



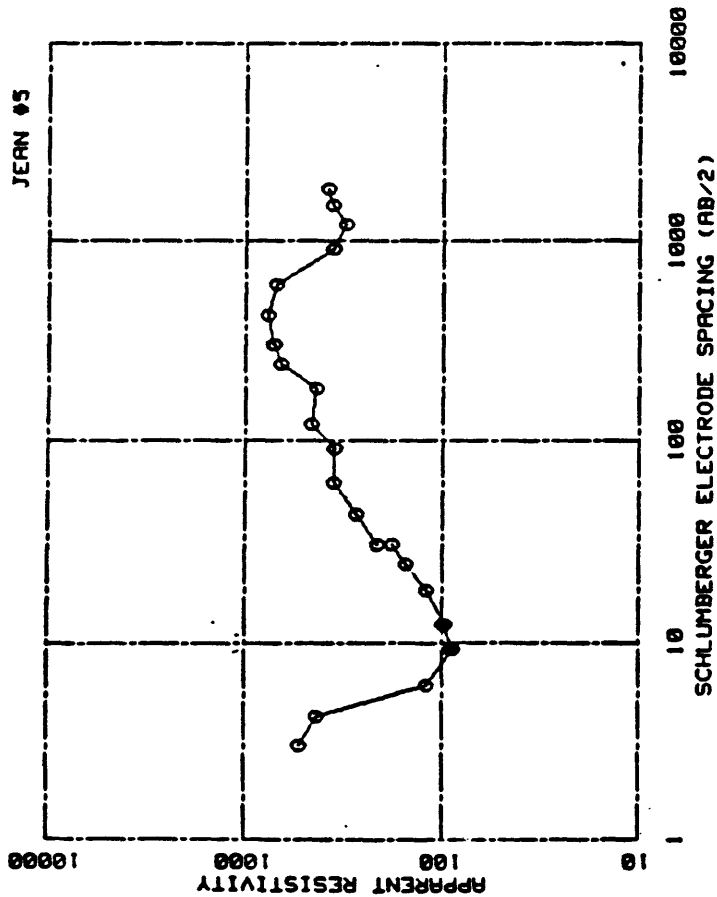




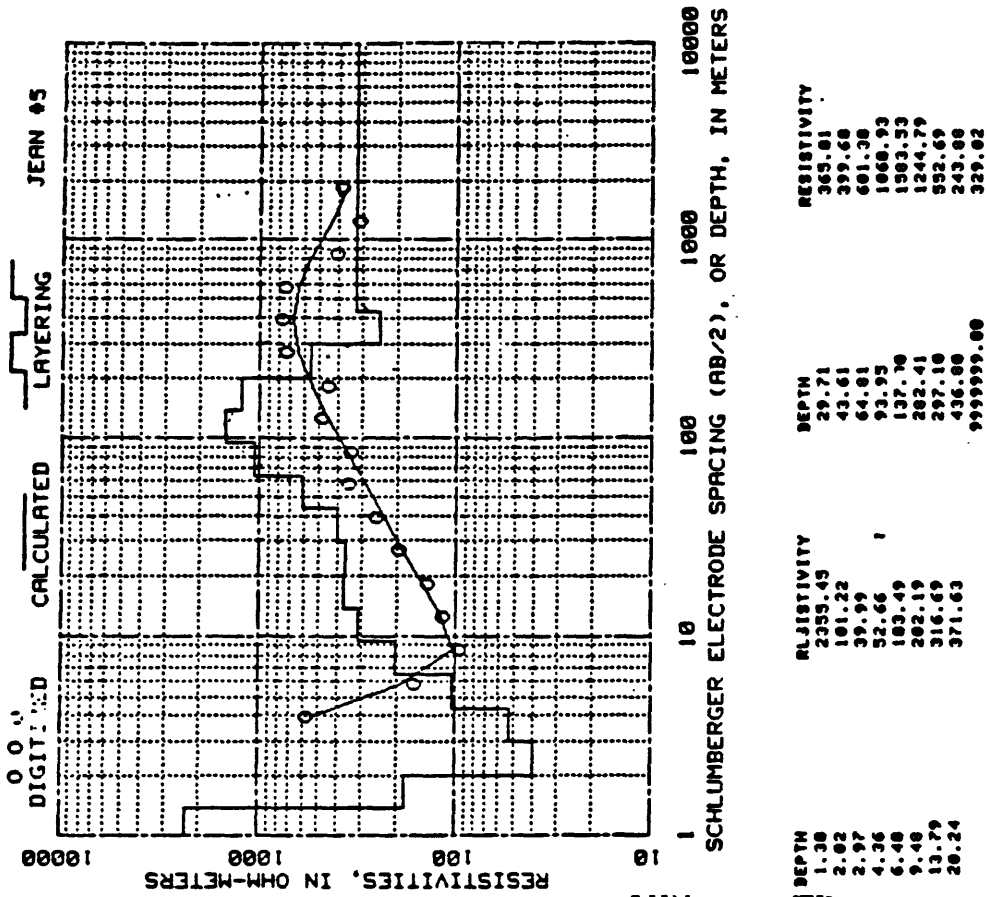
AB/2	OBSERVED RESISTIVITY	AB/2	OBSERVED RESISTIVITY
3.05	515.00	91.44	350.00
4.27	270.00	121.92	400.00
6.10	200.00	182.00	325.00
9.14	120.00	243.04	410.00
9.14	140.00	304.00	410.00
12.19	65.00	304.00	390.00
18.29	105.00	426.72	400.00
24.38	112.00	609.60	430.00
30.48	130.00	914.40	375.00
38.40	235.00	1219.20	191.00
42.67	180.00	914.40	490.00
60.96	250.00	1219.20	243.00
91.44	275.00	1524.00	165.00
121.92	320.00	1820.00	135.00
		2430.40	197.00



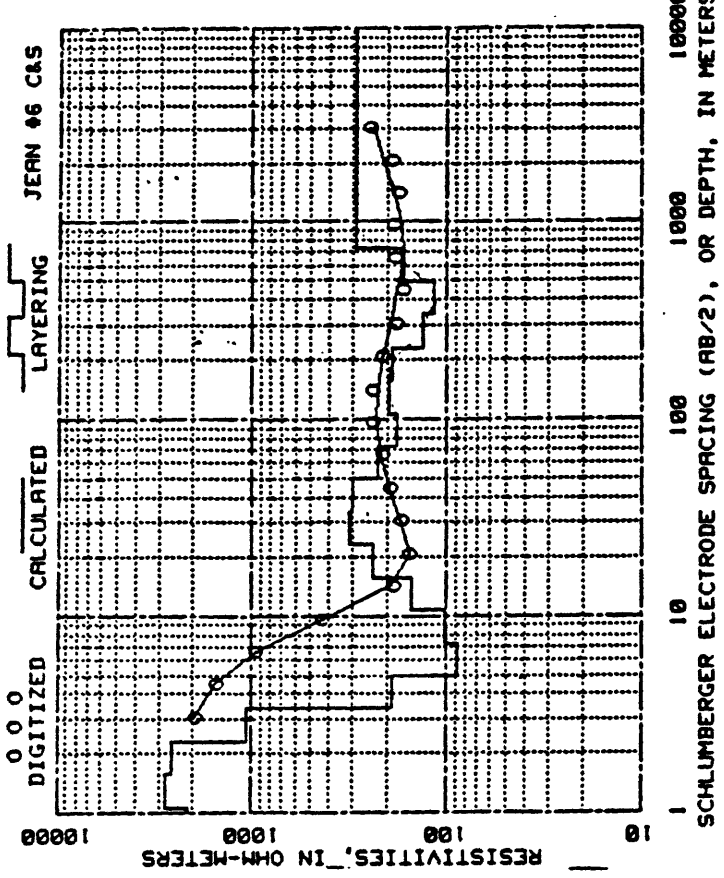
DEPTH	RESISTIVITY	DEPTH	RESISTIVITY
1.25	2030.74	39.62	309.05
1.04	1799.19	50.16	320.56
2.70	775.11	65.37	382.90
3.96	266.60	125.30	627.59
5.02	210.24	183.92	1010.05
8.54	206.61	269.95	1017.19
12.53	251.48	396.23	442.04
18.39	378.65	501.59	130.12
27.00	440.24	999999.00	159.60



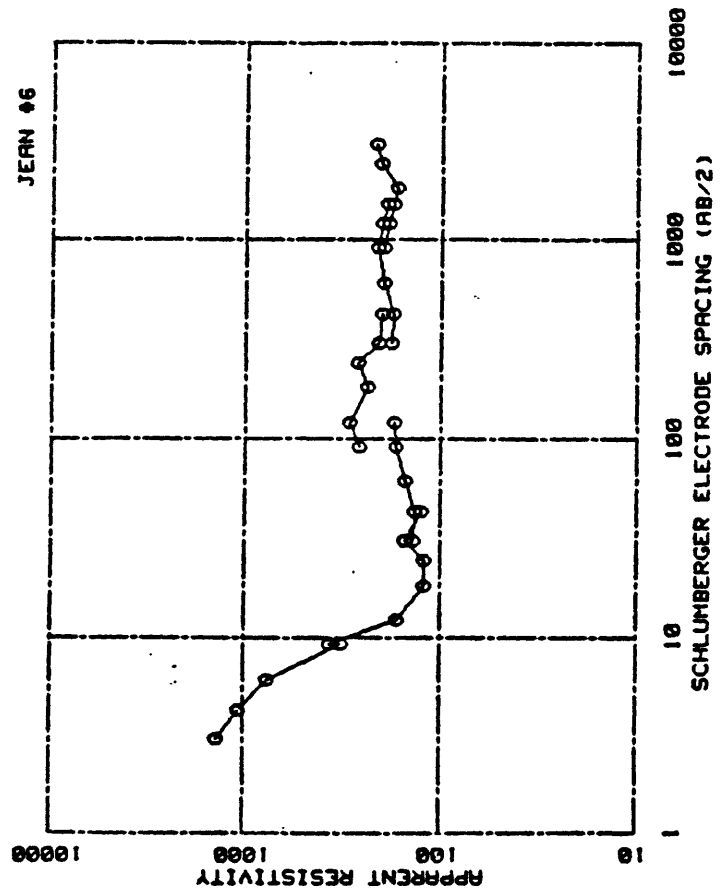
AB/2	OBSERVED RESISTIVITY	AB/2	OBSERVED RESISTIVITY
3.65	538.00	91.44	368.00
4.27	438.00	91.44	350.00
6.10	128.00	121.92	465.00
9.14	97.00	182.00	448.00
12.19	100.00	243.04	665.00
9.14	91.00	304.00	728.00
12.19	97.00	304.00	725.00
18.29	128.00	426.72	700.00
24.38	154.00	605.60	700.00
38.48	102.00	914.48	368.00
38.48	214.00	914.48	367.00
42.67	276.00	1219.20	312.00
60.96	368.00	1524.00	364.00
		1820.00	303.00



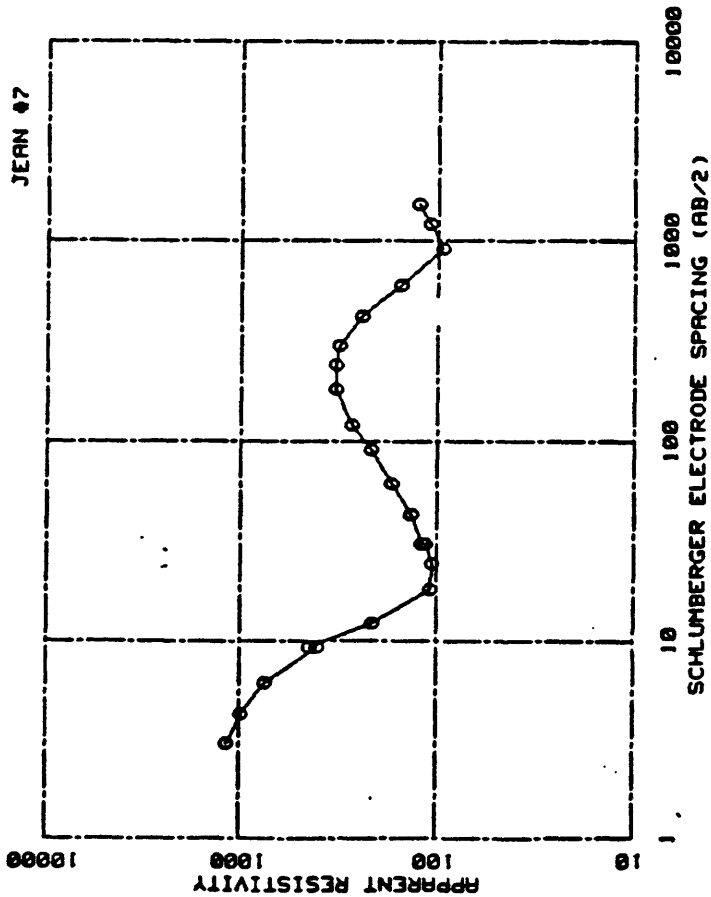
DEPTH	RESISTIVITY	DEPTH	RESISTIVITY
1.38	2355.45	29.71	365.01
2.02	181.22	43.61	399.68
2.97	39.99	64.01	601.38
4.36	52.66	93.95	1860.93
6.48	183.49	137.70	1503.53
9.40	202.19	202.41	1244.79
13.79	316.69	297.10	552.69
20.24	371.63	436.00	243.00
		999999.00	329.02



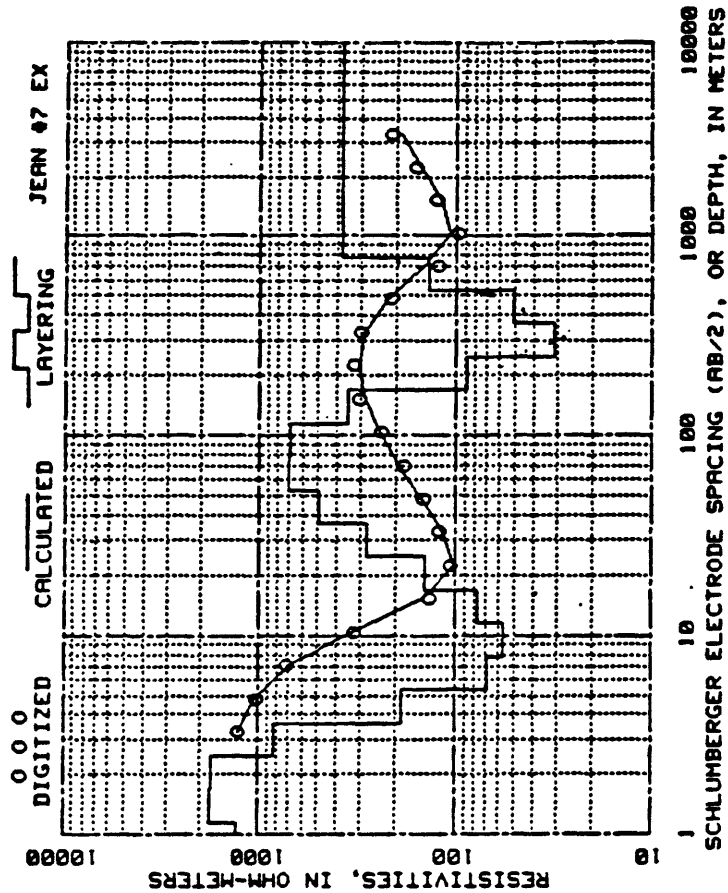
DEPTH	RESISTIVITY	DEPTH	RESISTIVITY
1.07	2130.25	33.74	314.06
1.57	2794.06	49.52	303.79
2.30	2506.96	72.68	222.50
3.37	1055.16	106.68	179.47
4.44	109.63	156.50	197.41
		228.84	190.67



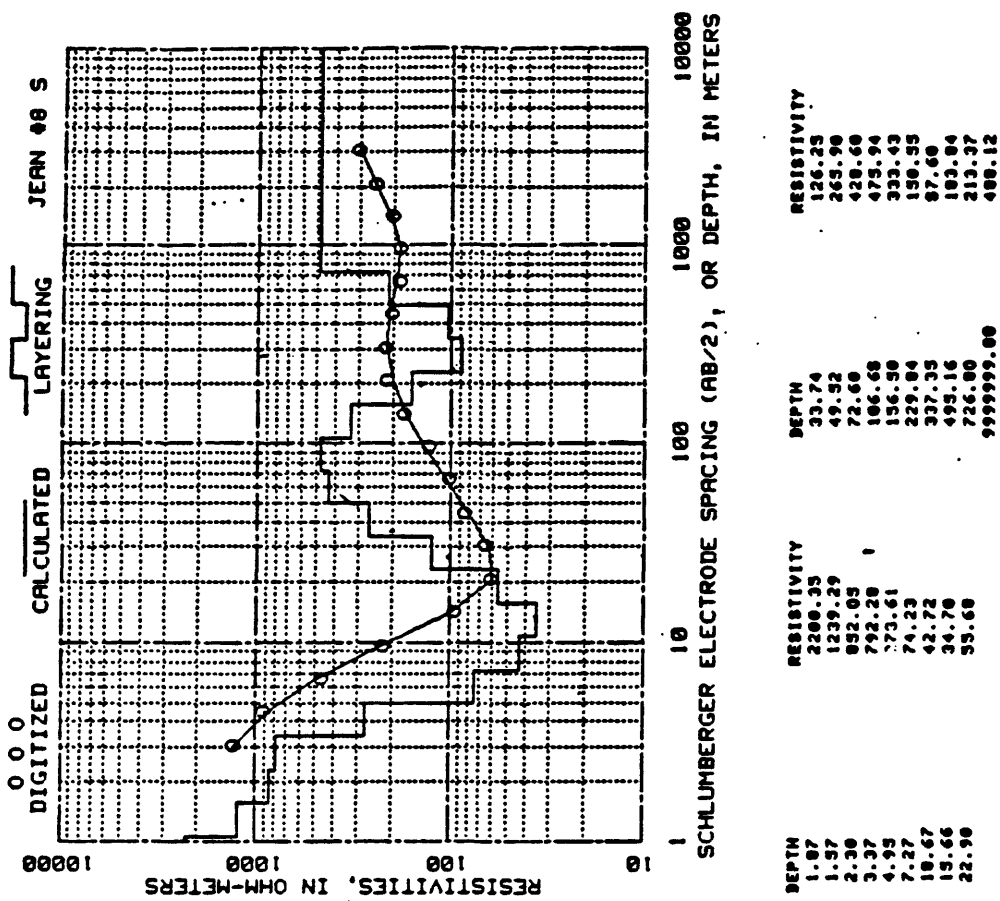
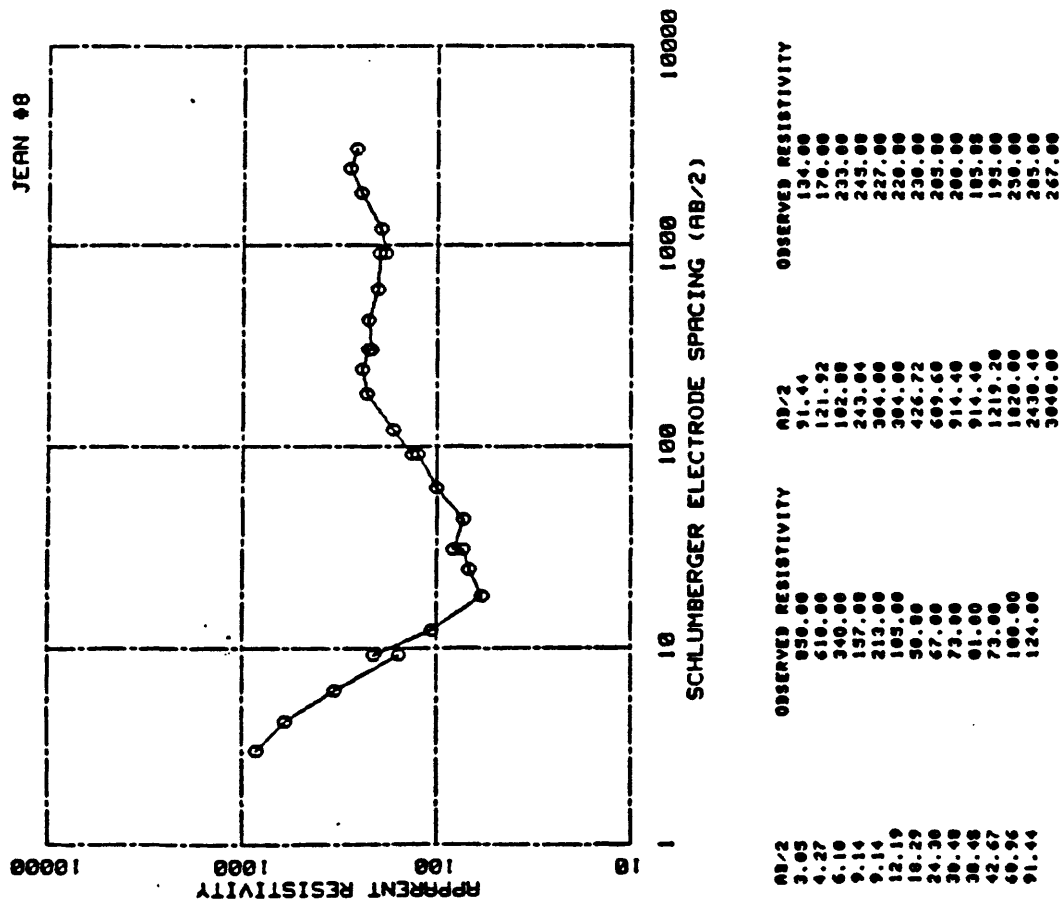
AB/2	OBSERVED RESISTIVITY	AB/2	OBSERVED RESISTIVITY
3.05	1375.00	121.92	290.00
4.27	1070.00	102.00	235.00
2.16	760.00	243.04	265.00
		222.00	200.00

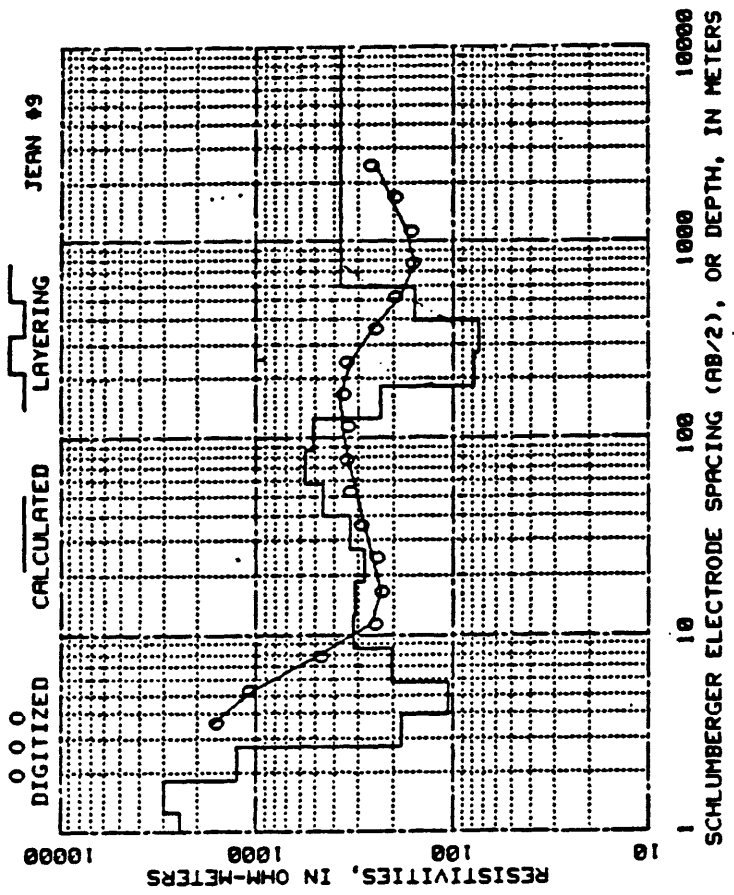


AB/2	OBSERVED RESISTIVITY	AB/2	OBSERVED RESISTIVITY
3.05	1175.00	91.44	215.00
4.27	900.00	91.44	215.00
6.16	750.00	121.92	272.00
9.14	400.00	102.00	325.00
9.14	440.00	243.04	325.00
12.19	210.00	304.00	315.00
18.29	100.00	304.00	315.00
24.38	105.00	426.72	240.00
30.48	114.00	609.60	155.00
30.48	110.00	914.40	95.00
42.67	136.00	1219.20	110.00
60.96	170.00	1524.00	125.00

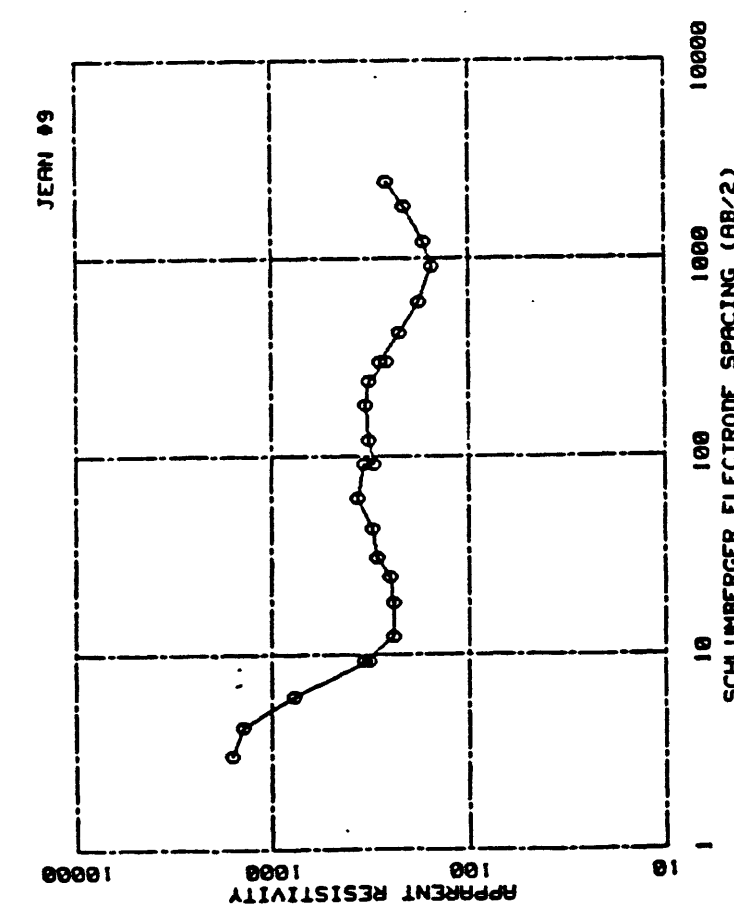


DEPTH	RESISTIVITY	DEPTH	RESISTIVITY
1.15	1314.04	36.30	279.00
1.69	1700.02	53.29	494.32
2.47	1765.30	70.21	706.47
3.63	036.74	114.08	607.49
5.33	105.41	160.50	354.01
7.02	69.12	247.33	87.34
11.40	56.69	363.03	31.17
16.05	77.22	532.03	50.76
24.73	142.56	702.12	137.55
		9999999.00	377.92

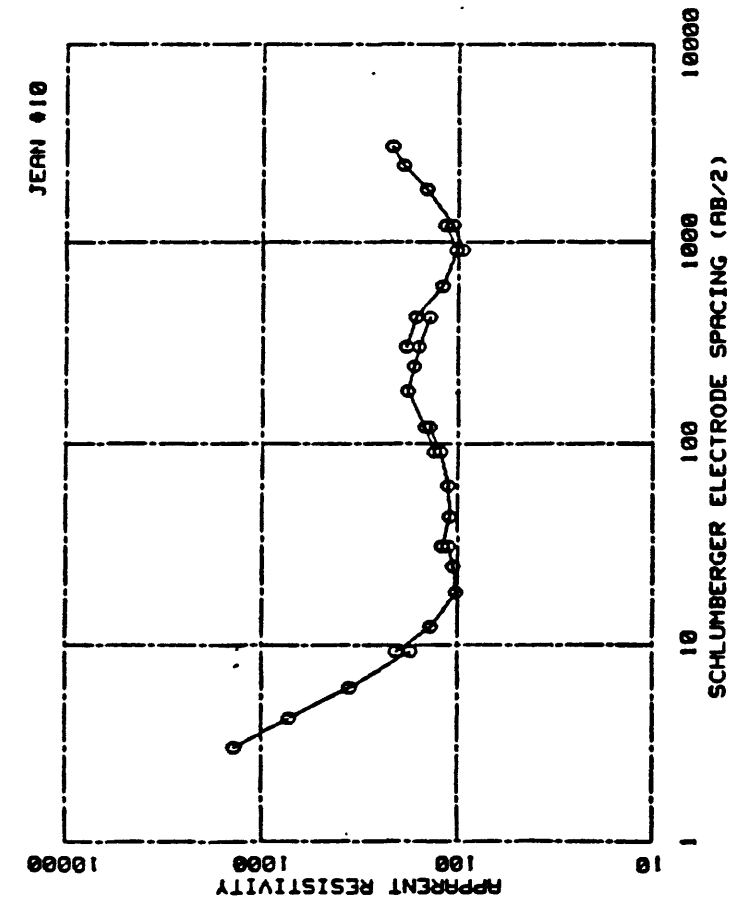




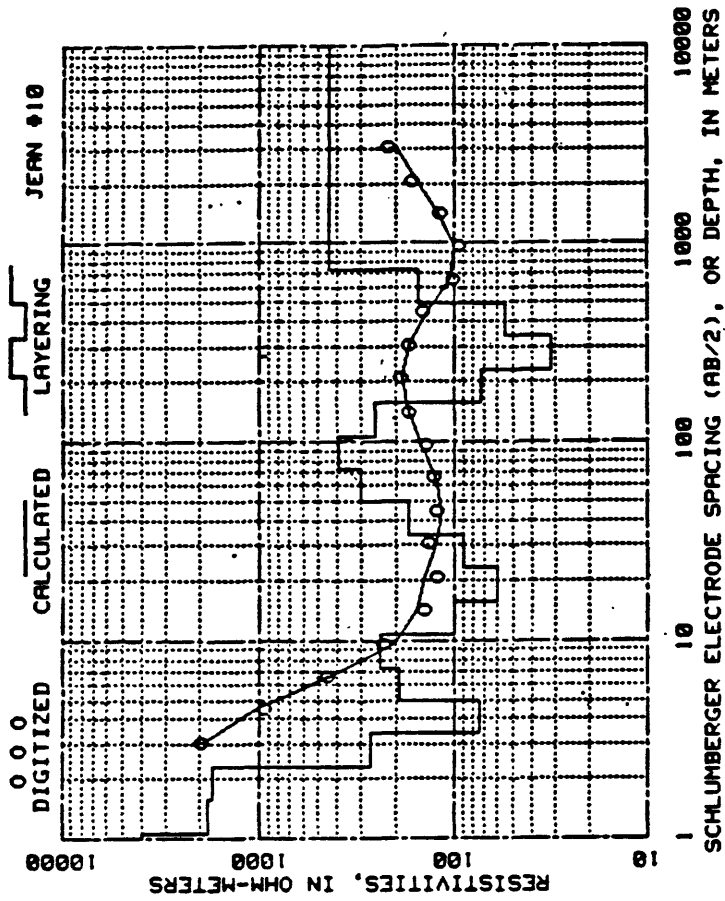
DEPTH	RESISTIVITY	DEPTH	RESISTIVITY
1.25	2482.64	39.61	332.60
1.84	2967.53	58.14	456.71
2.70	1263.37	85.34	567.54
3.96	182.12	125.27	512.30
5.81	184.31	183.67	234.00
8.53	204.91	269.00	77.00
12.53	319.00	396.13	72.00
18.39	314.17	581.44	156.09
26.99	283.16	999999.00	368.56



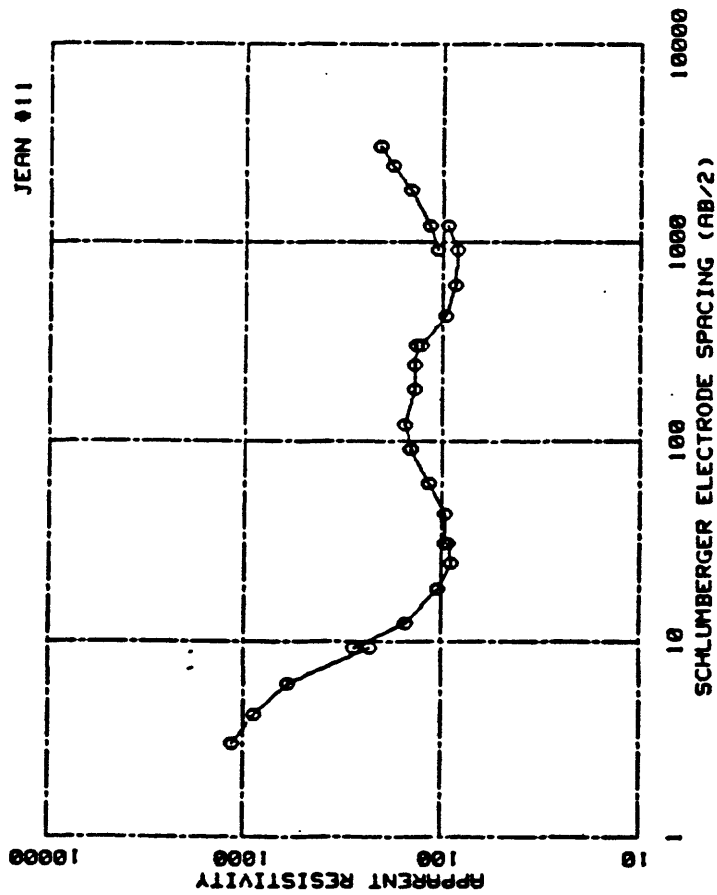
AB/2	OBSERVED RESISTIVITY	AB/2	OBSERVED RESISTIVITY
3.05	1600.00	91.44	305.00
4.27	1410.00	121.32	328.00
6.10	775.00	182.00	335.00
9.14	320.00	243.04	320.00
9.14	340.00	304.00	260.00
12.19	340.00	384.00	200.00
18.29	240.00	426.72	222.00
24.38	250.00	609.68	180.00
30.48	290.00	914.40	155.00
30.48	290.00	914.40	155.00
42.67	310.00	1219.20	150.00
60.96	360.00	1820.00	210.00
91.44	340.00	2430.40	260.00



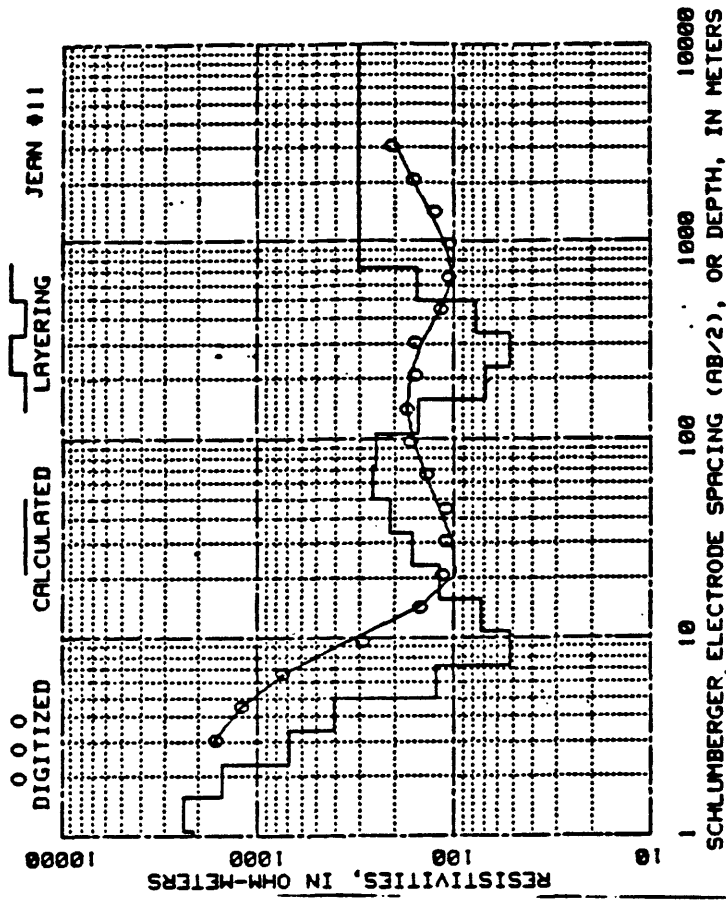
AB/2	OBSERVED RESISTIVITY	AB/2	OBSERVED RESISTIVITY
3.05	1300.00	121.92	147.00
4.27	730.00	102.00	102.00
6.10	350.00	243.04	102.00
9.14	174.00	304.00	100.00
12.19	207.00	426.72	100.00
18.29	130.00	304.00	100.00
24.30	102.00	426.72	100.00
30.40	111.00	609.60	100.00
42.67	120.00	914.40	102.00
60.96	109.60	1219.20	117.00
91.44	112.00	914.40	94.00
121.92	120.00	1020.00	100.00
91.44	130.00	2430.40	140.00
		3040.00	210.00



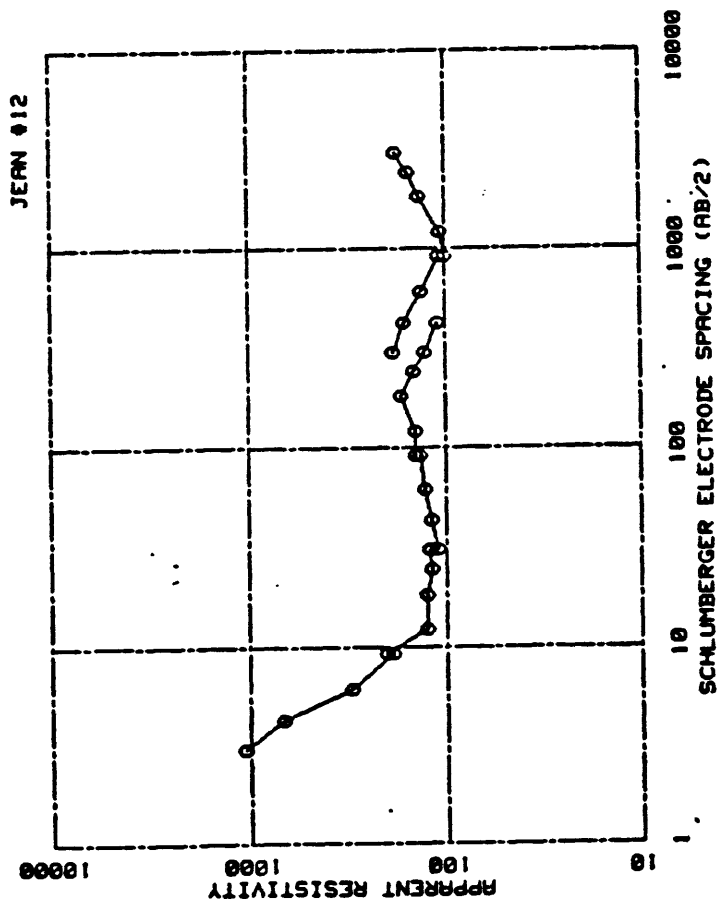
DEPTH	RESISTIVITY	DEPTH	RESISTIVITY
1.07	3966.97	33.74	90.00
1.57	1034.43	49.52	172.73
2.30	1732.22	72.60	302.96
3.37	269.10	106.60	392.95
4.93	73.95	156.30	256.79
7.27	192.62	229.04	73.22
10.67	240.10	337.35	31.95
15.66	100.50	495.16	94.92
22.90	60.67	726.00	132.45
		9999999.00	443.06



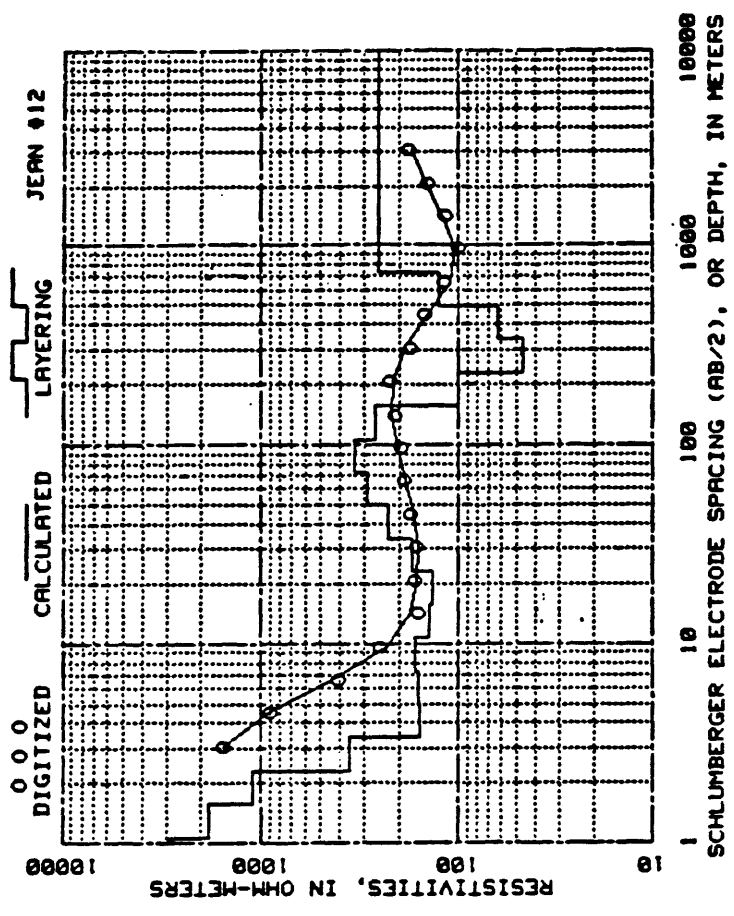
AB/2	OBSERVED RESISTIVITY	AB/2	OBSERVED RESISTIVITY
3.05	1150.00	121.92	155.00
4.27	800.00	162.00	137.00
6.10	600.00	243.04	130.00
9.14	230.00	304.00	136.00
12.19	270.00	304.00	127.00
18.29	151.00	426.72	97.00
24.30	103.00	609.60	66.00
30.40	92.00	914.40	95.00
42.67	96.00	1219.20	95.00
60.96	116.00	1219.20	185.00
91.44	143.00	1020.00	117.00
	142.00	2430.40	145.00
		3040.00	179.00
			207.00



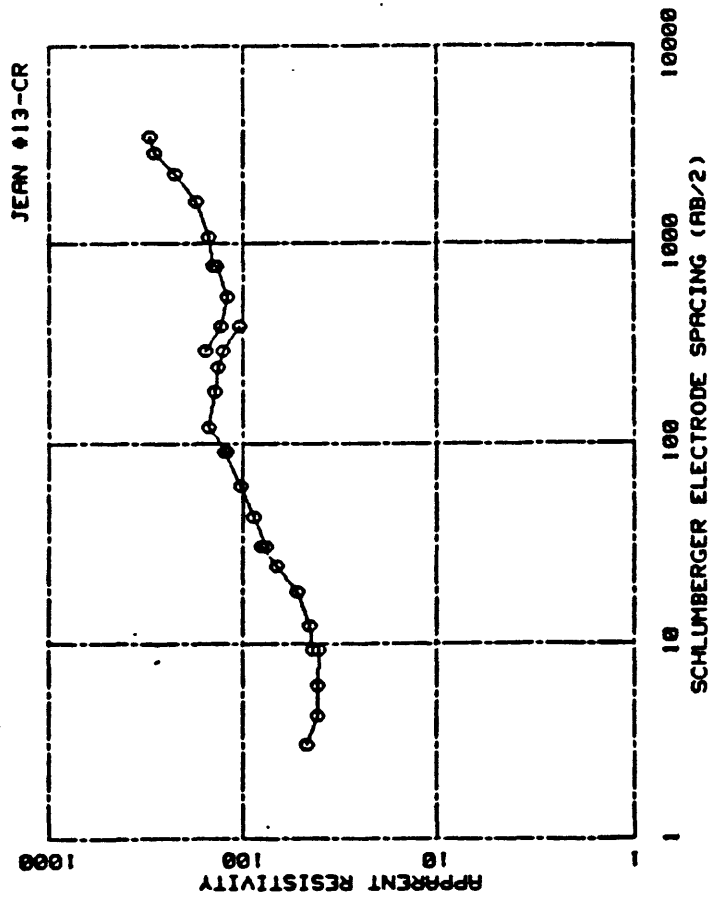
DEPTH	RESISTIVITY	DEPTH	RESISTIVITY
1.07	2126.61	33.74	162.57
1.37	2301.73	49.32	211.07
2.30	1531.04	72.68	260.02
3.37	609.69	106.60	249.72
4.95	400.04	156.50	151.14
7.27	123.05	229.04	69.03
10.67	51.70	337.35	51.36
15.66	22.39	495.16	77.49
22.96	117.37	726.00	152.90
		9999999.00	306.72



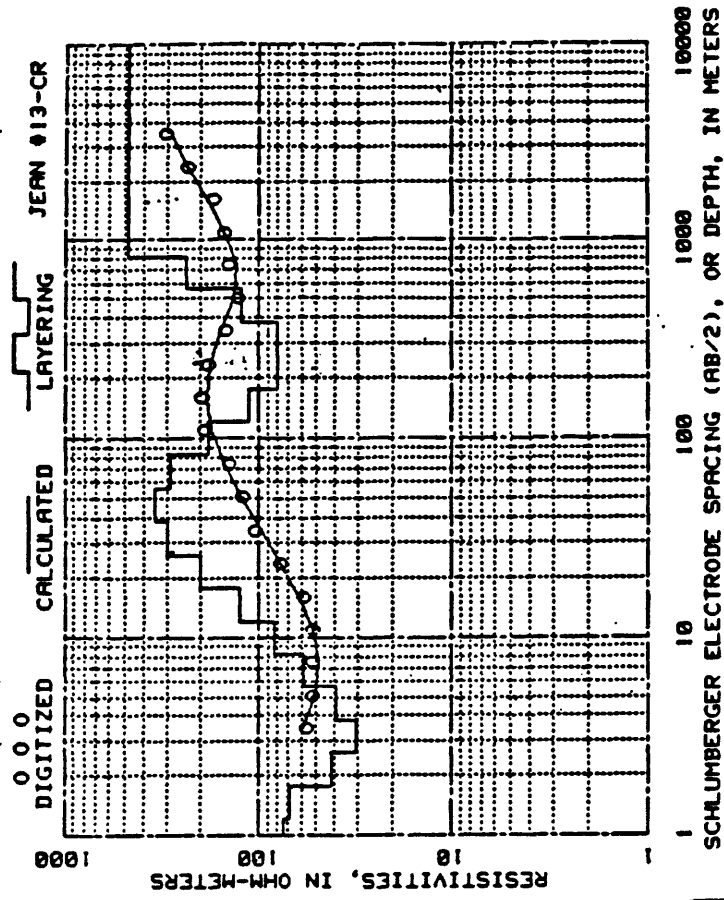
AB/2	OBSERVED RESISTIVITY	AB/2	OBSERVED RESISTIVITY
2.05	1060.00	121.92	143.00
4.27	600.00	162.00	170.00
6.10	310.00	243.04	145.00
9.14	100.00	304.00	127.00
12.19	205.00	426.72	110.00
16.29	126.00	584.00	107.00
24.30	110.00	826.72	163.00
30.40	120.00	114.40	132.00
38.40	110.00	914.40	107.00
42.67	110.00	1219.20	100.00
60.96	127.00	1820.00	106.00
91.44	135.00	2430.40	150.00
	143.00	3040.00	100.00



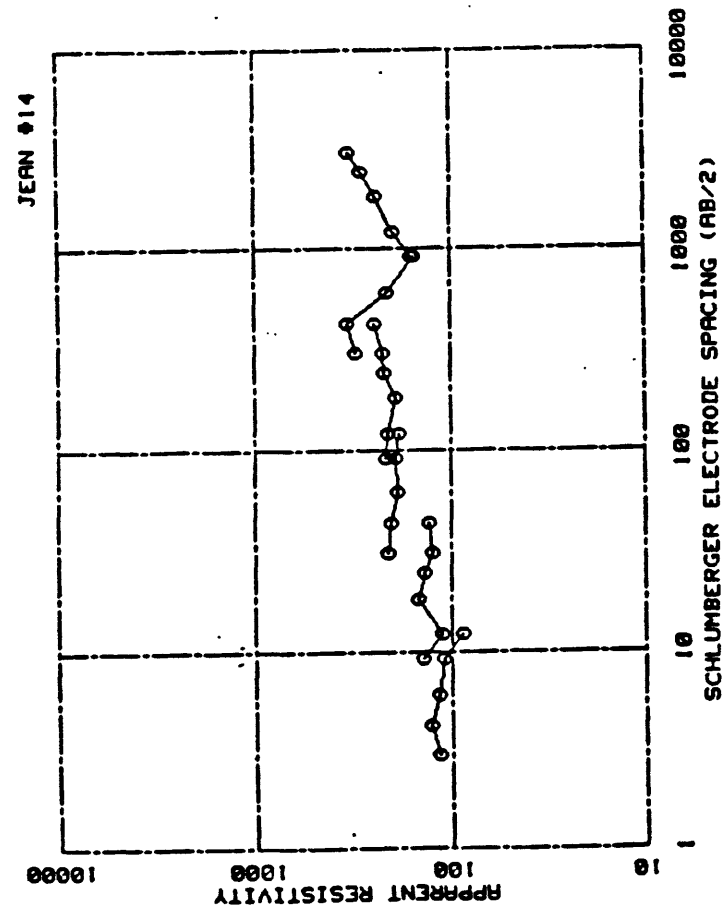
DEPTH	RESISTIVITY	DEPTH	RESISTIVITY
1.07	2907.09	33.74	170.90
1.57	1019.45	49.52	229.74
2.30	1102.33	72.60	290.33
3.37	360.70	106.68	339.27
4.95	156.30	156.50	265.62
7.27	159.00	229.04	100.30
10.67	165.52	337.35	46.52
15.66	141.39	495.16	62.09
22.90	135.19	726.00	125.40
		999999.00	254.30



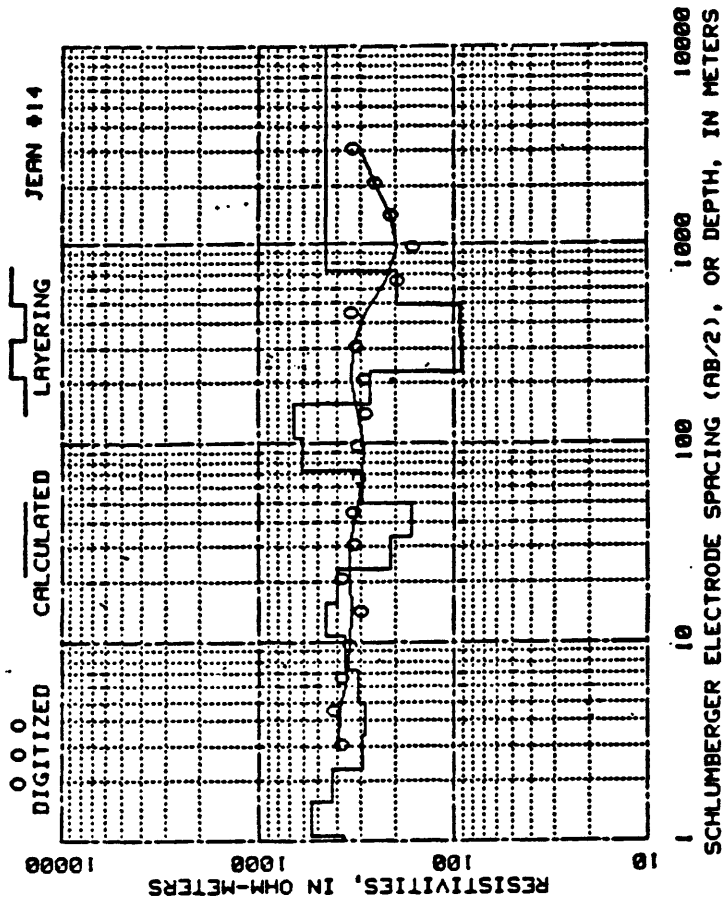
AB/2	OBSERVED RESISTIVITY	AB/2	OBSERVED RESISTIVITY
3.05	46.50	121.92	153.00
4.27	41.00	162.00	142.00
6.10	41.00	243.04	137.00
9.14	40.00	291.00	120.00
12.19	43.00	307.10	104.00
16.29	44.50	291.00	150.00
24.30	82.00	307.10	132.00
30.40	66.00	946.20	123.00
38.40	81.00	701.20	130.00
42.67	76.00	1079.60	145.00
60.96	89.00	1650.11	152.00
91.44	103.00	2262.53	170.00
91.44	127.00	2000.06	224.00
	122.00	3453.99	207.00
			304.00



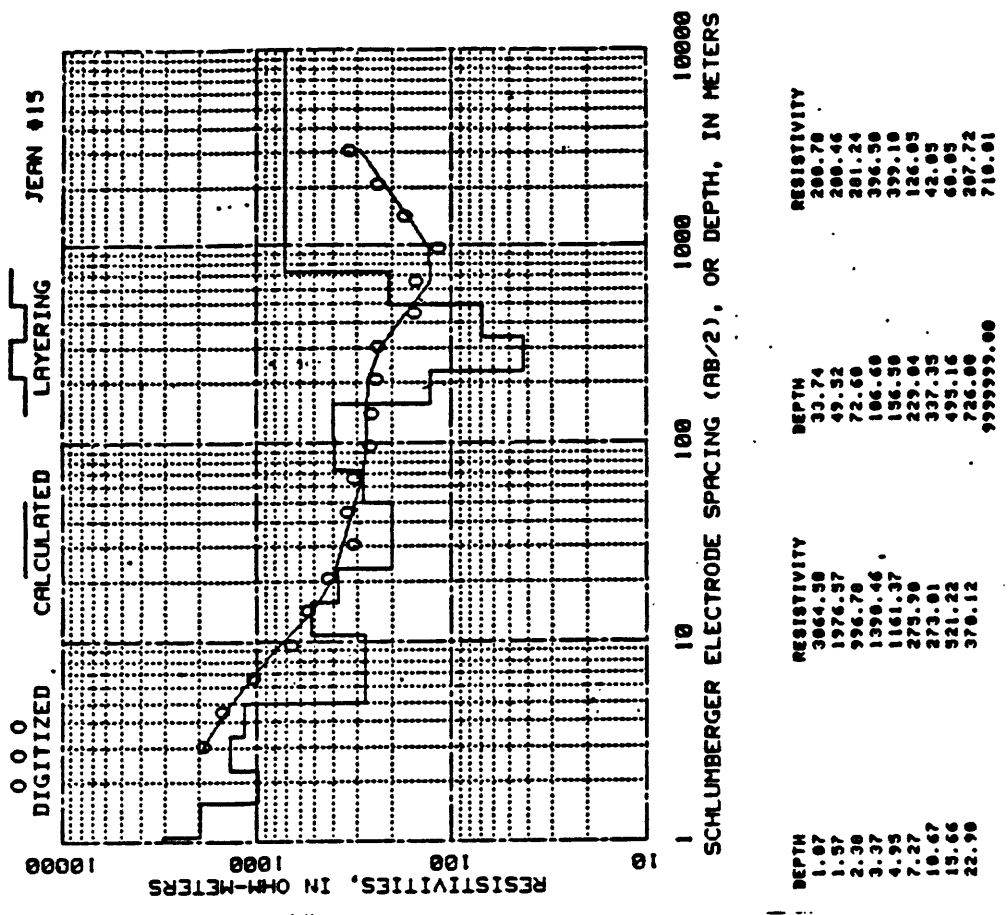
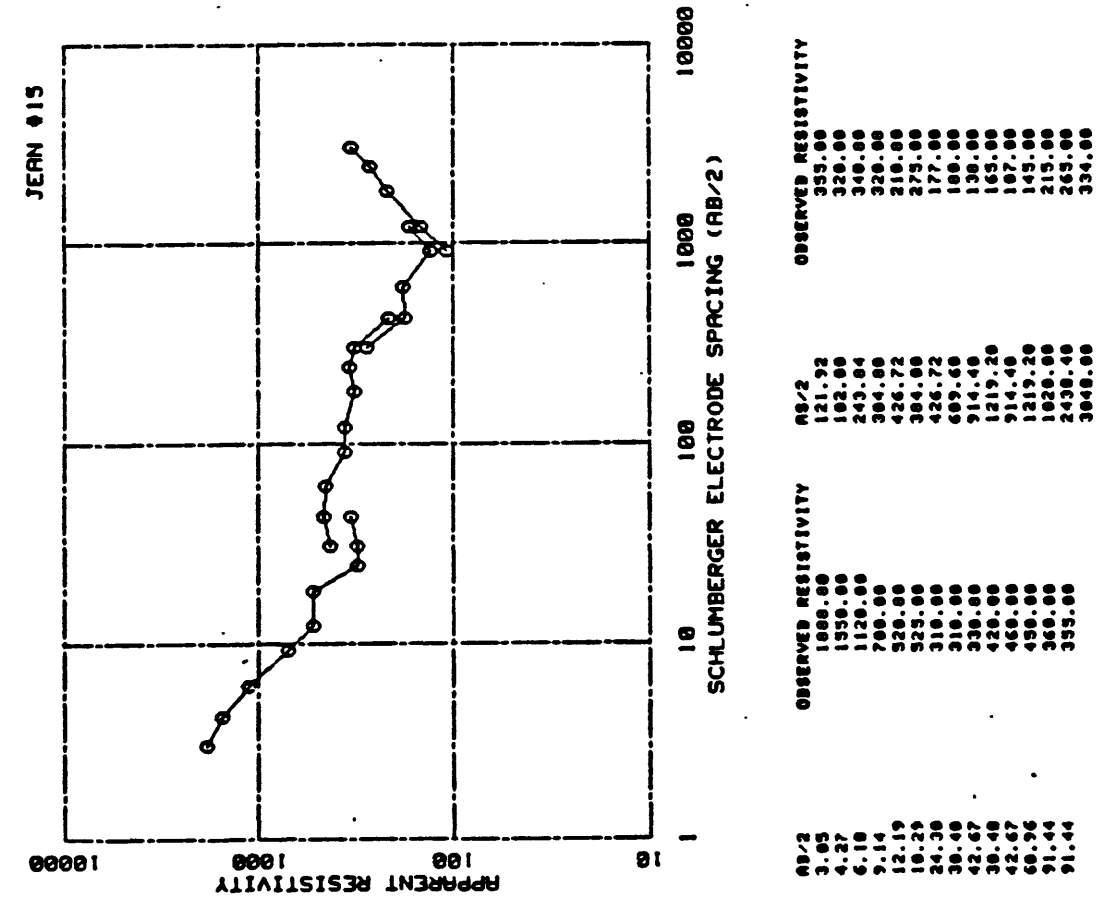
DEPTH	RESISTIVITY	DEPTH	RESISTIVITY
1.21	74.76	30.23	257.99
1.77	60.50	56.11	344.00
2.60	42.01	82.36	200.60
3.02	31.11	120.09	104.27
5.61	39.63	177.44	113.04
6.24	50.71	260.45	80.79
12.09	83.04	302.29	90.23
17.74	126.00	561.12	124.19
26.04	203.01	823.61	239.77
		9999999.00	475.39

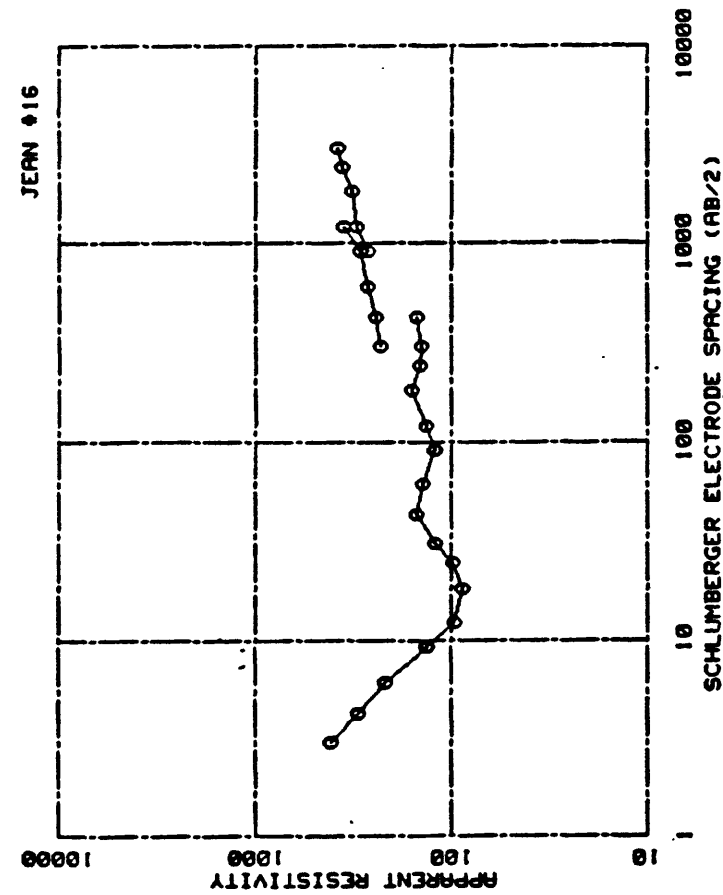


AB/2	OBSERVED RESISTIVITY	AB/2	OBSERVED RESISTIVITY
3.85	115.00	121.92	105.00
4.27	127.00	91.44	215.00
6.18	116.00	121.92	218.00
9.14	109.00	102.00	192.00
12.19	87.00	243.04	210.00
9.14	140.00	304.00	222.00
12.19	111.00	426.72	244.00
10.29	147.00	304.00	307.00
24.38	130.00	426.72	340.00
42.67	126.00	609.60	210.00
30.40	130.00	914.40	155.00
42.67	212.00	914.40	160.00
30.40	205.00	1219.20	195.00
42.67	190.00	1020.00	240.00
60.96	192.00	2430.40	205.00
91.44		3040.00	330.00

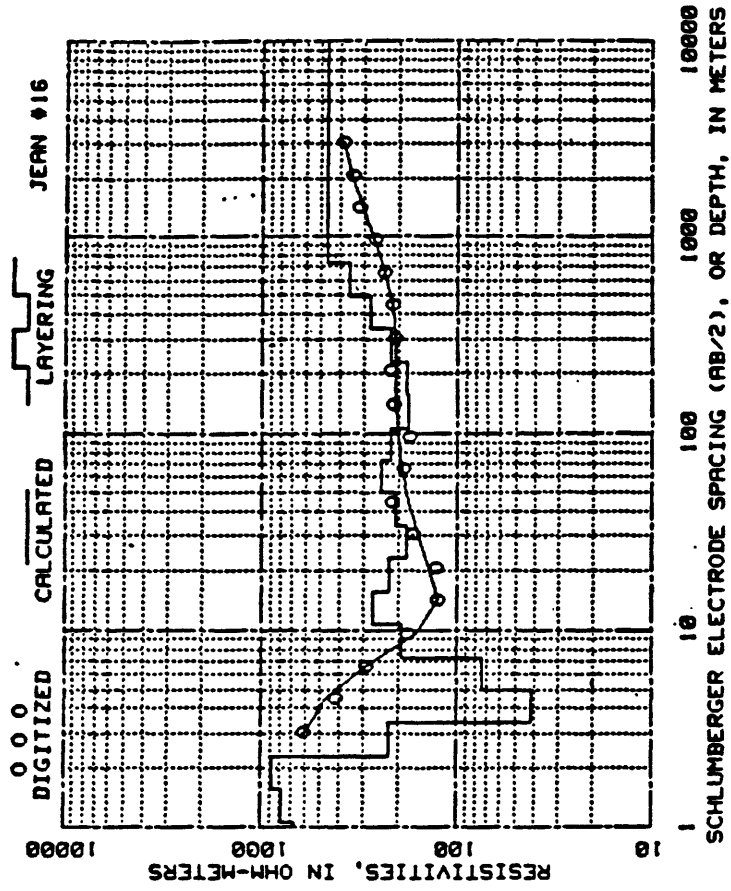


DEPTH	RESISTIVITY	DEPTH	RESISTIVITY
1.07	378.00	33.74	212.74
1.37	540.62	49.52	166.04
1.97	426.06	72.60	290.91
3.37	290.17	106.68	608.41
4.95	206.24	156.50	608.99
7.27	311.49	229.94	271.39
10.67	365.75	337.35	90.62
15.66	456.41	495.16	93.04
22.90	399.02	726.90	197.51
		9999999.00	456.56

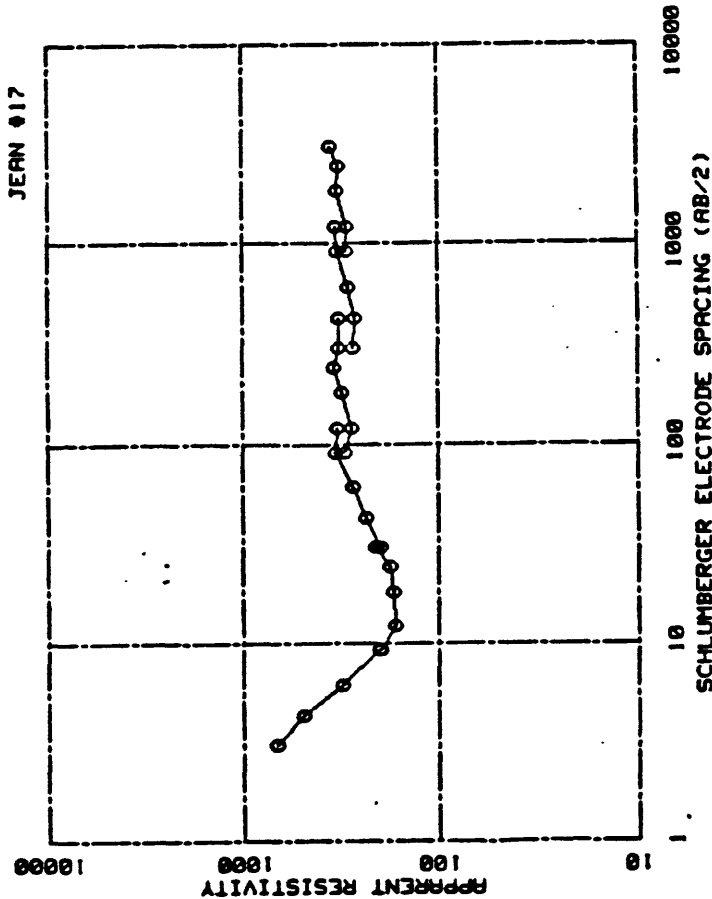




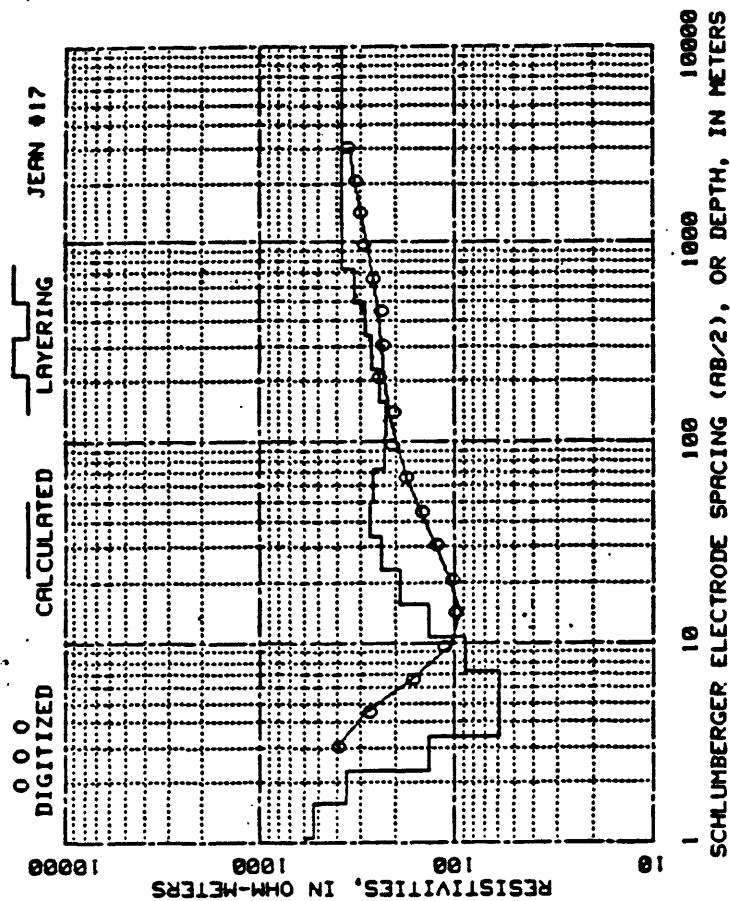
AB/2	OBSERVED RESISTIVITY	AB/2	OBSERVED RESISTIVITY
3.65	428.00	121.92	135.00
4.27	305.00	161.00	161.00
6.10	210.00	243.04	145.00
9.14	132.00	304.80	144.00
9.14	136.00	426.72	150.00
12.19	97.00	304.80	234.00
18.29	87.00	426.72	240.00
24.38	90.00	609.60	270.00
38.48	120.00	914.40	293.00
42.67	120.00	1219.20	353.00
60.96	140.00	914.40	270.00
91.44	123.00	1219.20	307.00
91.44	121.00	1820.00	320.00
		2430.40	363.00
		3048.00	369.00



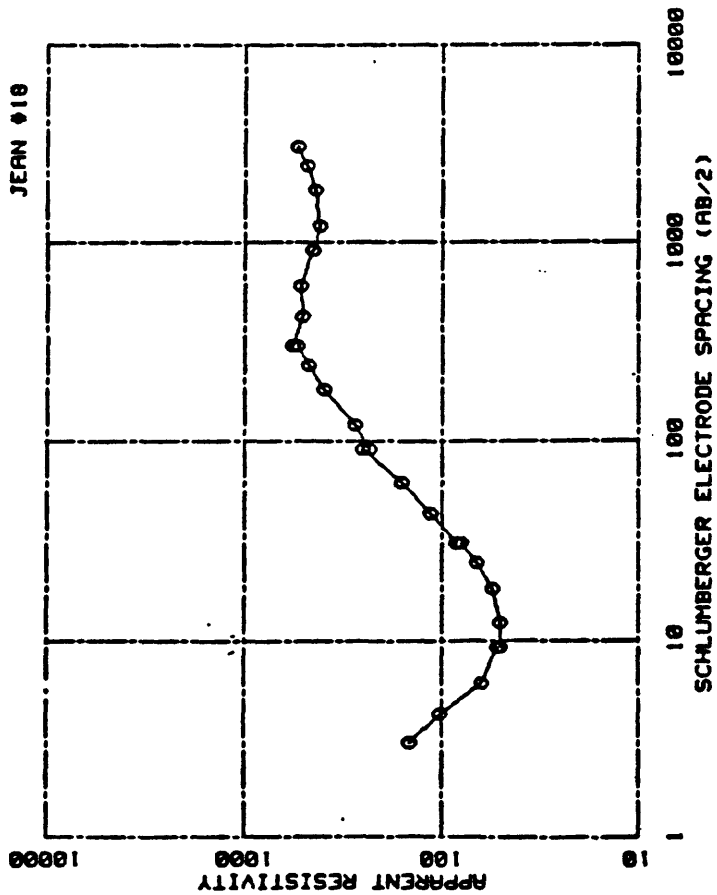
DEPTH	RESISTIVITY	DEPTH	RESISTIVITY
1.07	672.50	33.74	101.01
1.57	794.92	49.32	207.50
2.30	978.73	72.60	243.79
3.37	225.67	106.60	210.07
4.99	41.29	156.30	179.17
7.27	73.59	229.04	101.74
10.67	192.69	337.35	221.92
13.66	260.00	435.16	279.33
22.90	222.13	726.00	337.51
		999999.00	403.20



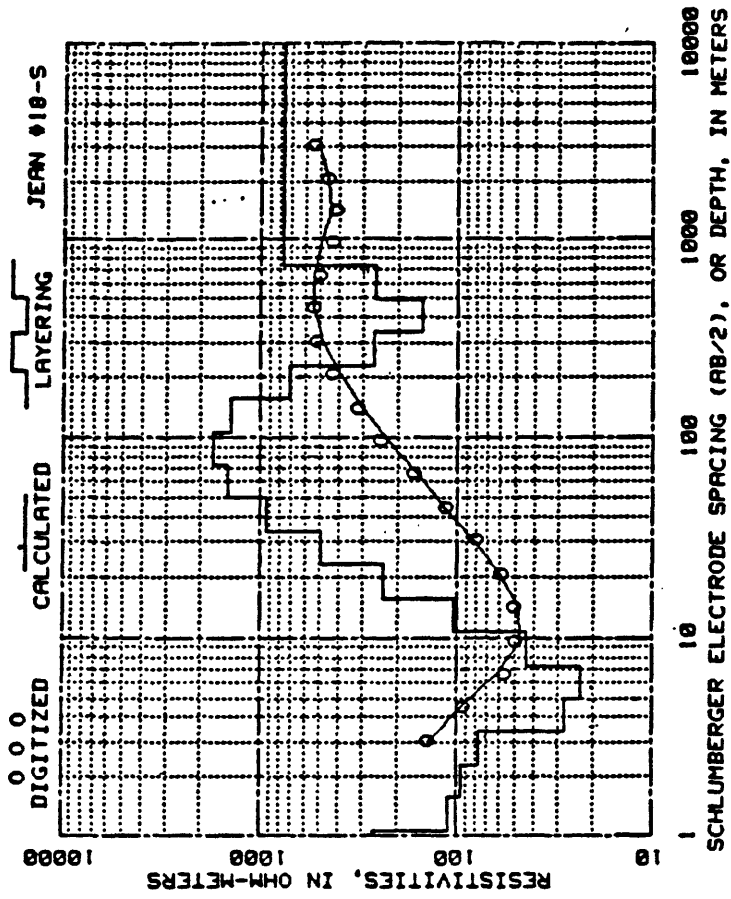
AB/2	OBSERVED RESISTIVITY	AB/2	OBSERVED RESISTIVITY
3.05	605.00	121.92	275.00
4.27	495.00	102.00	310.00
6.10	310.00	243.04	340.00
9.14	200.00	304.00	320.00
12.19	195.00	320.00	320.00
16.29	167.00	270.00	265.00
24.38	176.00	200.00	200.00
30.40	206.00	914.40	320.00
42.67	197.00	1219.20	330.00
60.96	232.00	914.40	292.00
91.44	270.00	1219.20	292.00
121.92	325.00	1020.00	320.00
91.44	295.00	2430.40	320.00
		3040.00	350.00



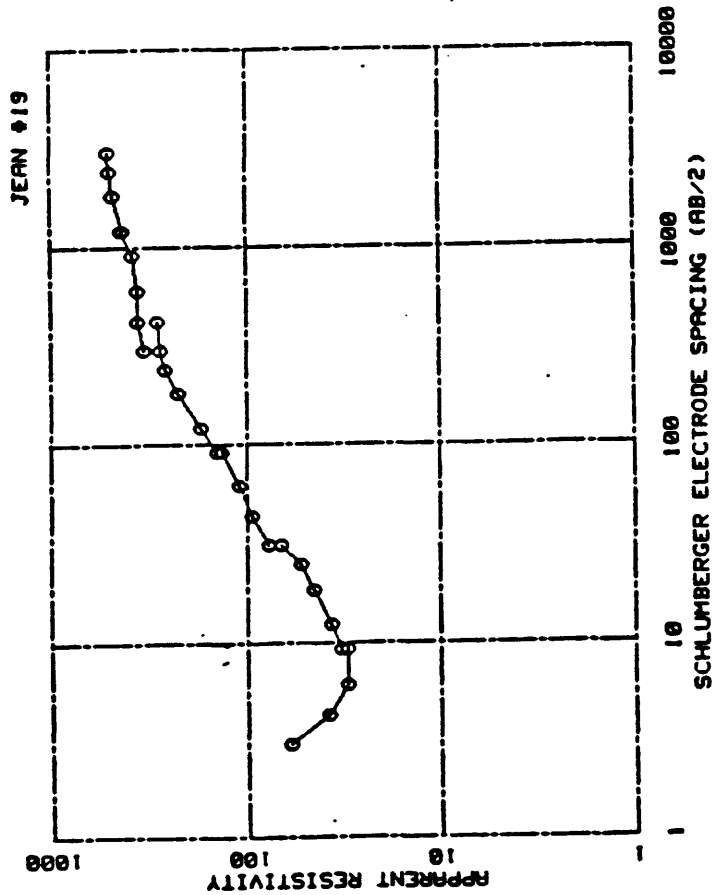
DEPTH	RESISTIVITY	DEPTH	RESISTIVITY
1.07	500.22	33.74	237.22
1.57	530.37	49.92	260.96
2.30	356.27	72.60	290.41
3.37	133.96	106.60	327.04
4.95	50.54	156.50	222.50
7.27	59.13	229.04	243.40
10.67	87.59	337.35	263.90
15.66	134.41	495.16	205.33
22.90	107.70	726.00	325.19
		999999.00	300.90



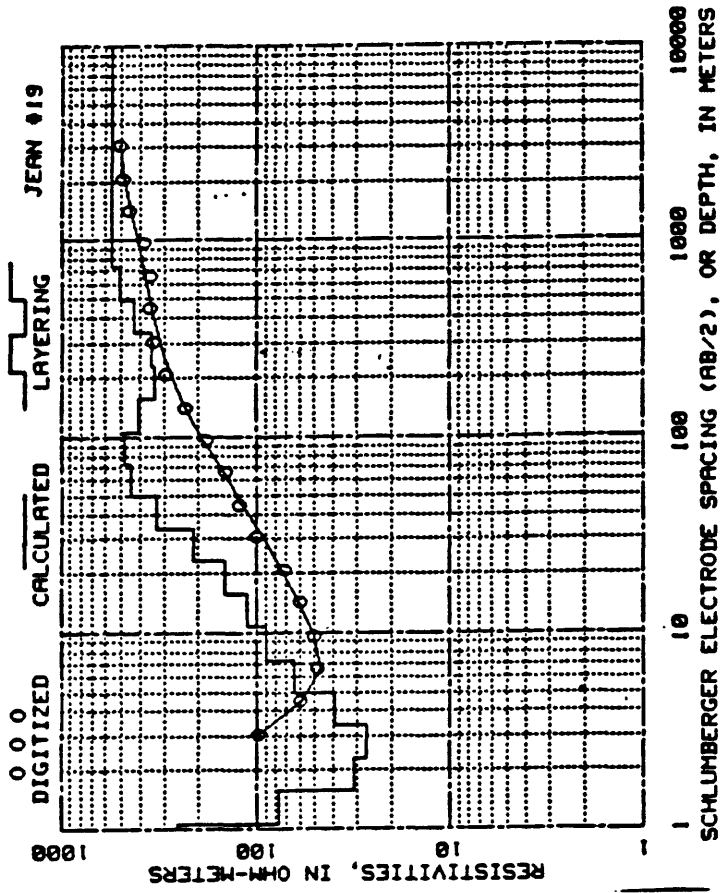
AB/2	OBSERVED RESISTIVITY	AB/2	OBSERVED RESISTIVITY
3.05	148.00	91.44	231.00
4.27	102.00	121.92	275.00
6.10	63.00	182.00	392.00
9.14	52.00	243.04	475.00
12.19	50.00	304.00	540.00
18.29	53.00	364.00	570.00
24.30	66.00	426.72	810.00
30.40	80.00	607.60	520.00
38.40	84.00	914.40	455.00
42.67	114.00	1219.20	415.00
68.96	160.00	1820.00	440.00
91.44	250.00	2430.40	400.00
		3040.00	540.00



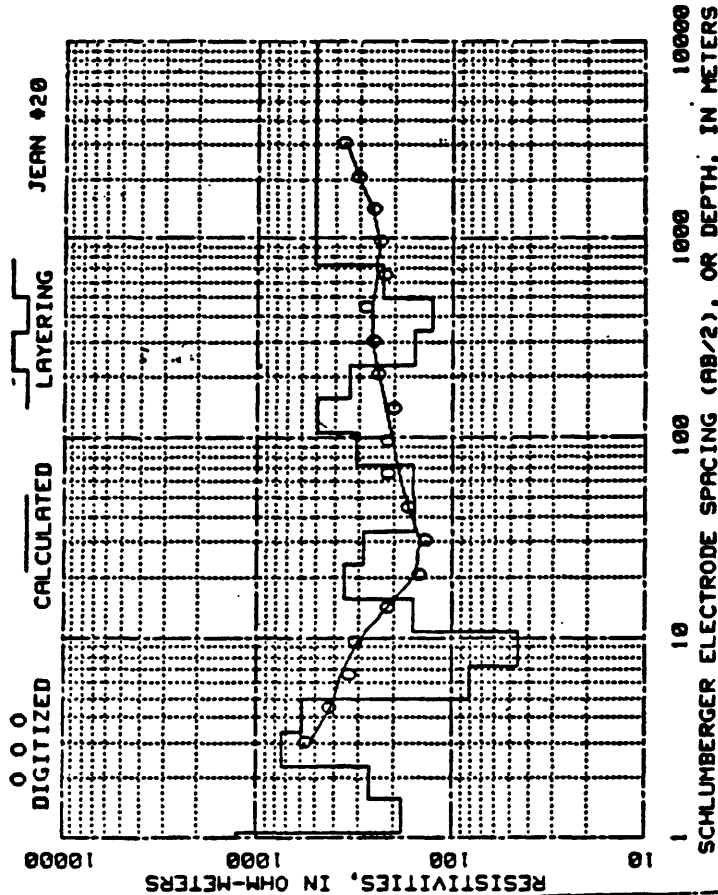
DEPTH	RESISTIVITY	DEPTH	RESISTIVITY
1.07	264.95	33.74	496.01
1.37	189.64	49.52	923.23
2.30	94.34	72.00	1466.19
3.37	76.06	106.60	1740.31
4.95	27.01	156.50	1414.90
7.27	23.09	229.04	717.06
10.67	43.01	337.35	267.70
15.66	102.57	495.16	152.39
22.90	230.60	726.00	260.46
		9999999.00	767.90



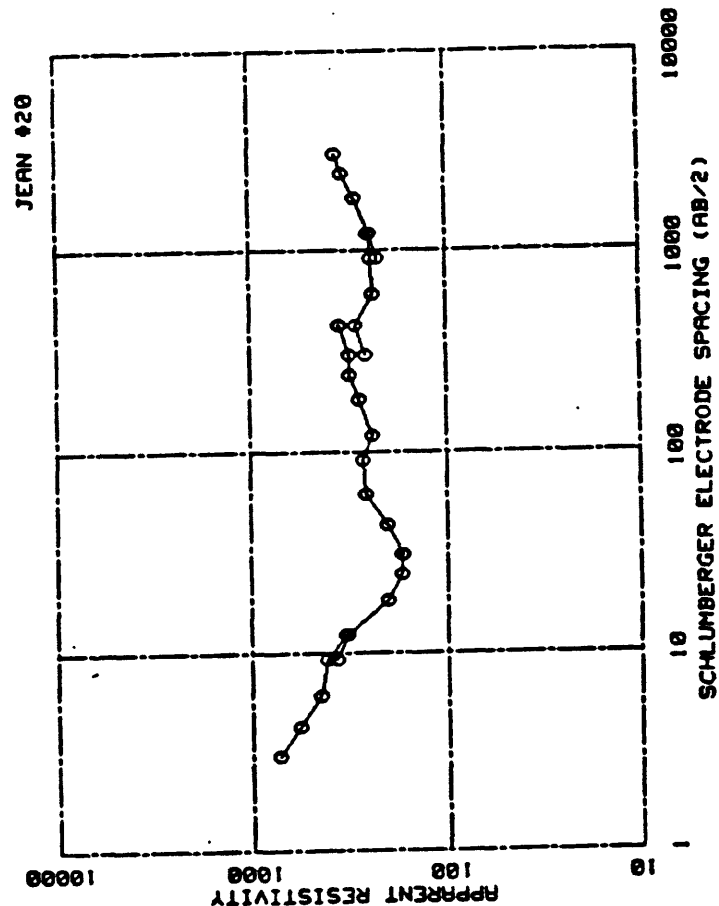
AB/2	OBSERVED RESISTIVITY	AB/2	OBSERVED RESISTIVITY
3.85	59.50	121.52	173.00
4.27	38.00	182.00	225.00
6.10	38.00	243.04	260.00
9.14	38.00	304.00	280.00
12.19	32.50	426.72	290.00
18.29	36.50	584.00	336.00
24.38	44.50	826.72	360.00
38.48	52.00	1114.00	360.00
56.48	66.00	1519.20	300.00
82.67	70.00	2119.20	435.00
118.96	95.00	2920.00	427.00
171.44	116.00	4020.00	400.00
248.96	137.00	5520.00	300.00
356.96	145.00	7620.00	310.00



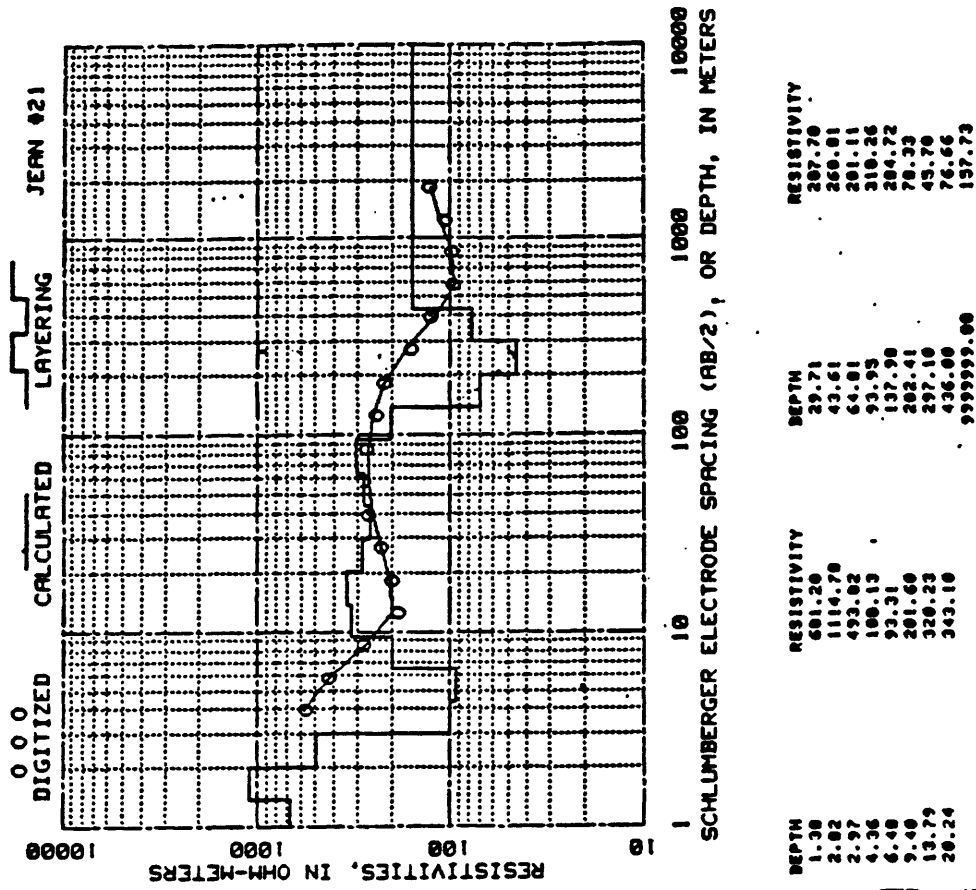
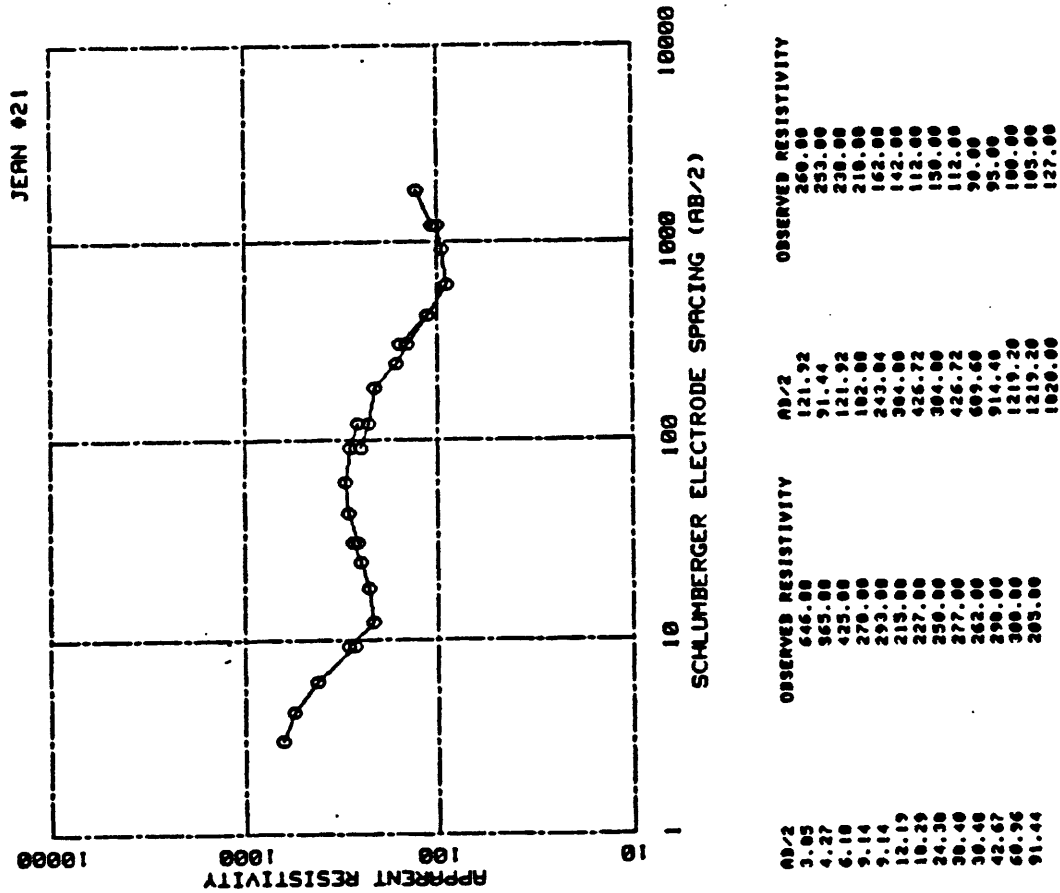
DEPTH	RESISTIVITY	DEPTH	RESISTIVITY
1.07	250.10	33.74	215.05
1.97	76.95	49.52	329.40
2.30	31.61	72.60	447.21
3.37	26.91	106.60	475.90
4.95	39.19	156.50	403.00
7.27	63.72	229.04	337.40
10.67	89.97	337.95	349.47
15.66	112.32	495.16	426.00
22.90	146.39	726.00	509.63
		999.999.00	560.07

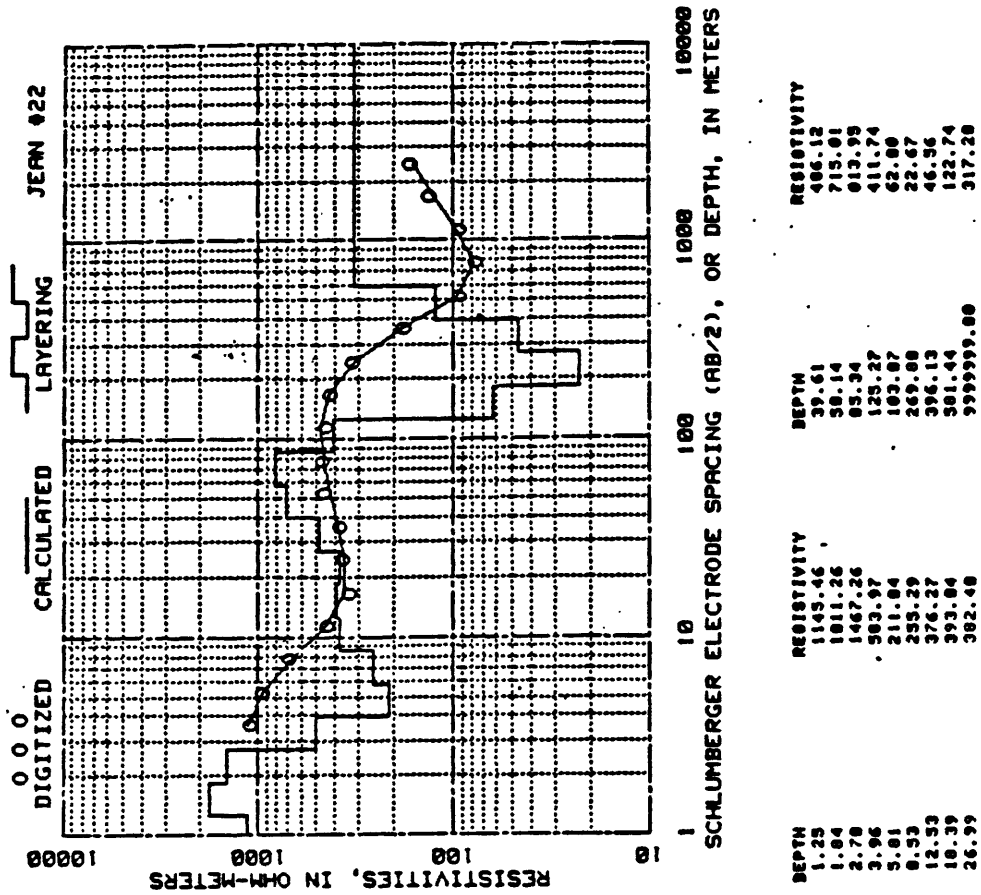
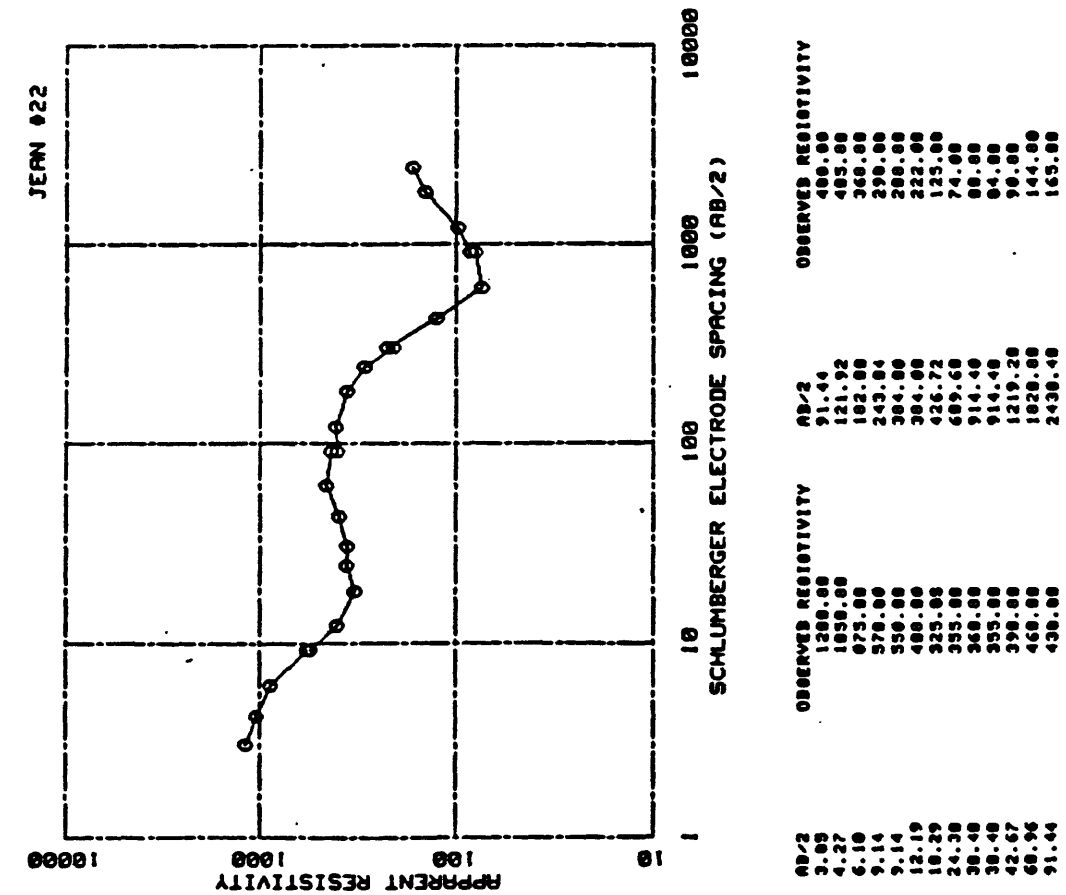


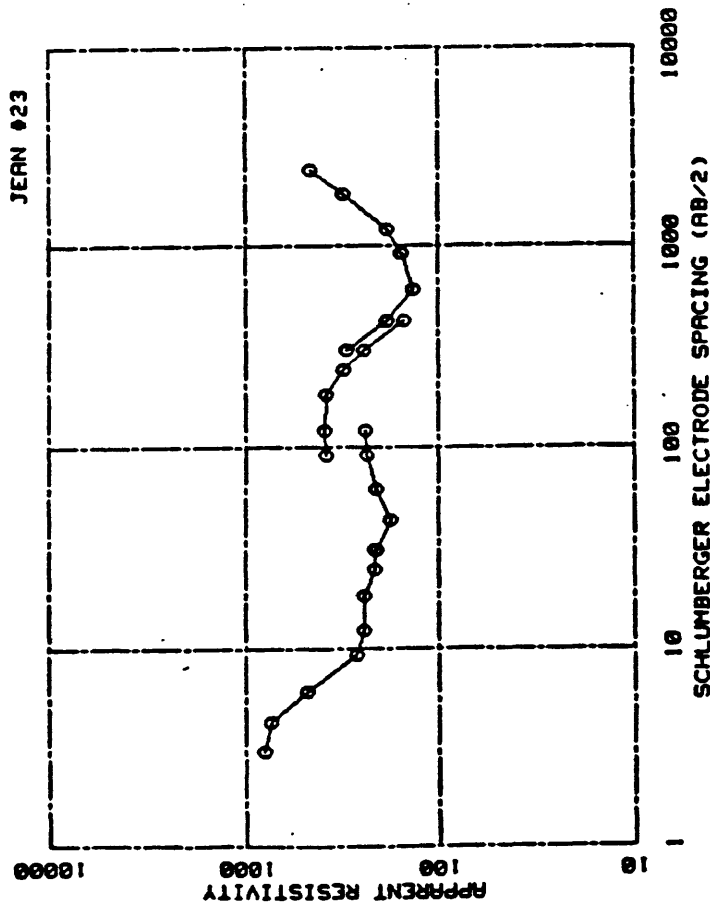
DEPTH	RESISTIVITY	DEPTH	RESISTIVITY
1.07	1249.67	33.74	200.60
1.37	101.00	49.52	195.51
2.30	262.05	72.60	190.72
3.37	750.51	106.60	315.49
4.95	579.35	156.50	409.21
7.27	81.37	229.04	348.63
10.67	45.23	337.35	195.54
15.66	159.24	495.16	120.63
22.90	357.21	726.00	220.51
		999999.00	500.49



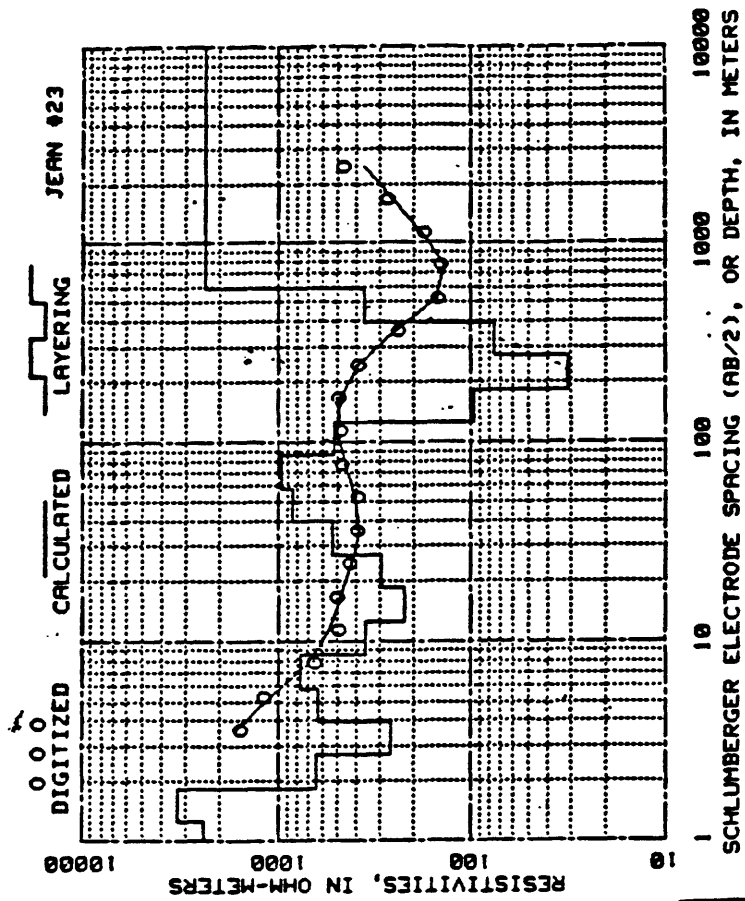
AB/2	OBSERVED RESISTIVITY	AB/2	OBSERVED RESISTIVITY
3.05	730.00	121.92	240.00
4.27	570.00	102.00	200.00
6.10	450.00	243.04	315.00
9.14	420.00	304.00	315.00
12.19	335.00	426.72	350.00
9.14	375.00	304.00	260.00
12.19	325.00	426.72	290.00
10.20	205.00	609.60	235.00
24.30	173.00	914.40	240.00
30.40	173.00	1219.20	250.00
30.40	170.00	914.40	235.00
42.67	203.00	1219.20	245.00
60.96	260.00	1020.00	290.00
91.44	270.00	2430.40	337.00
	265.00	3040.00	366.00



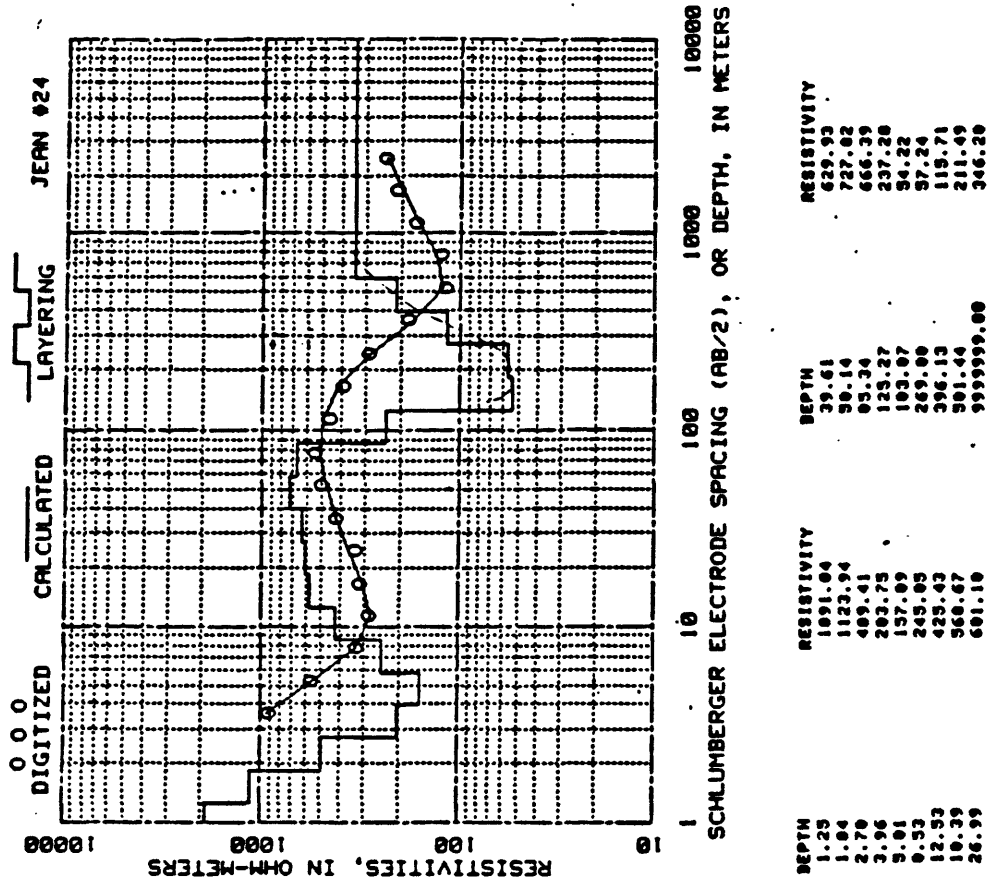
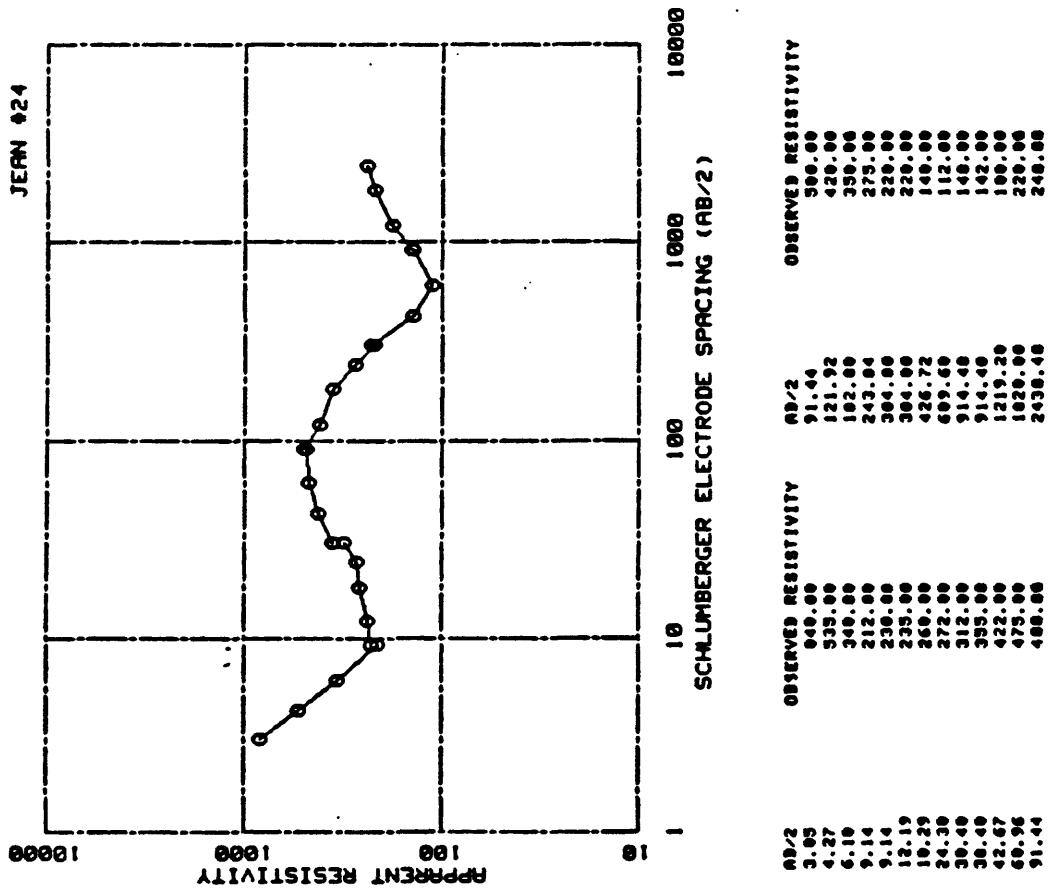


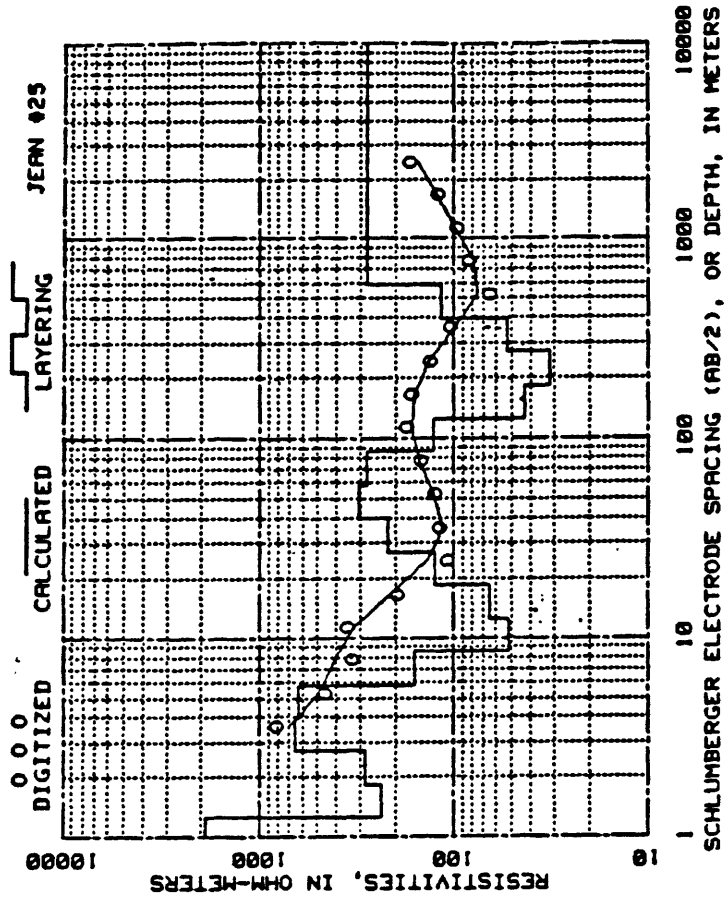


AB/2	OBSERVED RESISTIVITY	AB/2	OBSERVED RESISTIVITY
3.55	880.88	91.44	389.00
4.27	740.00	121.92	390.00
6.10	400.00	102.00	305.00
9.14	270.00	243.04	315.00
9.14	270.00	304.00	244.00
12.19	245.00	426.72	150.00
10.29	245.00	364.00	305.00
24.30	215.00	426.72	106.00
30.40	215.00	609.60	136.00
30.40	210.00	914.40	154.00
42.67	100.00	914.40	156.00
60.96	230.00	1219.20	105.00
91.44	1020.00	1020.00	315.00
121.92	240.00	2430.40	478.88

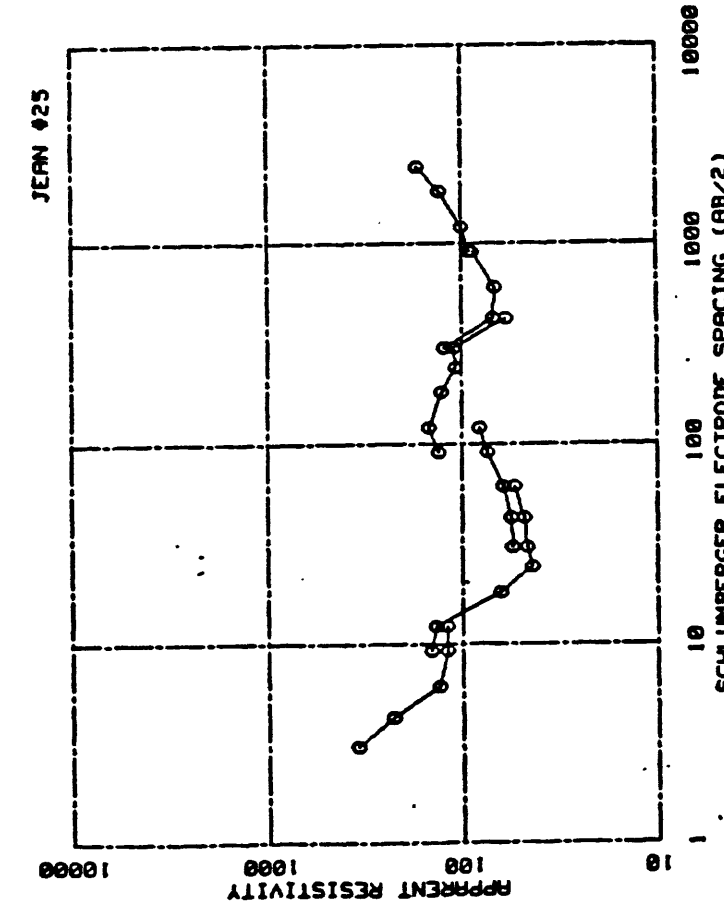


DEPTH	RESISTIVITY	DEPTH	RESISTIVITY
1.25	2451.94	39.61	527.21
1.04	3299.10	58.14	856.33
2.70	646.35	85.34	966.94
3.96	265.35	125.27	523.66
5.81	620.43	103.07	93.92
0.52	771.03	269.00	31.07
12.53	356.02	396.13	74.97
18.39	225.53	581.44	368.35
26.99	296.02	999999.00	2370.10

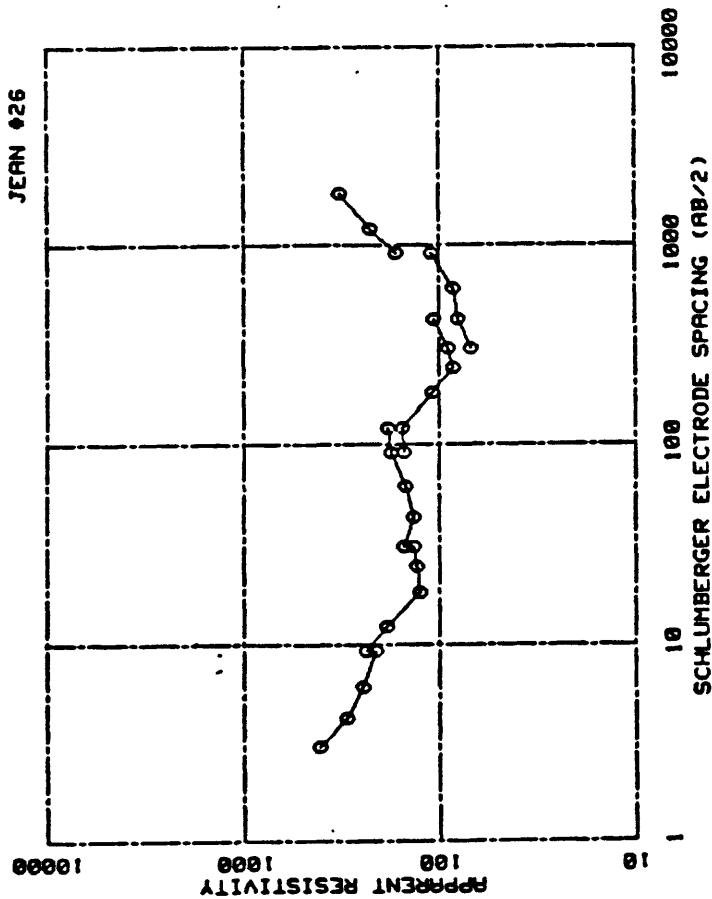




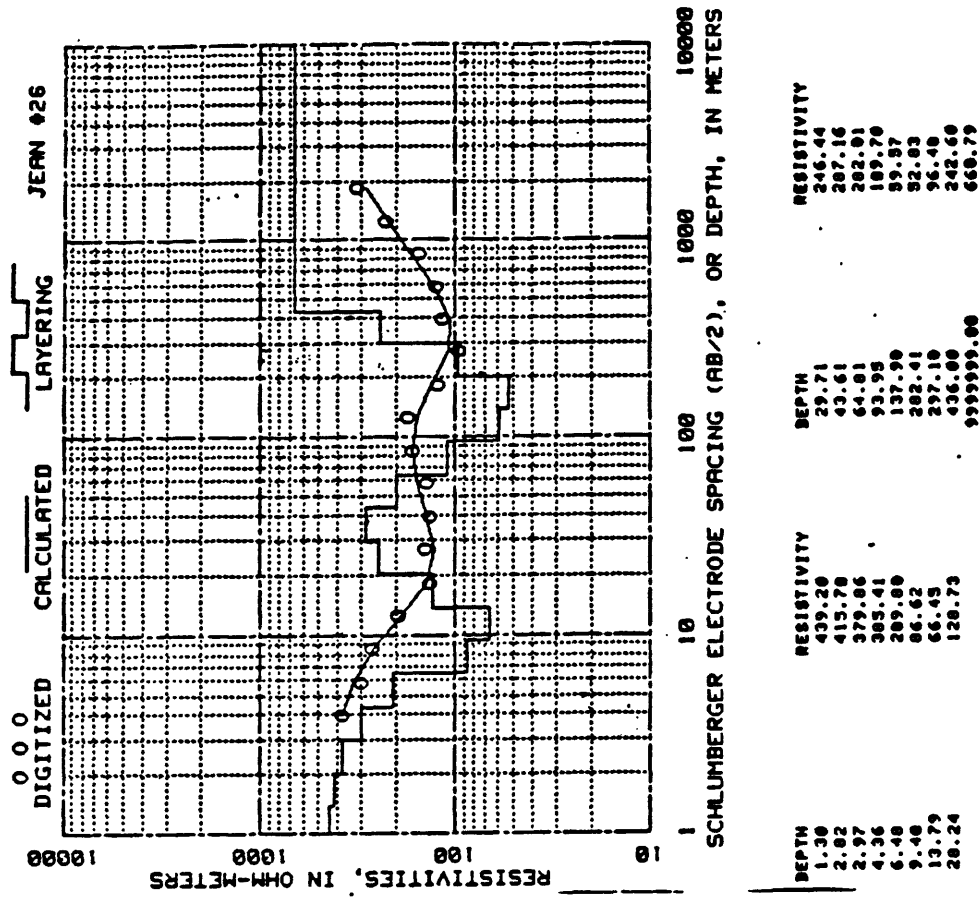
AB/2	OBSERVED RESISTIVITY	AB/2	OBSERVED RESISTIVITY
3.05	346.00	91.44	74.00
4.37	229.00	121.92	82.00
6.10	132.00	91.44	133.00
9.14	120.00	121.92	147.00
12.19	120.00	102.00	120.00
9.14	145.00	243.04	100.00
12.19	130.00	304.00	110.00
10.29	64.00	426.72	85.20
24.38	44.00	304.00	122.00
30.48	46.30	426.72	69.00
42.67	40.00	609.60	67.00
68.96	34.00	914.40	87.00
30.48	35.00	1219.20	91.00
42.67	56.00	1020.00	130.00
60.96	61.00	2430.40	170.00



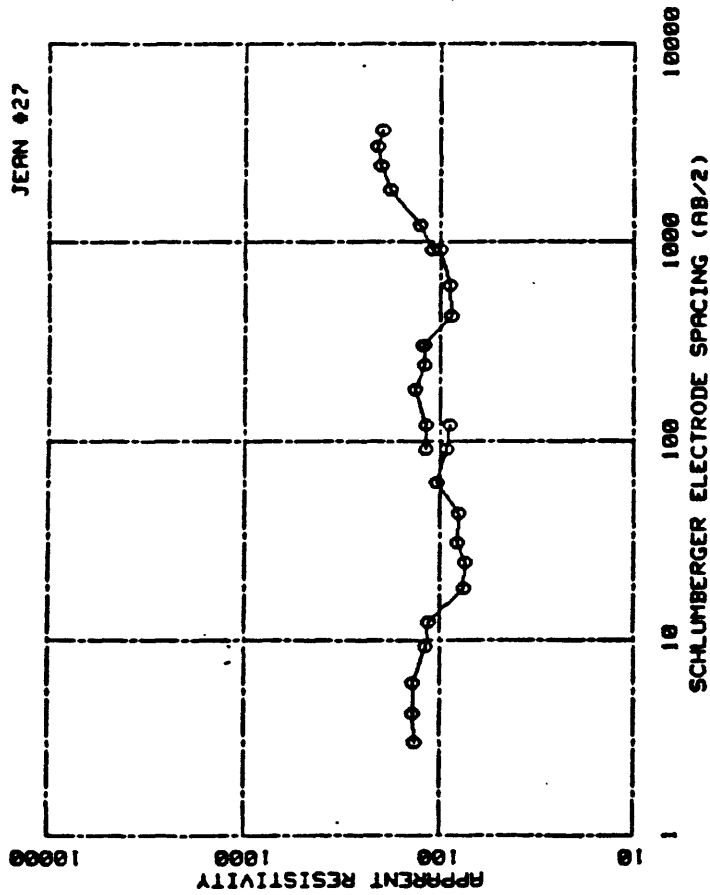
DEPTH	RESISTIVITY	DEPTH	RESISTIVITY
1.25	1909.31	39.61	219.61
1.04	237.15	50.14	310.24
2.70	206.61	85.34	202.30
3.96	659.67	125.27	127.66
5.01	624.20	103.87	42.66
0.53	160.50	269.00	31.77
10.39	81.76	396.13	92.30
26.99	65.45	501.44	116.40
	124.00	999999.00	279.29



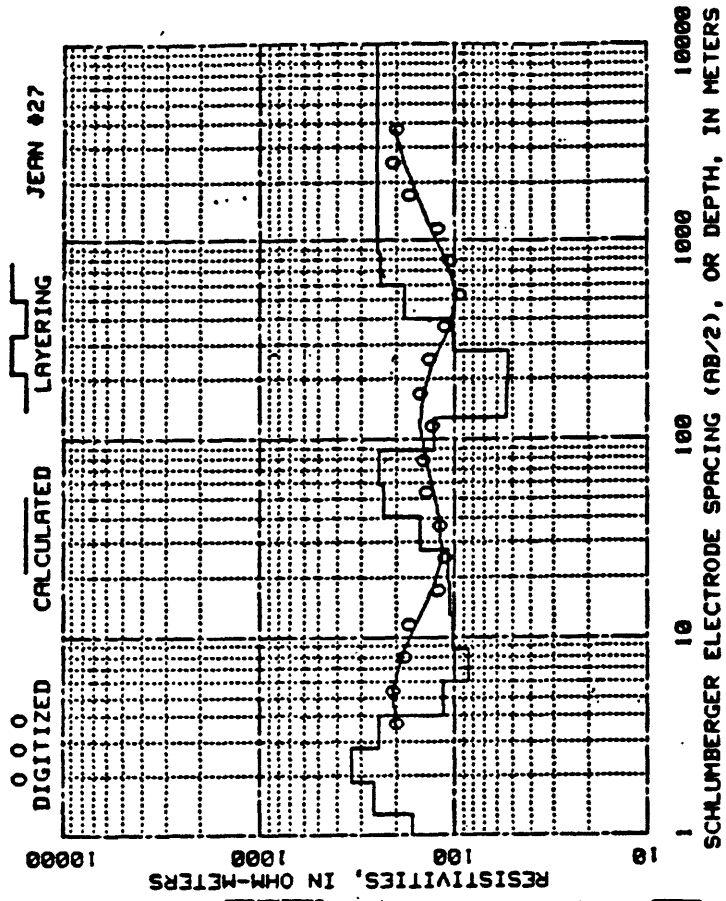
AB/2	OBSERVED RESISTIVITY	AB/2	OBSERVED RESISTIVITY
3.05	405.00	121.92	182.00
4.27	295.00	91.44	150.00
6.10	245.00	121.92	134.00
9.14	210.00	102.00	107.00
12.19	235.00	84.00	84.00
16.29	185.00	304.00	90.00
24.30	125.00	426.72	105.00
36.40	129.00	304.00	60.00
50.40	134.00	426.72	80.00
62.67	150.00	609.60	04.00
68.96	136.00	914.40	110.00
91.44	140.00	914.40	165.00
	175.00	1219.20	223.00
		1020.00	320.00



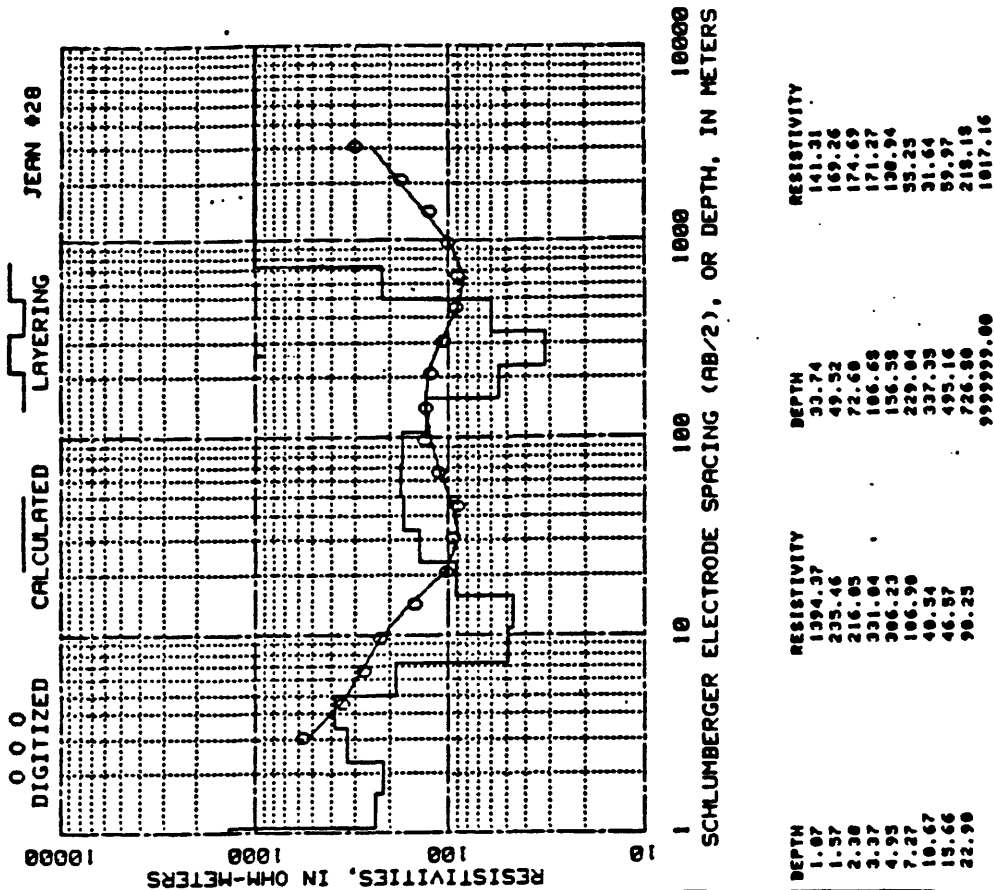
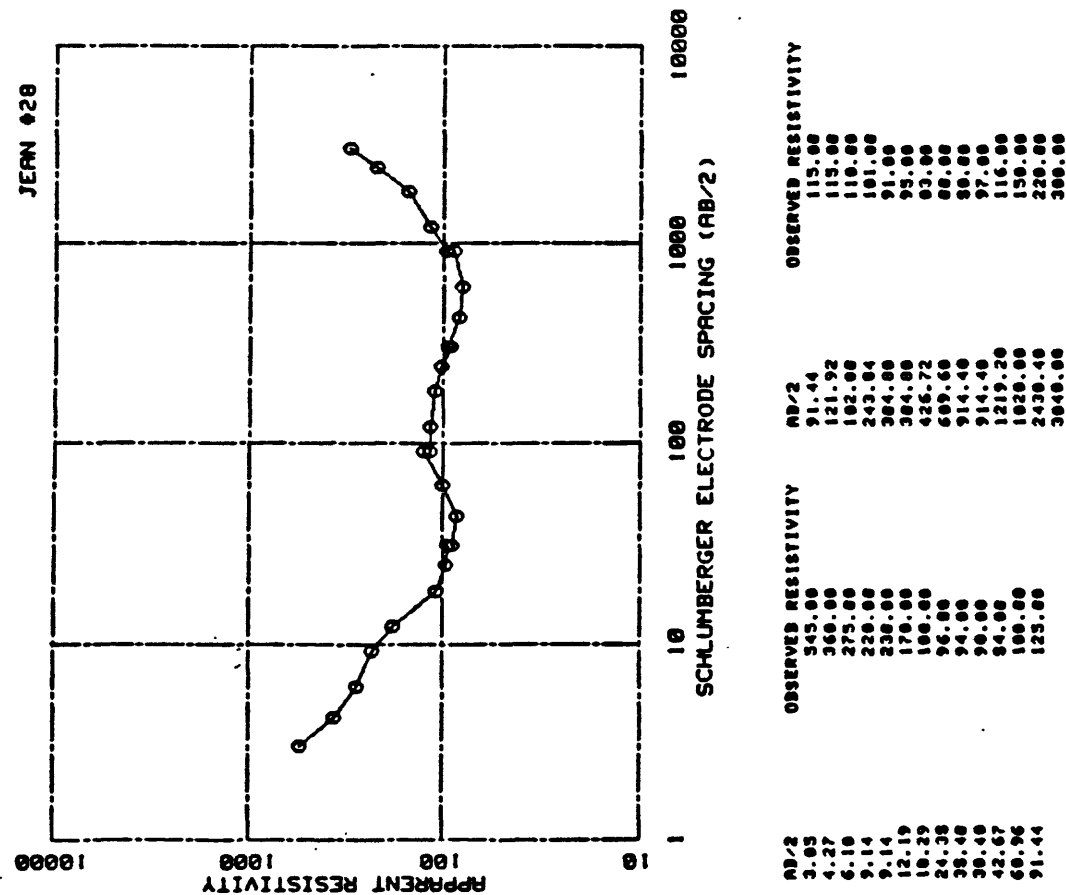
DEPTH	RESISTIVITY	DEPTH	RESISTIVITY
1.30	439.20	29.71	246.44
2.02	415.70	43.61	207.16
2.97	379.06	64.01	202.01
4.36	305.41	93.95	189.70
6.40	289.00	137.90	59.57
9.40	86.62	202.41	52.03
13.79	66.45	297.10	96.40
20.24	120.73	436.00	242.60
		999999.00	660.79

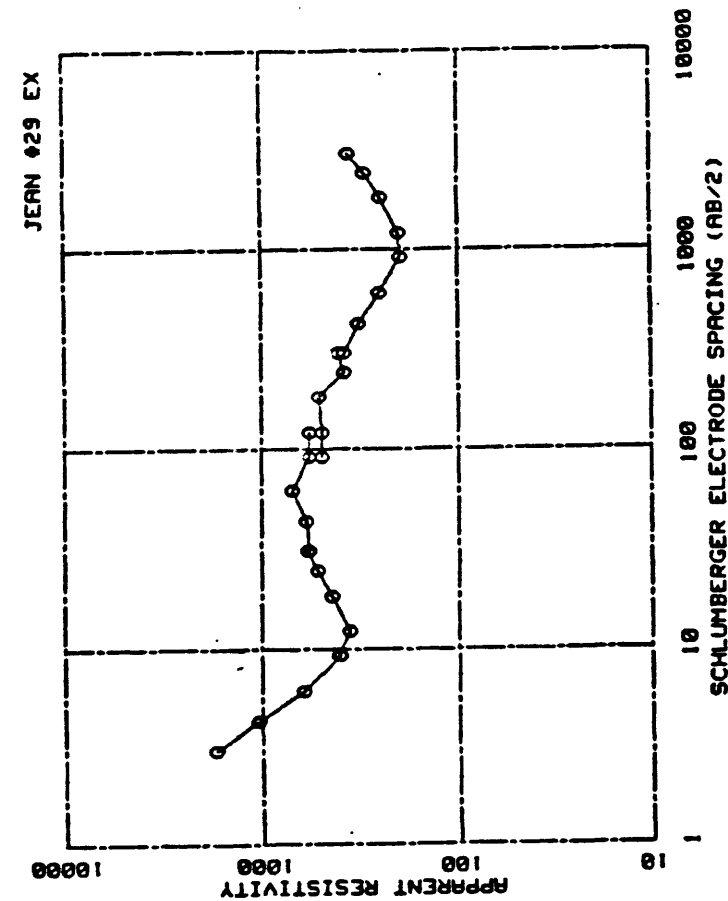


AB/2	OBSERVED RESISTIVITY	AB/2	OBSERVED RESISTIVITY
3.65	135.00	91.44	110.00
4.27	137.00	131.92	110.00
6.10	137.00	182.84	136.00
9.14	118.00	243.84	128.00
9.14	118.00	384.00	128.00
12.19	114.00	384.00	122.00
16.29	76.00	426.72	97.00
24.38	74.00	609.60	90.00
30.48	81.00	914.40	100.00
30.48	82.00	914.40	110.00
42.67	80.00	1219.20	120.00
60.96	103.00	1820.00	102.00
91.44	92.00	2438.40	205.00
121.92	90.00	3848.00	218.00
		3657.60	202.00

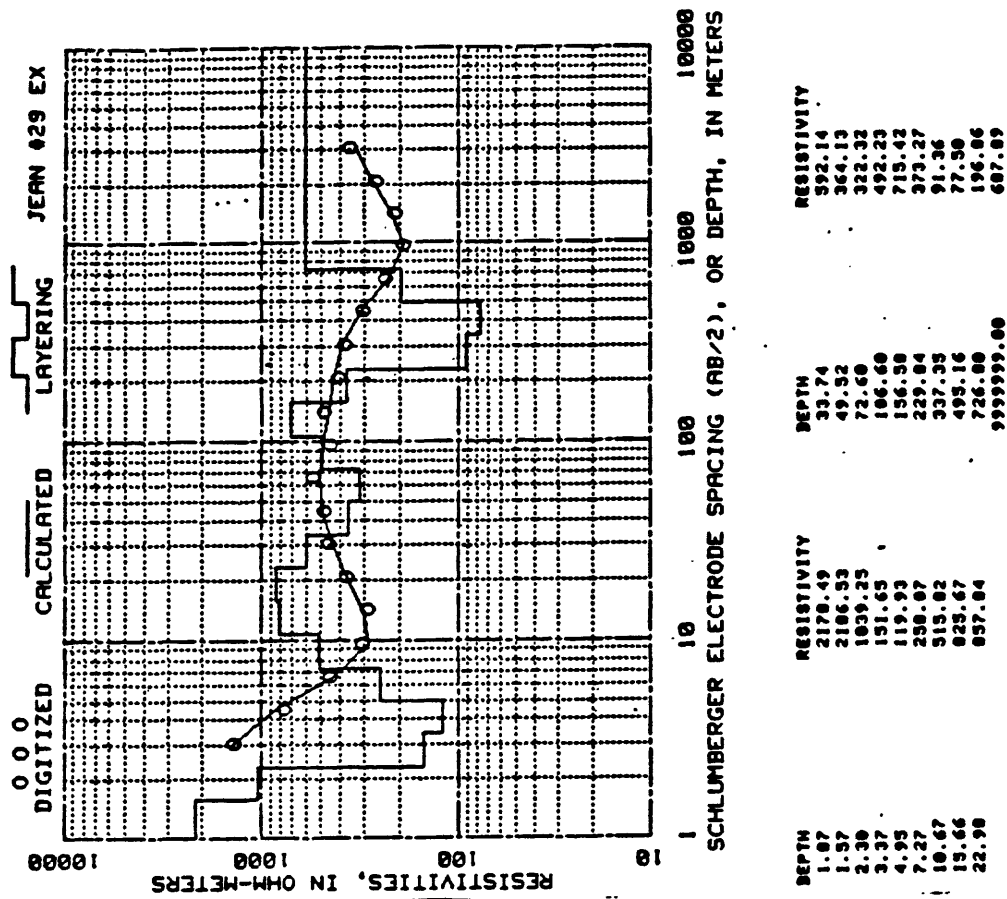


DEPTH	RESISTIVITY	DEPTH	RESISTIVITY
1.20	163.78	46.40	149.60
1.00	259.50	59.42	231.50
2.76	335.84	87.22	244.94
4.03	245.71	120.02	120.00
5.94	114.92	187.90	93.39
9.72	83.00	278.00	93.16
12.00	102.27	404.02	101.09
16.79	105.72	594.20	101.27
27.50	107.33	872.16	241.61
		9999999.00	249.29

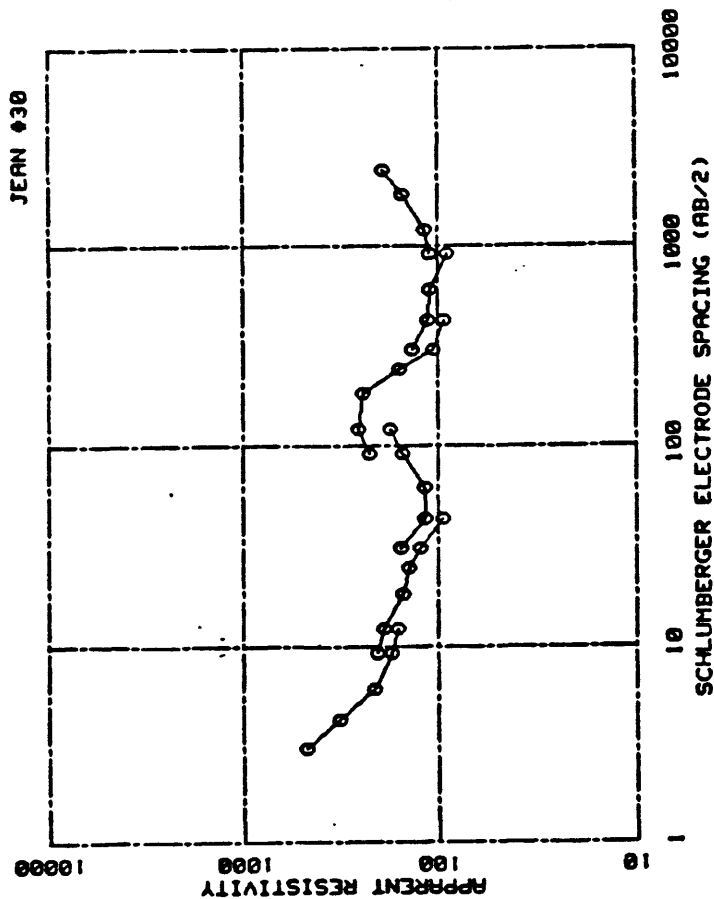




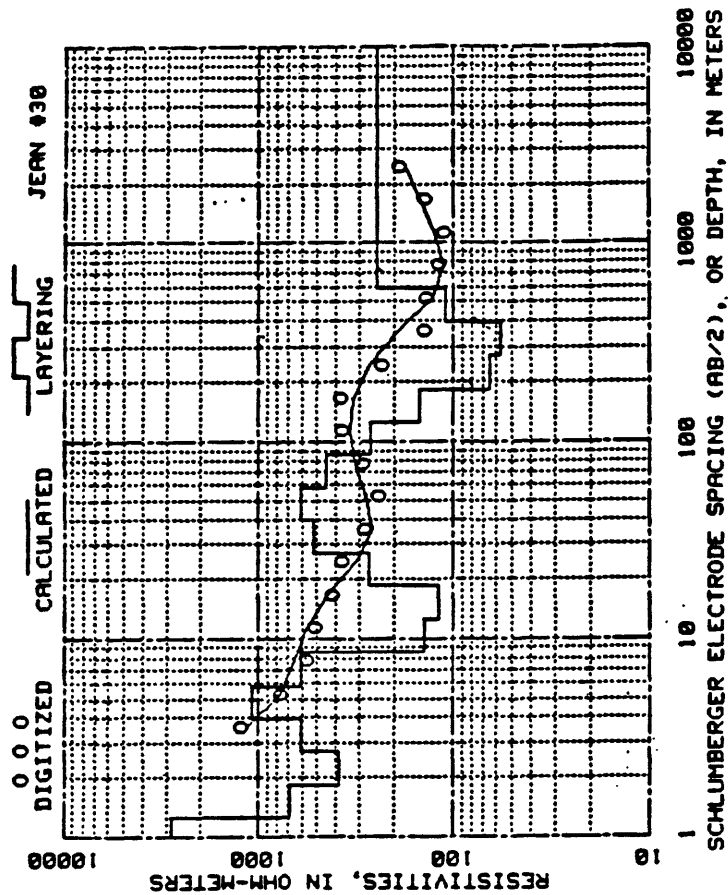
AB/2	OBSERVED RESISTIVITY	AB/2	OBSERVED RESISTIVITY
3.05	1730.00	121.92	570.00
4.27	1050.00	91.44	490.00
6.10	623.00	121.92	490.00
9.14	400.00	102.00	310.00
12.19	400.00	243.84	300.00
16.29	355.00	304.00	400.00
24.38	440.00	304.00	300.00
30.48	520.00	426.72	320.00
42.67	570.00	609.60	250.00
60.96	570.00	914.40	190.00
91.44	570.00	1219.20	200.00
		1020.00	245.00
		2430.40	295.00
		3040.00	355.00



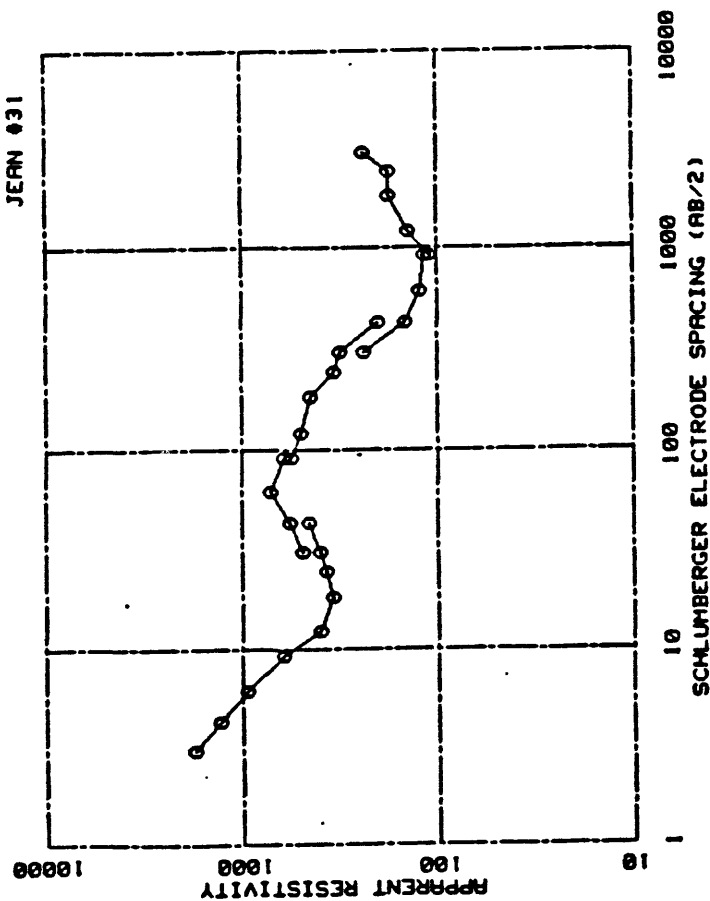
DEPTH	RESISTIVITY	DEPTH	RESISTIVITY
1.07	2170.49	33.74	392.14
1.57	2106.53	49.52	364.13
2.30	1039.25	72.60	322.32
3.37	151.65	106.60	492.23
4.95	119.93	156.50	715.42
7.27	250.07	229.04	373.27
10.67	515.02	337.35	91.36
15.66	825.67	495.16	77.50
22.90	057.04	726.00	196.06
		9999999.00	607.09



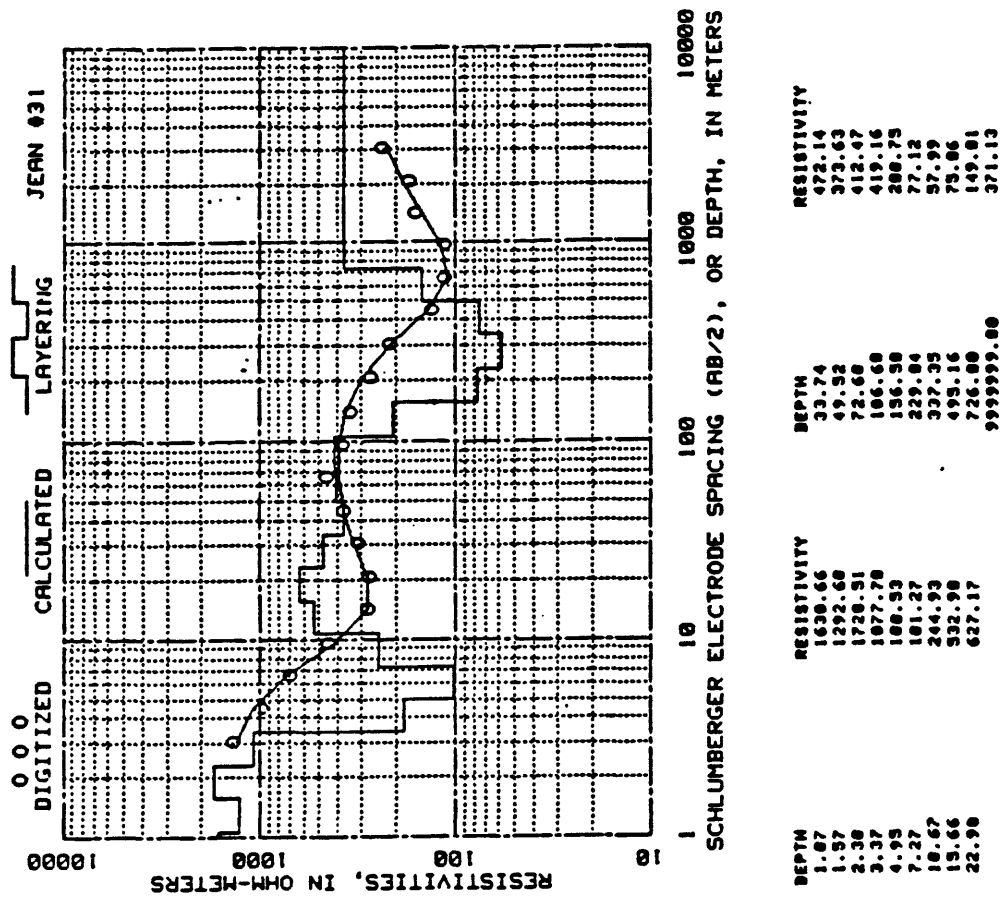
AB/2	OBSERVED RESISTIVITY	AB/2	OBSERVED RESISTIVITY
3.85	471.00	121.92	175.00
4.27	320.00	91.44	235.00
6.10	210.00	121.92	257.00
9.14	172.00	182.00	240.00
12.19	160.00	243.04	157.00
9.14	203.00	304.00	106.00
12.19	100.00	426.72	92.00
10.29	150.00	304.00	135.00
24.30	140.00	426.72	112.00
30.40	120.00	609.60	110.00
30.40	95.00	914.40	90.00
30.40	42.67	135.00	110.00
42.67	116.00	1219.20	115.00
60.96	113.00	1020.00	150.00
91.44	152.00	2430.40	109.00

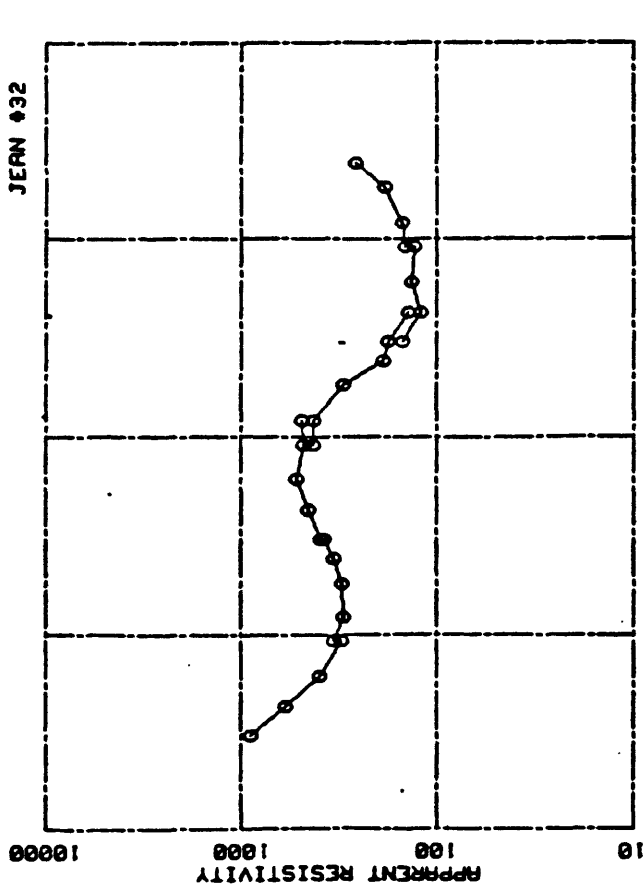


DEPTH	RESISTIVITY	DEPTH	RESISTIVITY
1.25	2021.37	39.61	521.40
1.94	693.57	56.14	610.37
2.70	304.00	83.34	440.93
3.96	609.70	123.27	267.79
5.81	1000.10	183.07	147.49
8.53	607.10	269.00	64.70
12.53	150.07	396.13	56.33
10.39	110.91	501.44	109.07
26.99	272.56	999999.00	246.60

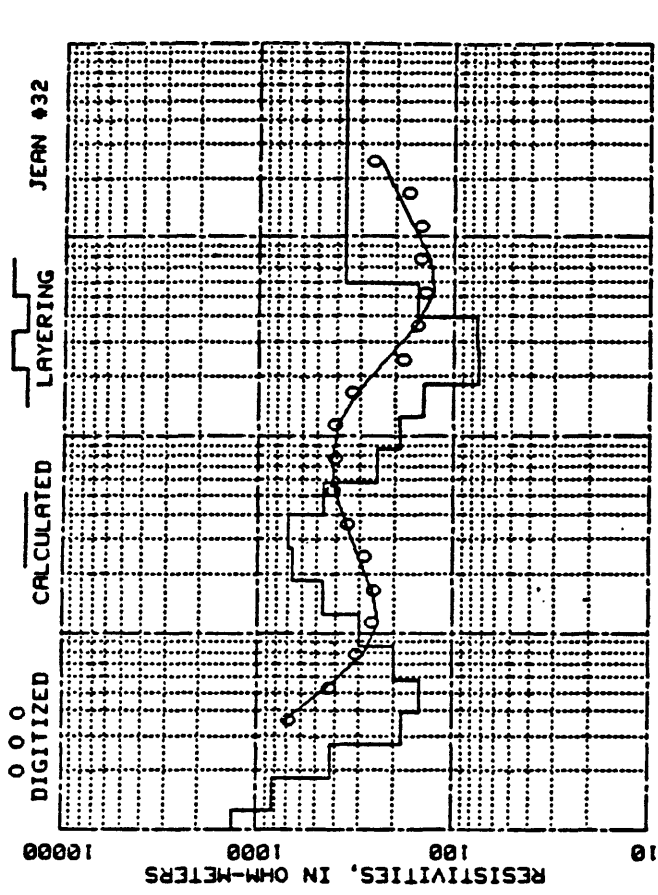


AB/2	OBSERVED RESISTIVITY	AB/2	OBSERVED RESISTIVITY
3.05	1776.00	91.44	565.00
4.27	1320.00	121.92	565.00
6.10	950.00	162.00	450.00
9.14	620.00	243.04	340.00
12.19	400.00	304.00	315.00
18.29	345.00	426.72	280.00
24.38	370.00	584.00	235.00
38.48	400.00	689.60	145.00
42.67	460.00	914.40	123.00
58.48	492.00	914.40	115.00
62.67	570.00	1219.20	110.30
68.96	715.00	1620.00	140.00
91.44	610.00	2430.00	175.00
		3040.00	177.00
			235.00

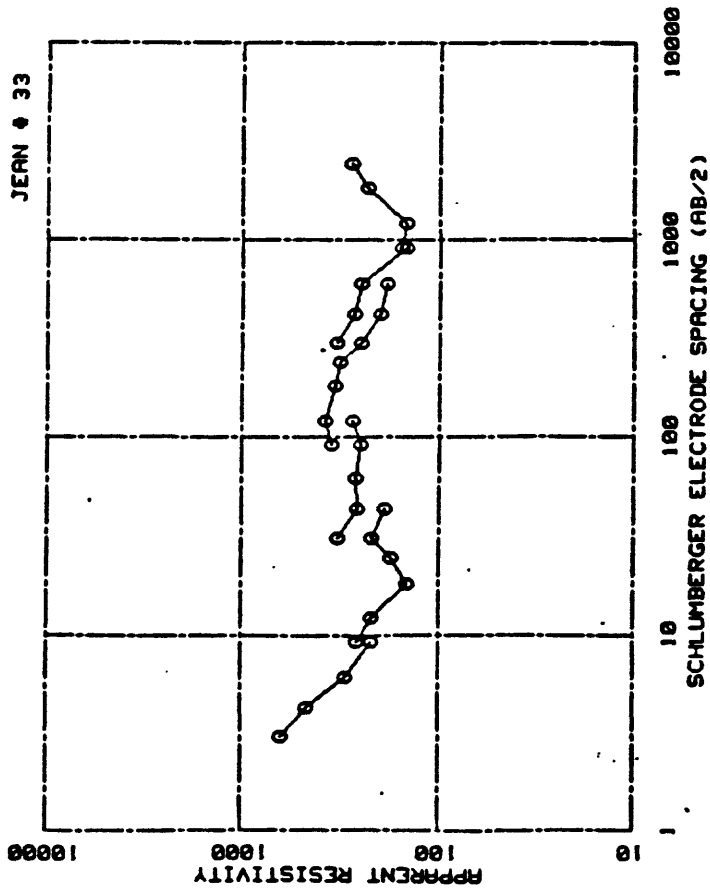




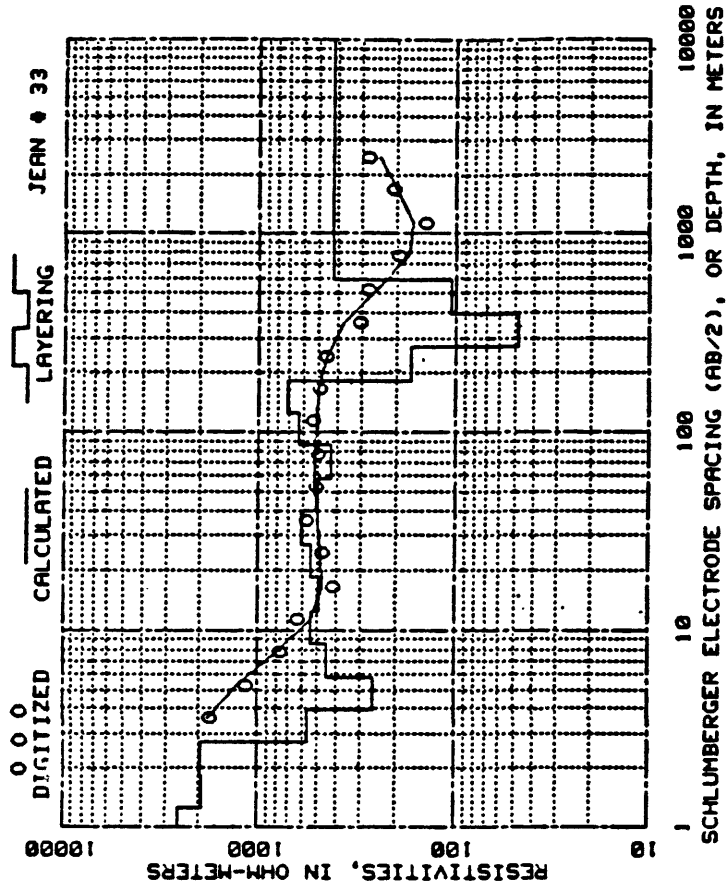
AB/2	OBSERVED RESISTIVITY	AB/2	OBSERVED RESISTIVITY
3.85	900.00	91.44	430.00
3.27	600.00	121.92	430.00
4.27	400.00	162.00	302.00
6.10	310.00	243.04	190.00
9.14	300.00	304.00	100.00
12.19	300.00	426.72	140.00
16.29	307.00	504.00	132.00
24.36	330.00	426.72	120.00
36.48	300.00	609.60	135.00
50.40	390.00	914.40	130.00
68.96	435.00	914.40	145.00
91.44	520.00	1219.20	152.00
121.92	400.00	1620.00	104.60
	495.00	2430.40	262.00



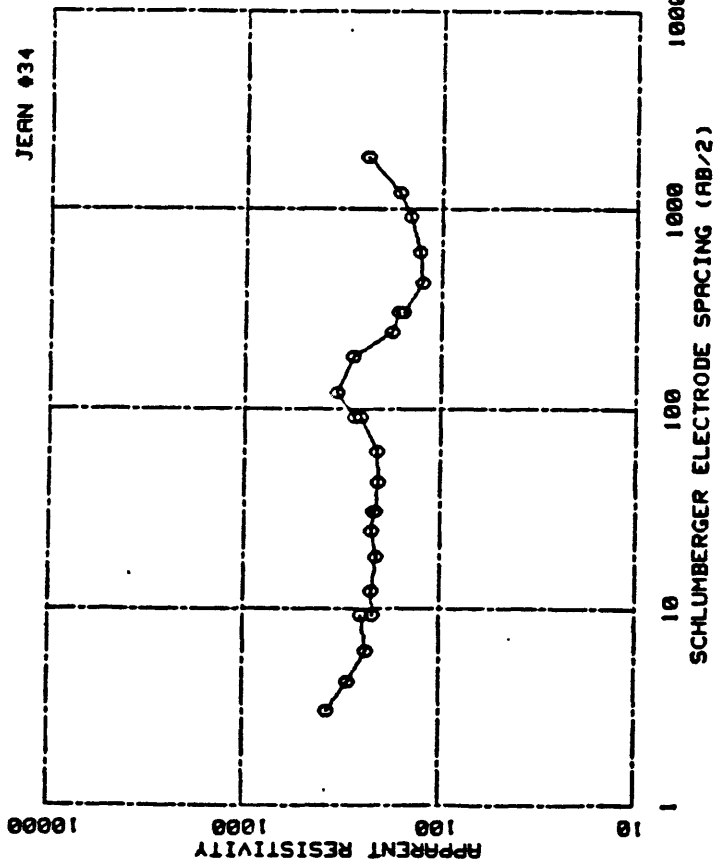
AB/2	OBSERVED RESISTIVITY	AB/2	OBSERVED RESISTIVITY
3.85	900.00	91.44	430.00
3.27	600.00	121.92	430.00
4.27	400.00	162.00	302.00
6.10	310.00	243.04	190.00
9.14	300.00	304.00	100.00
12.19	300.00	426.72	140.00
16.29	307.00	504.00	132.00
24.36	330.00	426.72	120.00
36.48	300.00	609.60	135.00
50.40	390.00	914.40	130.00
68.96	435.00	914.40	145.00
91.44	520.00	1219.20	152.00
121.92	400.00	1620.00	104.60
	495.00	2430.40	262.00



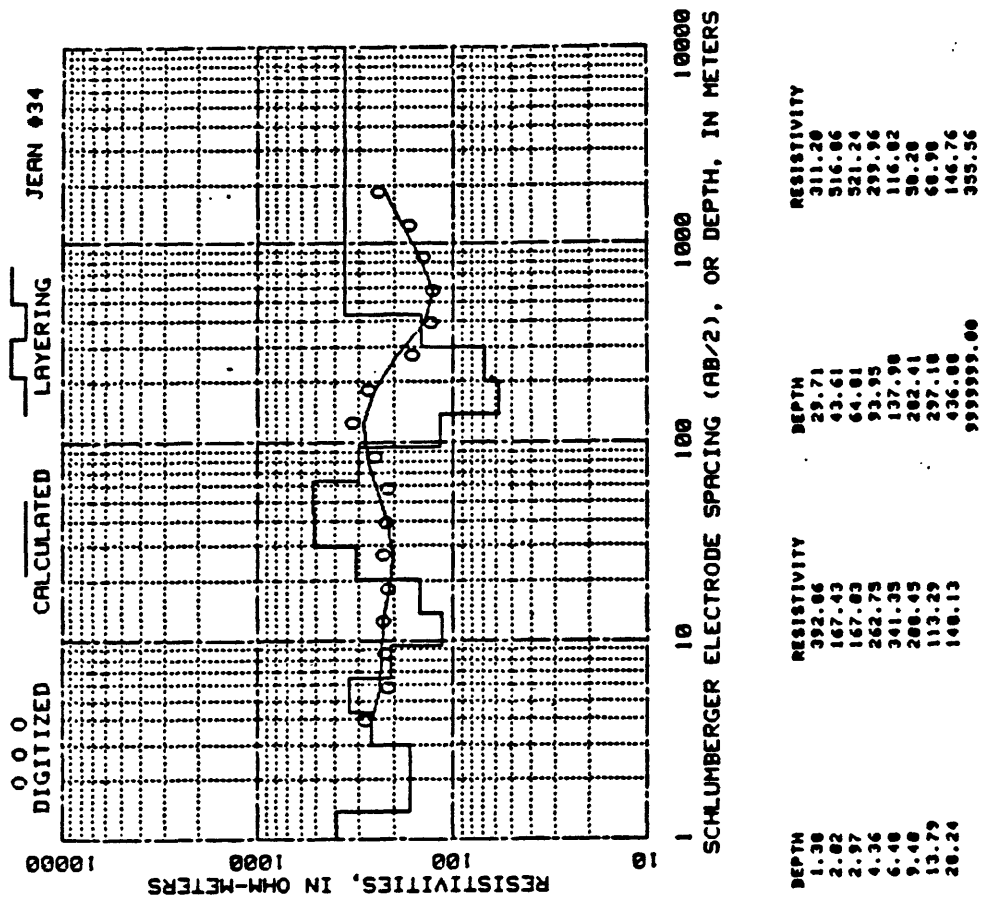
AB/2	OBSERVED RESISTIVITY	AB/2	OBSERVED RESISTIVITY
3.85	638.00	91.44	350.00
4.27	465.00	121.92	300.00
6.18	295.00	192.00	340.00
9.14	228.00	243.84	320.00
9.14	268.00	304.00	250.00
12.19	228.00	426.72	200.00
18.29	145.00	609.60	185.00
24.38	174.00	304.00	335.00
38.48	228.00	426.72	268.00
42.67	198.00	609.60	250.00
38.48	325.00	914.40	140.00
42.67	262.00	1219.20	156.00
68.96	265.00	140.00	140.00
91.44	250.00	1828.00	231.00
121.92	275.00	2438.40	203.00



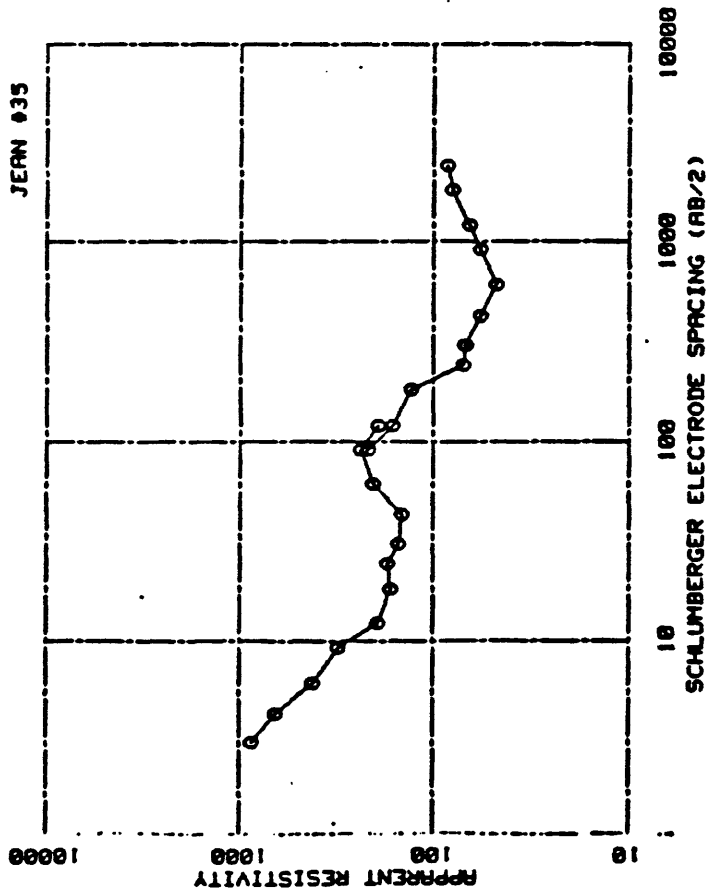
DEPTH	RESISTIVITY	DEPTH	RESISTIVITY
1.25	2591.05	39.61	603.76
1.84	1937.48	58.14	498.14
3.70	1903.17	85.34	428.46
3.96	558.33	125.27	624.27
5.81	261.86	183.97	720.96
8.53	445.54	269.08	168.70
12.93	548.74	396.13	47.96
18.39	498.66	501.44	185.55
26.99	537.68	999999.00	427.73



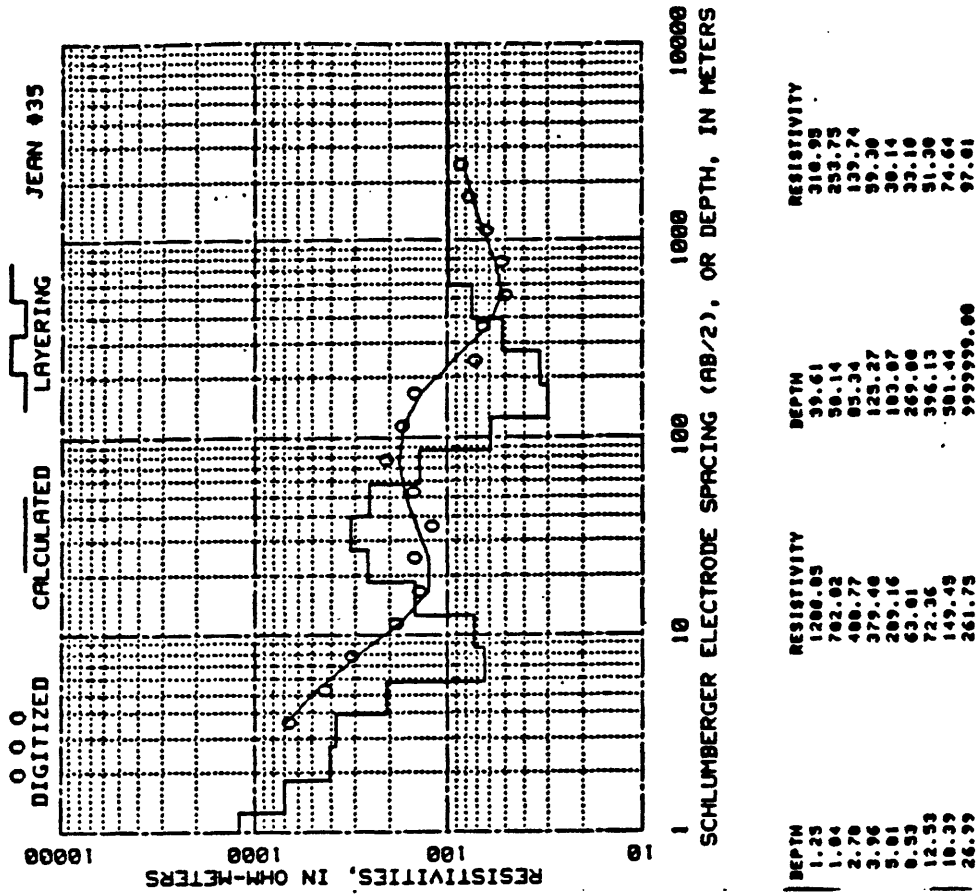
AB/2	OBSERVED RESISTIVITY	AB/2	OBSERVED RESISTIVITY
3.09	372.00	91.44	255.00
4.27	298.00	91.44	277.00
6.10	235.00	121.92	338.00
9.14	250.00	182.00	200.00
9.14	221.00	243.04	188.00
12.19	224.00	304.00	165.00
16.29	212.00	304.00	150.00
24.38	225.00	426.72	124.00
30.48	210.00	609.60	130.00
30.48	215.00	914.40	145.00
42.67	209.00	1219.20	165.00
60.96	210.00	1820.00	242.00



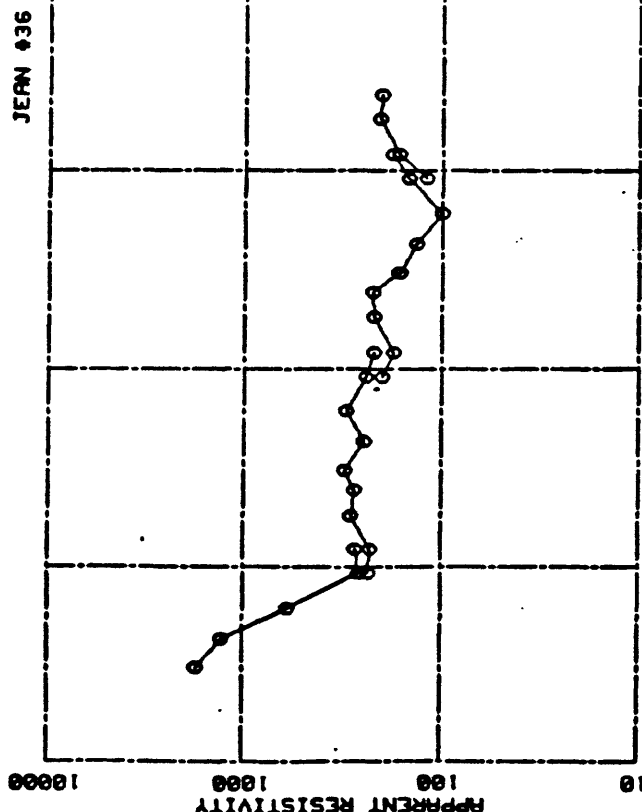
DEPTH	RESISTIVITY	DEPTH	RESISTIVITY
1.38	392.06	29.71	311.20
2.82	167.43	43.61	516.06
2.97	167.03	64.01	521.24
4.36	262.75	93.95	299.96
6.40	341.35	137.90	116.02
9.40	200.45	202.41	50.20
13.79	113.25	297.10	60.90
20.24	140.13	436.00	146.76
		999999.00	355.56



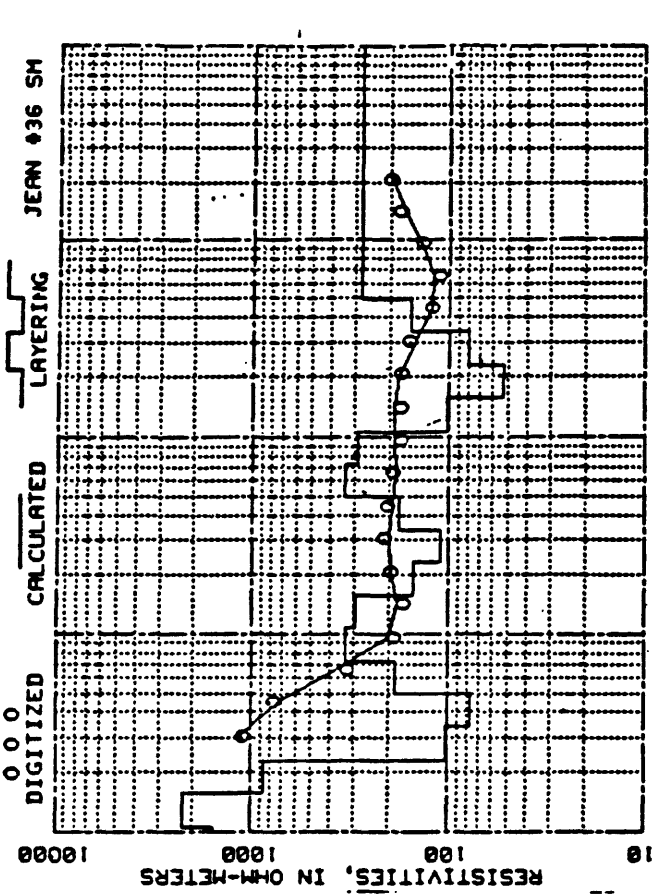
AB/2	OBSERVED RESISTIVITY	AB/2	OBSERVED RESISTIVITY
3.05	860.00	121.92	191.00
4.27	655.00	91.44	215.00
6.10	420.00	121.92	163.00
9.14	310.00	102.00	130.00
9.14	310.00	243.04	70.00
12.19	191.00	304.00	67.30
16.29	166.00	304.00	60.00
24.70	172.00	426.72	57.00
30.40	150.00	609.60	47.40
30.40	150.00	914.40	57.00
42.57	145.00	1219.20	65.00
60.86	205.00	1020.00	80.40
91.44	235.00	2430.40	04.00



DEPTH	RESISTIVITY	DEPTH	RESISTIVITY
1.25	1200.05	39.61	310.95
1.94	702.02	56.14	259.75
2.70	400.77	85.34	139.74
3.96	379.40	125.27	99.30
9.01	209.16	103.07	30.14
0.53	63.01	269.00	32.10
12.53	72.36	396.13	51.90
10.39	149.49	501.44	74.64
26.99	261.75	999999.00	97.01



AB/2	OBSERVED RESISTIVITY	AB/2	OBSERVED RESISTIVITY
3.05	121.92	230.00	230.00
4.27	1275.00	200.00	200.00
6.10	1275.00	175.00	175.00
9.14	590.00	210.00	210.00
12.19	262.00	222.00	222.00
9.14	260.00	167.00	167.00
12.19	233.00	154.00	154.00
10.29	230.00	136.00	136.00
24.30	207.00	99.00	99.00
30.40	277.00	609.60	609.60
30.40	306.00	914.40	914.40
42.67	306.00	1219.20	1219.20
60.96	245.00	100.00	100.00
91.44	300.00	120.00	120.00
	240.00	165.00	165.00
		206.00	206.00
		203.00	203.00



DEPTH	RESISTIVITY	DEPTH	RESISTIVITY
1.07	1502.31	33.74	109.22
1.37	2243.67	49.32	100.24
2.30	873.27	72.60	336.19
3.37	102.60	106.60	292.47
4.93	76.37	156.30	101.63
7.27	104.46	229.04	52.91
10.67	332.65	337.35	60.10
15.66	295.06	495.16	156.14
22.90	150.19	999999.00	279.41

Figure Captions

Figure 1. Map showing location of Schlumberger sounding stations and drill holes. Wells in blue designate potable water, wells in red designate marginal or unacceptable water.

Figure 2. Bar diagram showing distribution of TDS (total dissolved solids) in wells. Locations are approximately projected along road from Jean to Goodsprings.

Figure 3. Graph showing method to transform resistivity distribution with depth from a step function to continuous variation.

Figure 4. Geoelectric cross sections A-A', B-B', and C-C' showing variation of interpreted true resistivity with depth. Depth in meters. Contours in Ohm-m. Vertical exaggeration $\times 2$.

Figure 5. Geoelectric cross sections D-D' and E-E' showing variation of interpreted true resistivity with depth. Depth in meters. Contours in Ohm-m. Vertical exaggeration $\times 2$.

Figure 6. Geoelectric cross section F-F' showing variation of interpreted true resistivity with depth. Fault shown separates high resistivity Paleozoic limestone (on the left) from Mesozoic sandstone on the right. Question marks designate uncertainty of interpretation at depth because of short soundings. Depth in meters. Contours in Ohm-m. Vertical exaggeration $\times 2$.

Figure 7. Map showing interpreted true resistivity at a depth of 100 m (330 feet).

Figure 8. Map showing interpreted true resistivity at a depth of 200 m (650 feet).

Figure 9. Map showing interpreted true resistivity at a depth of 300 m (approximately 1000 feet).

Figure 10. Map showing interpreted true resistivity at a depth of 400 m (1300 feet).

Figure 11. Aerial view of the Jean area.

Figure 12. Block diagram G-G', composed of parts of sections A-A' and E-E', showing interpreted true resistivity with depth. Depth in meters. Contours in Ohm-m. Vertical exaggeration $\times 2$.

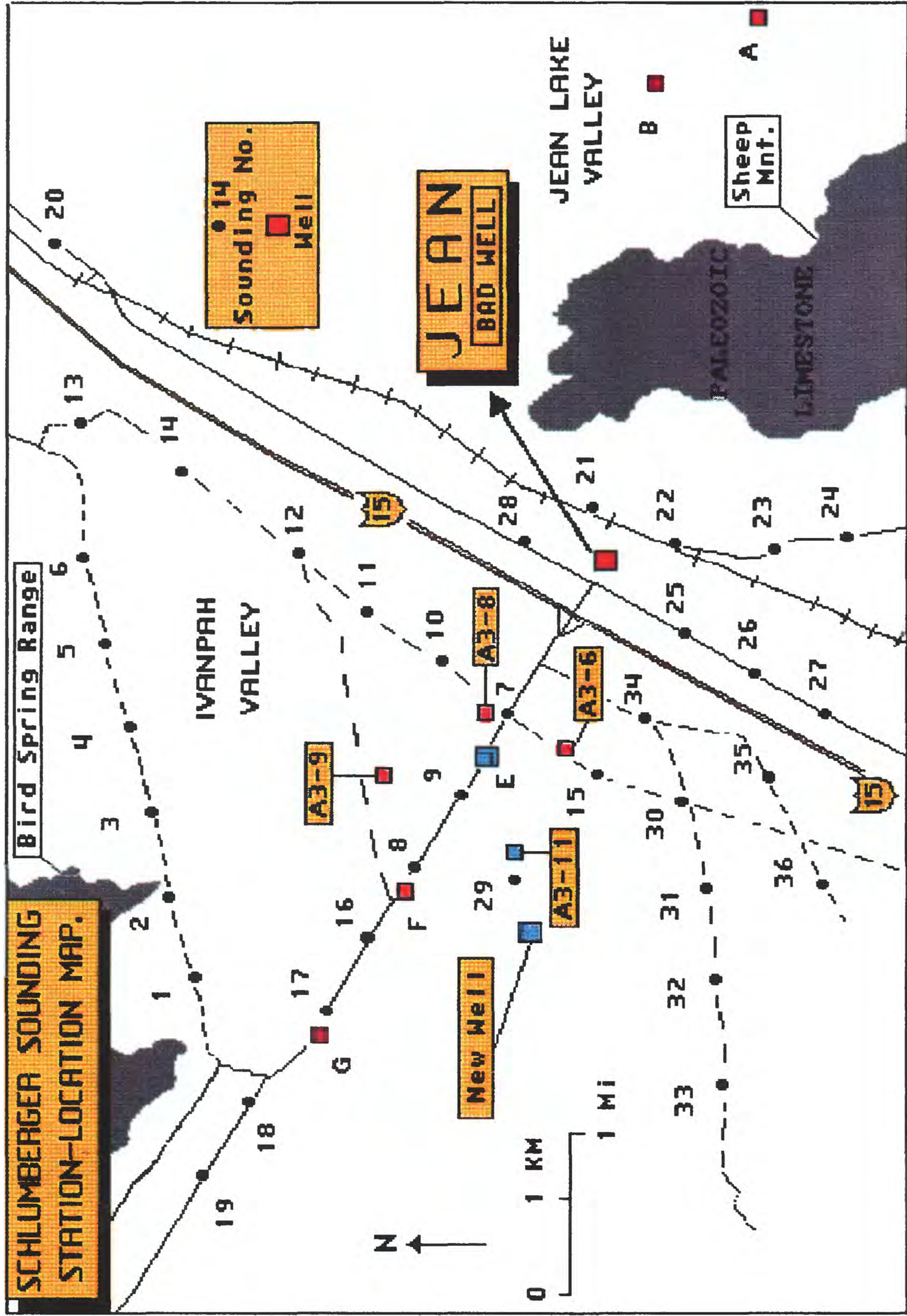


Fig. 1

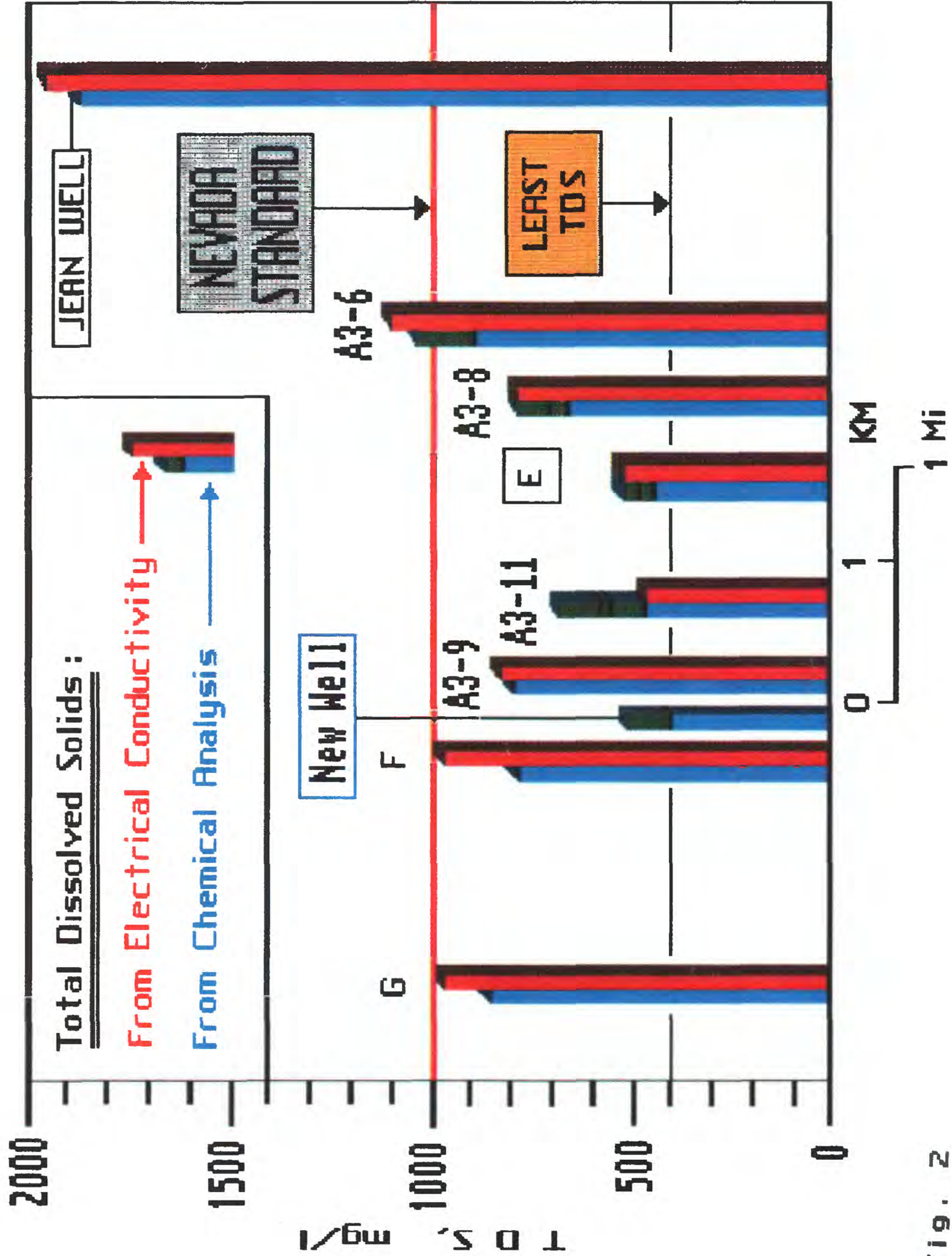


Fig. 2

10000

1000

100

10

Resistivity, Ohm - M

TO GENERATE MAPS AND CROSS SECTIONS :

Step Function

Continuous Variation



JEAN #10

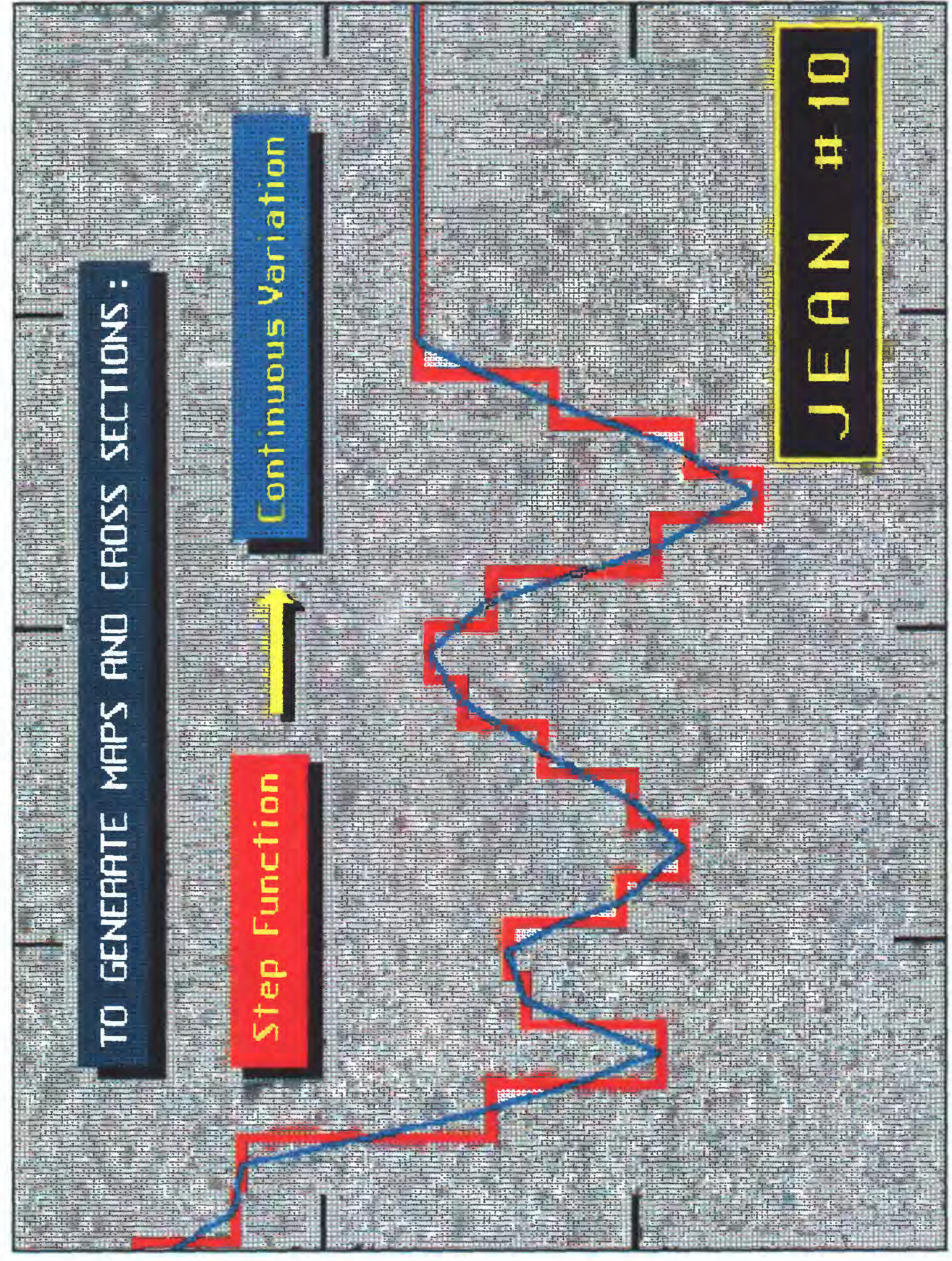
Depth, Meters

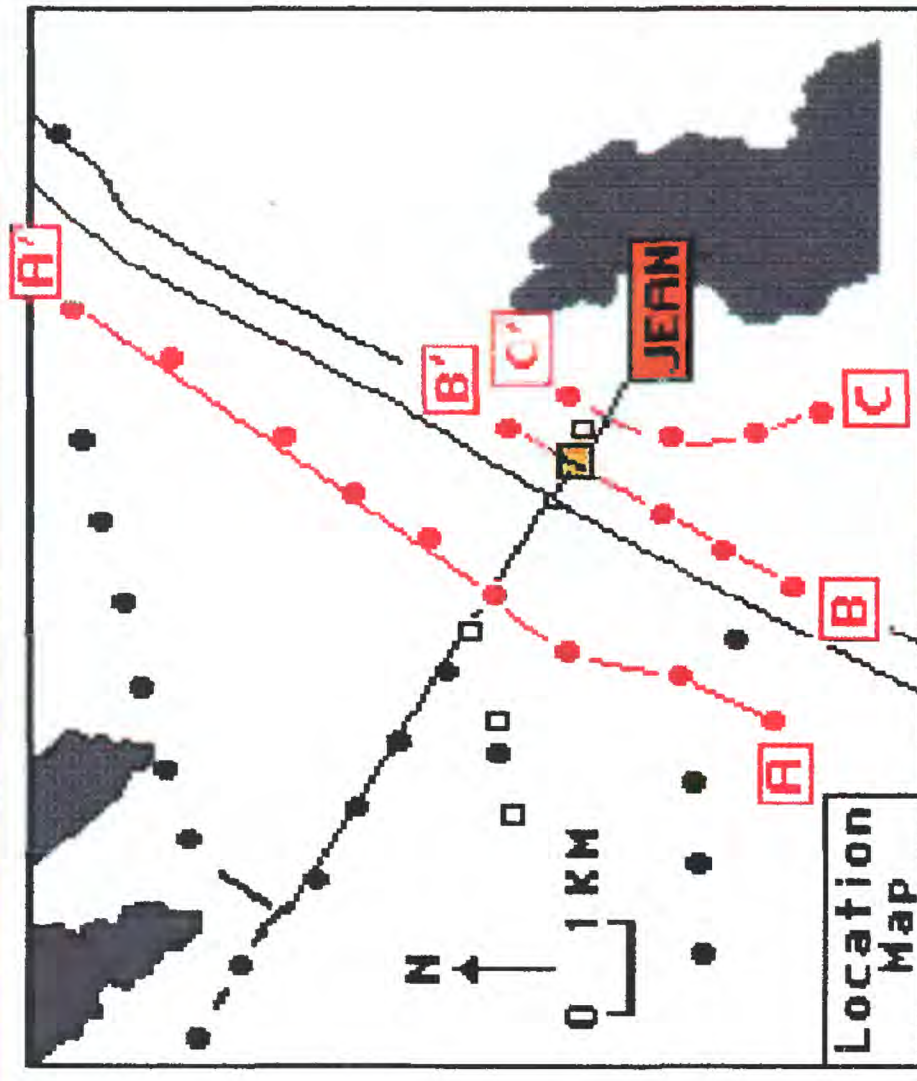
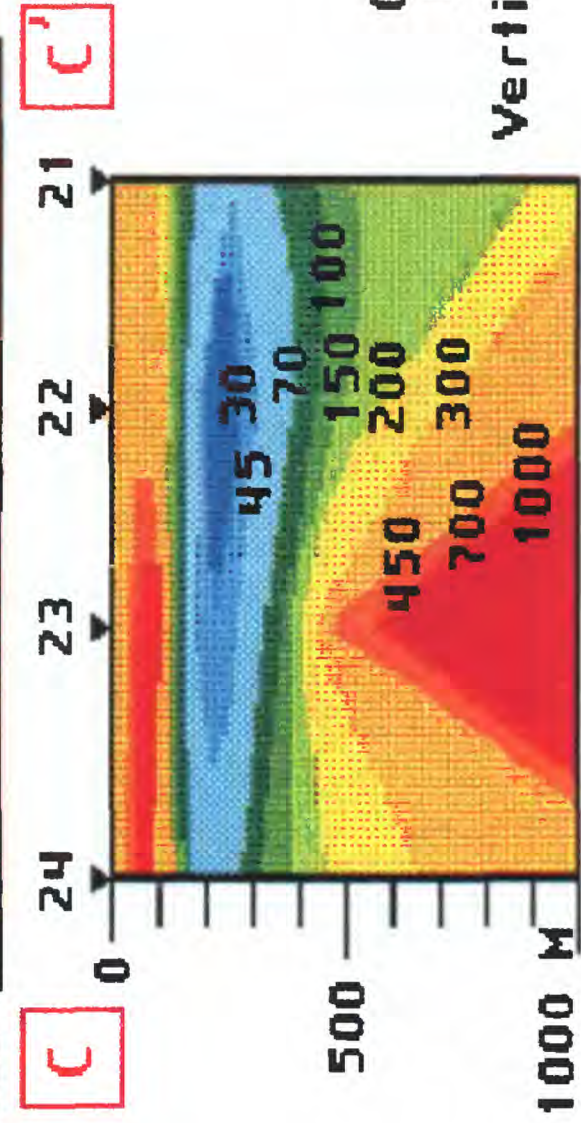
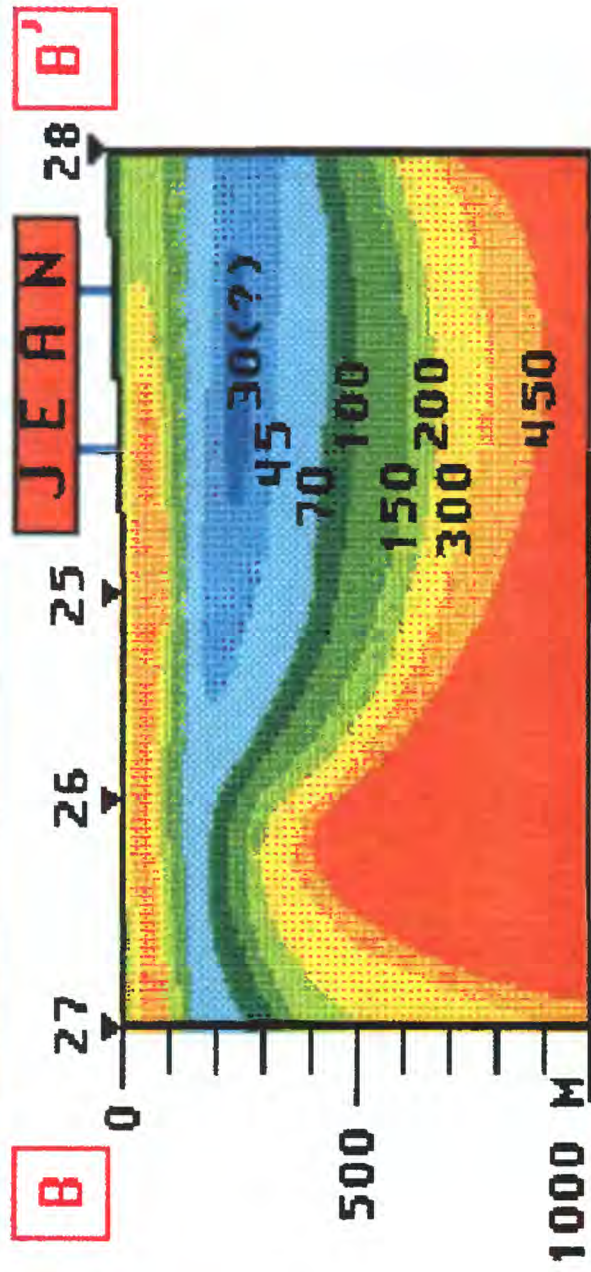
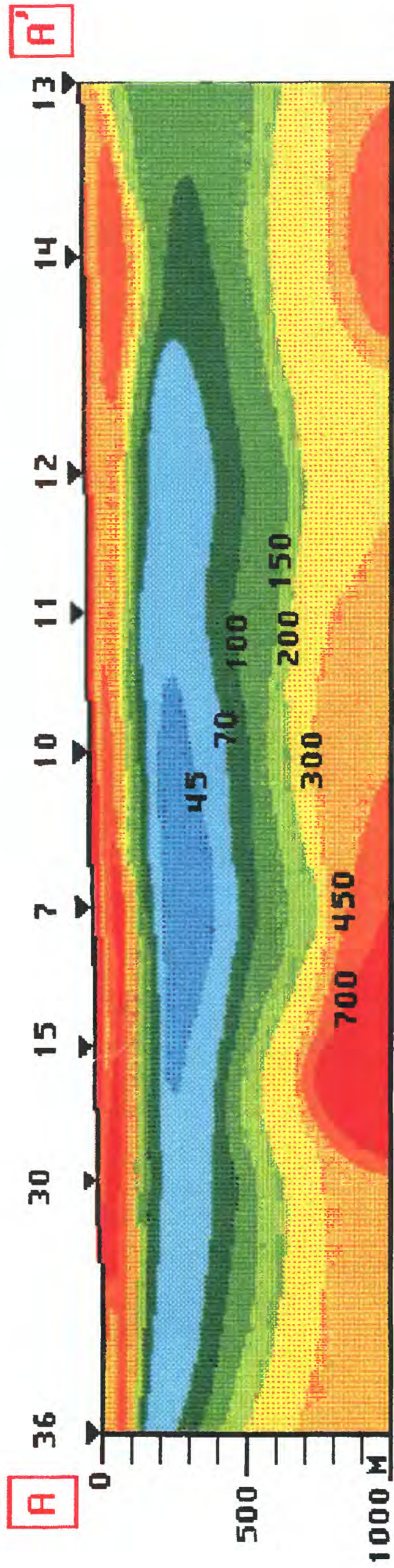
10

100

1000

10000





Interpreted
True Resistivity
Sections. Contours
in Ohm-M.

Vertical Exaggeration X 2

Fig. 4

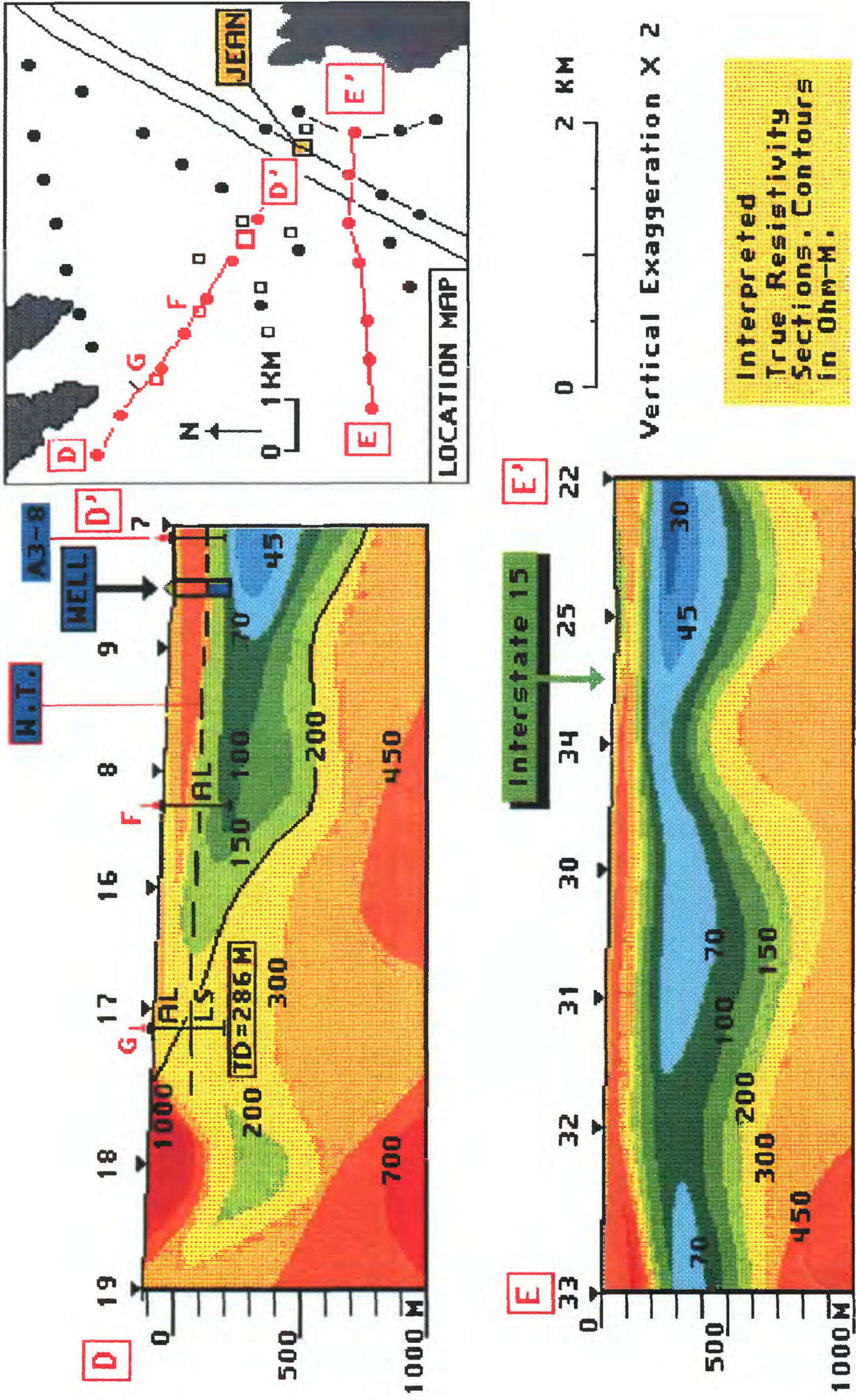
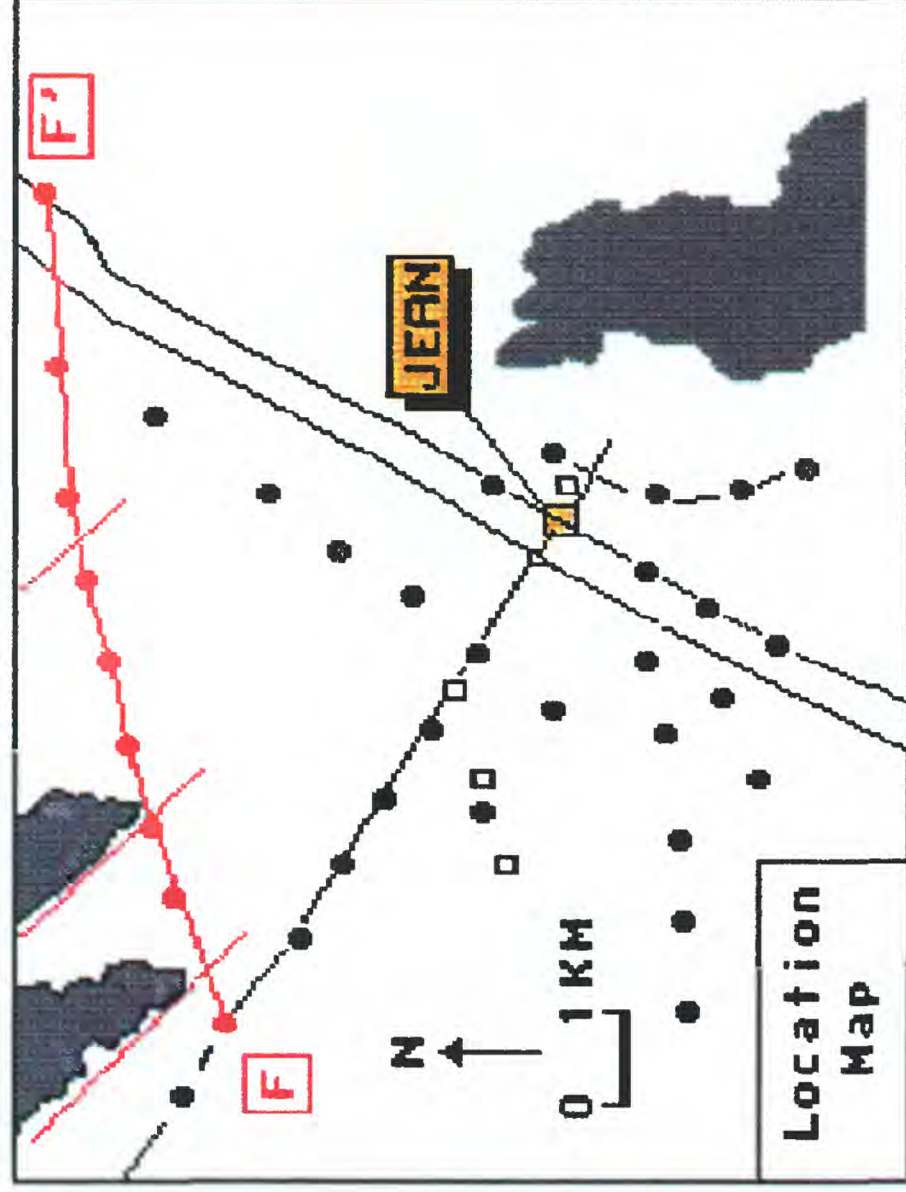
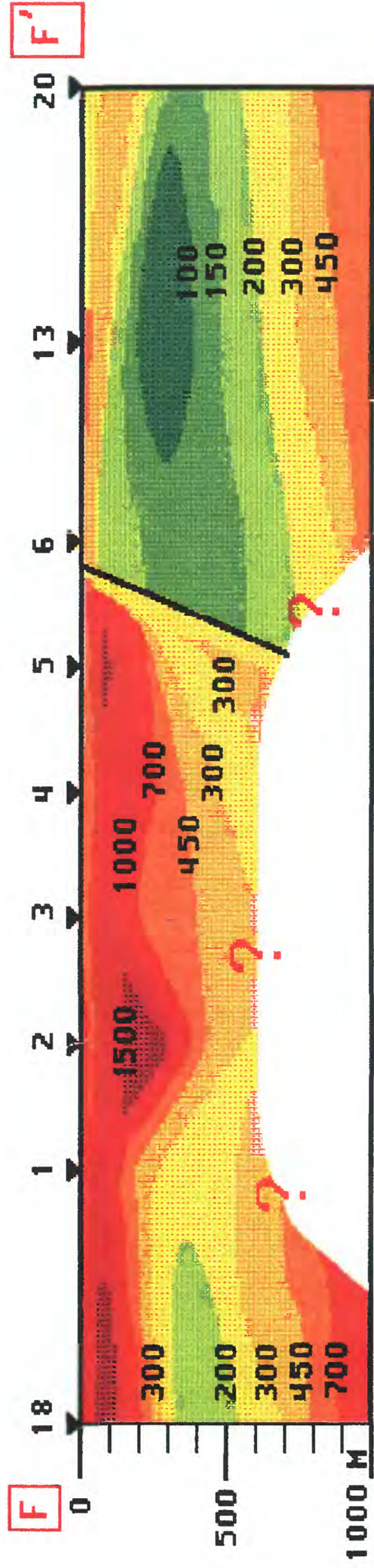


Fig. 5



0 2 KM

Vertical Exaggeration X 2

Interpreted True
Resistivity Section
(Contours in Ohm-M).

Fig. 6

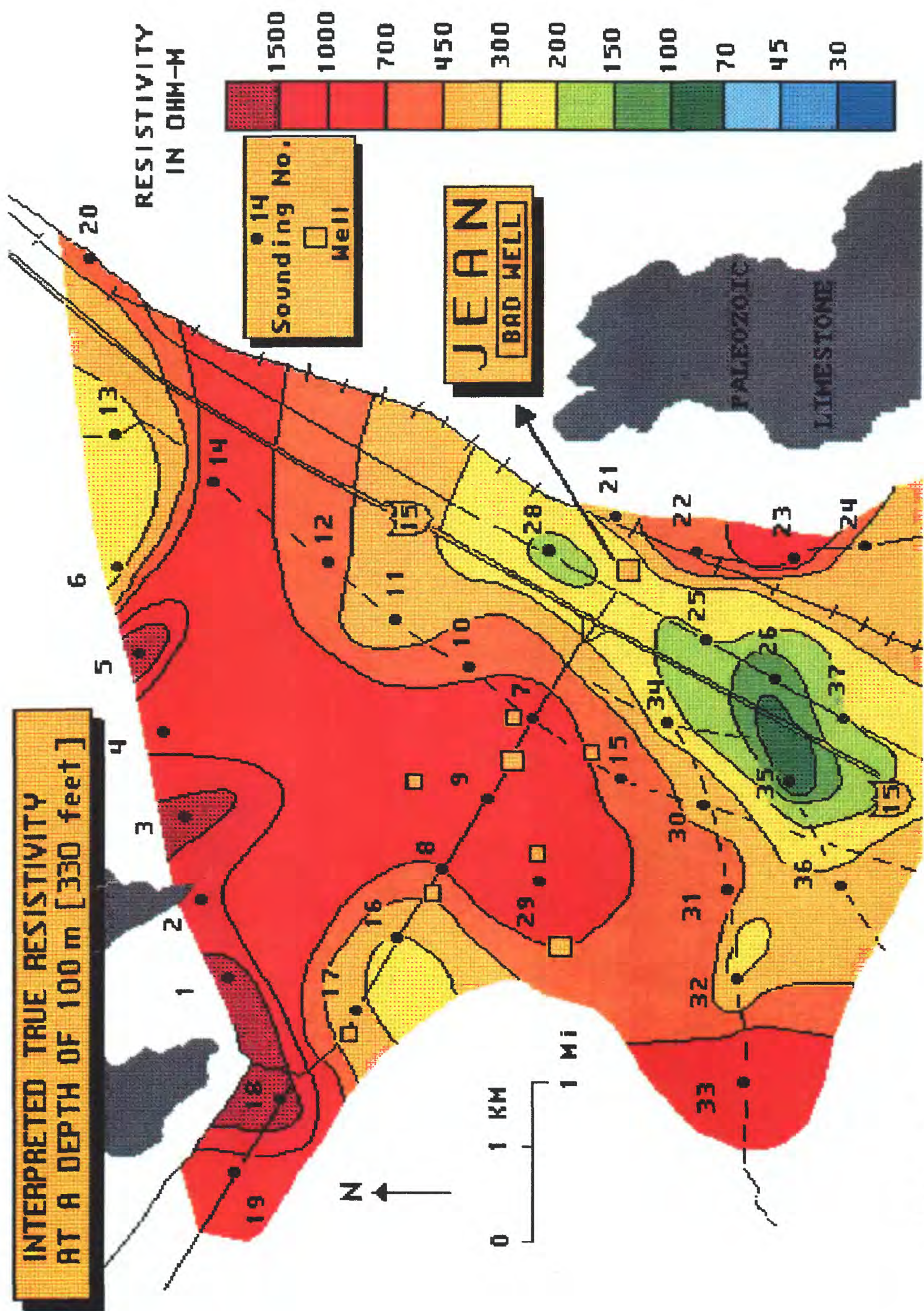


Fig. 7

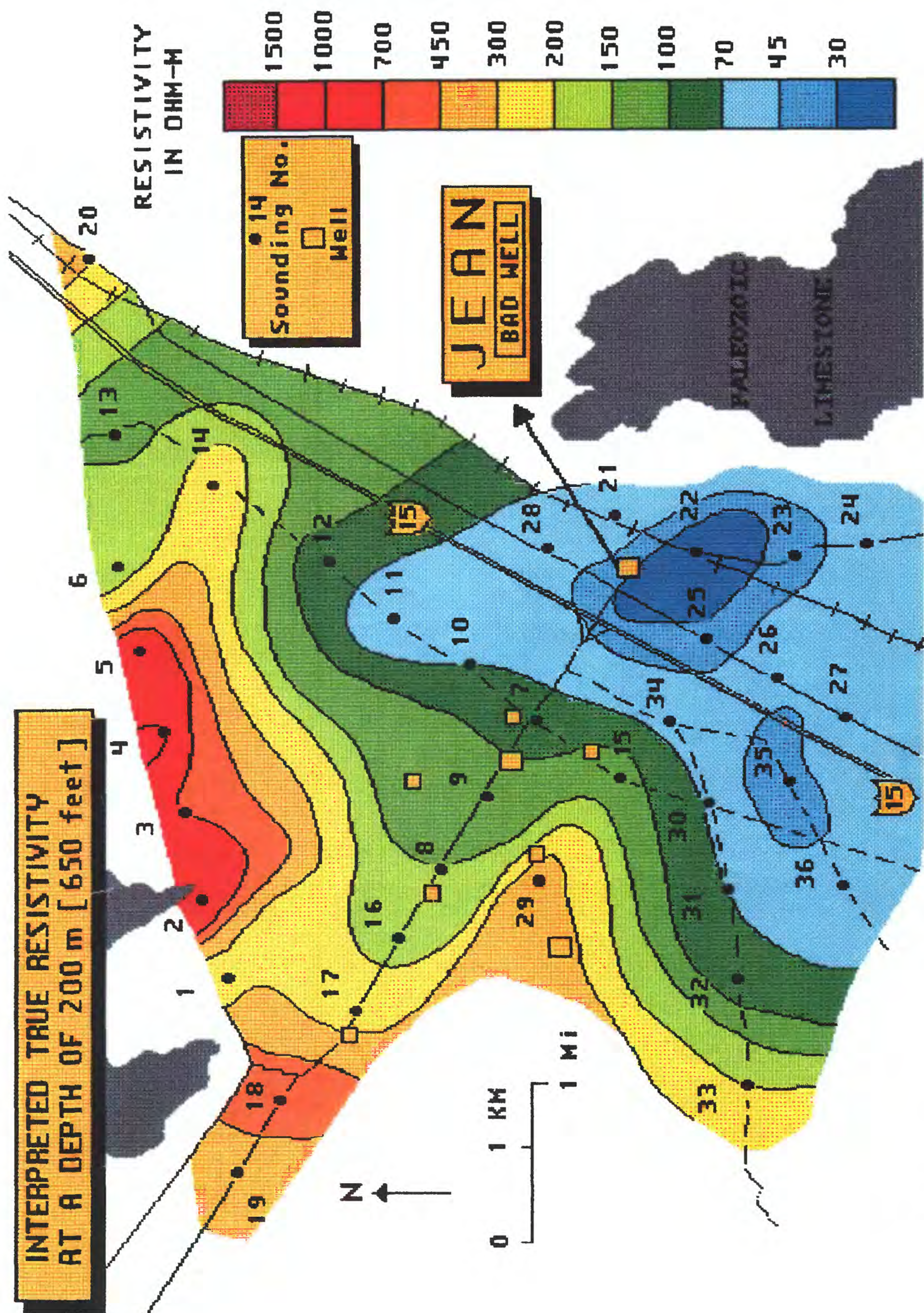


Fig. 8

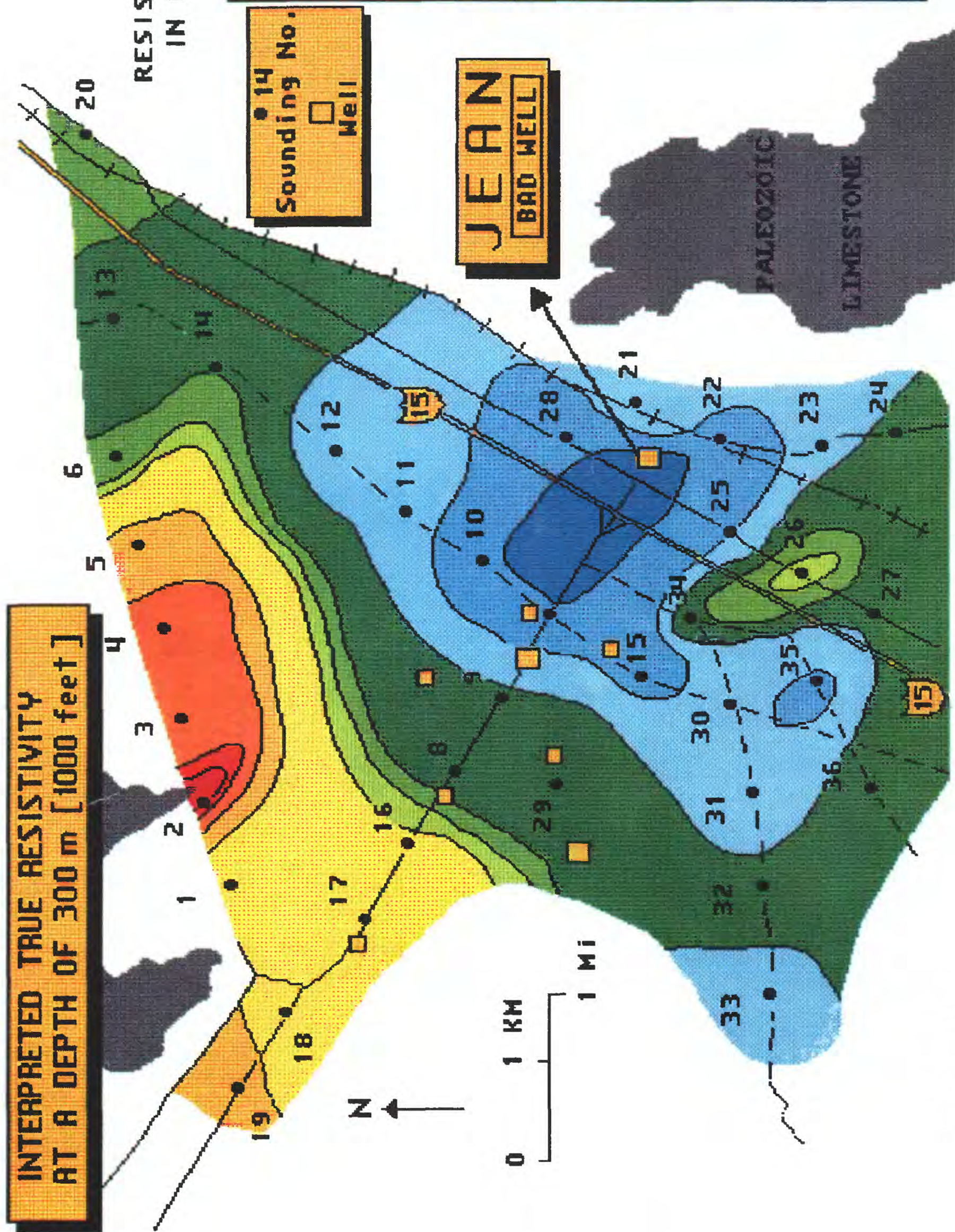


Fig. 9

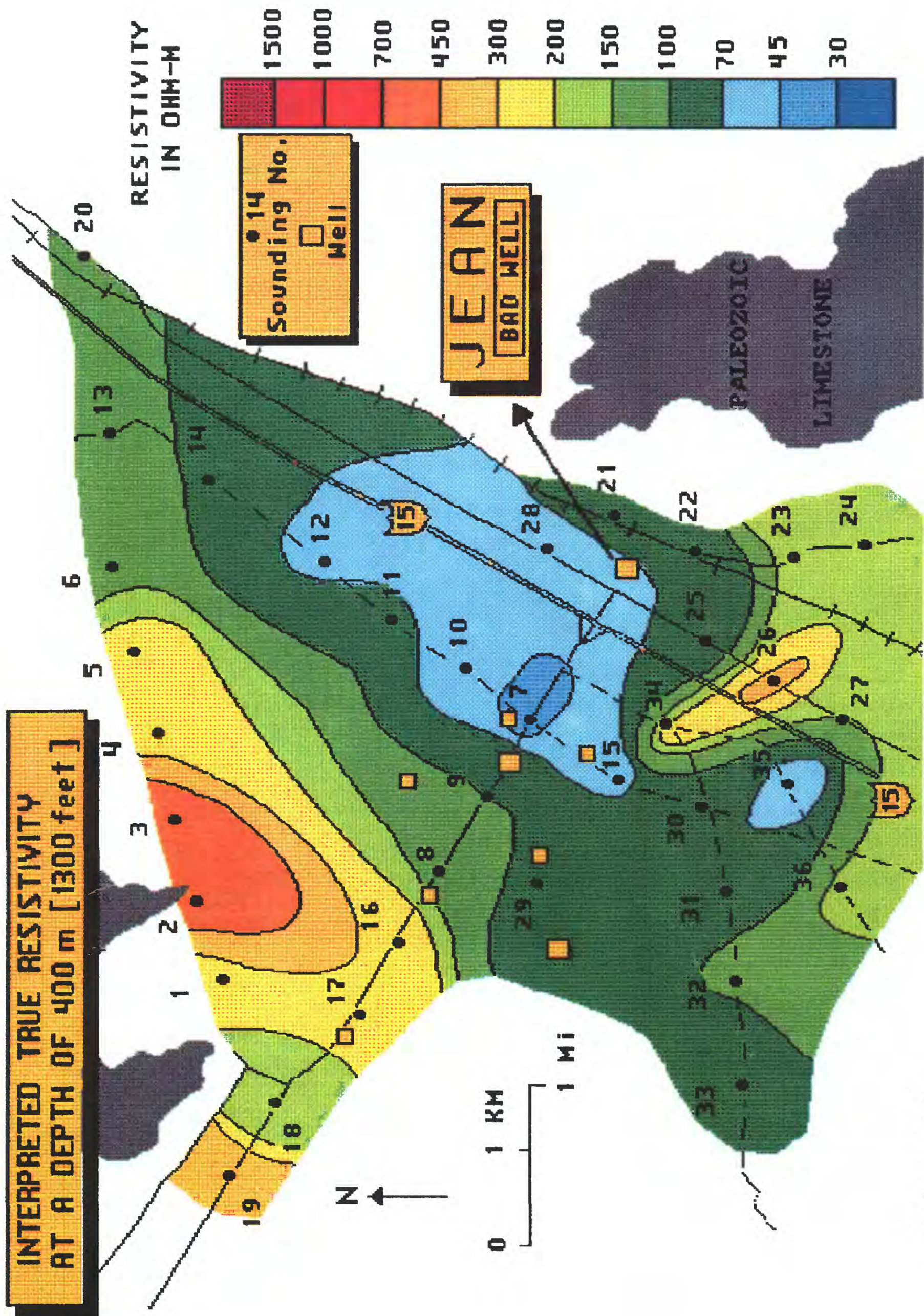


Fig. 10

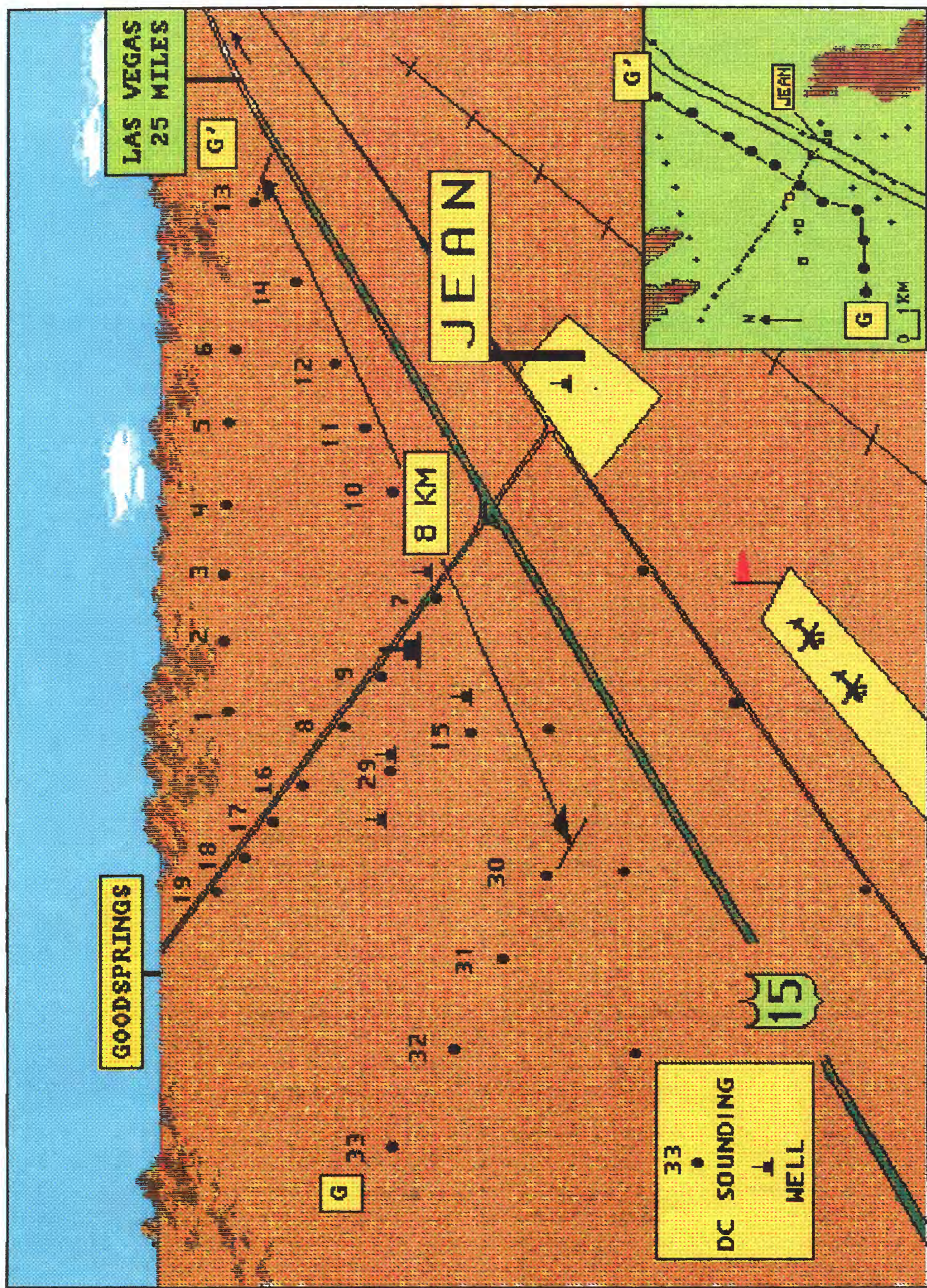


Fig. 11

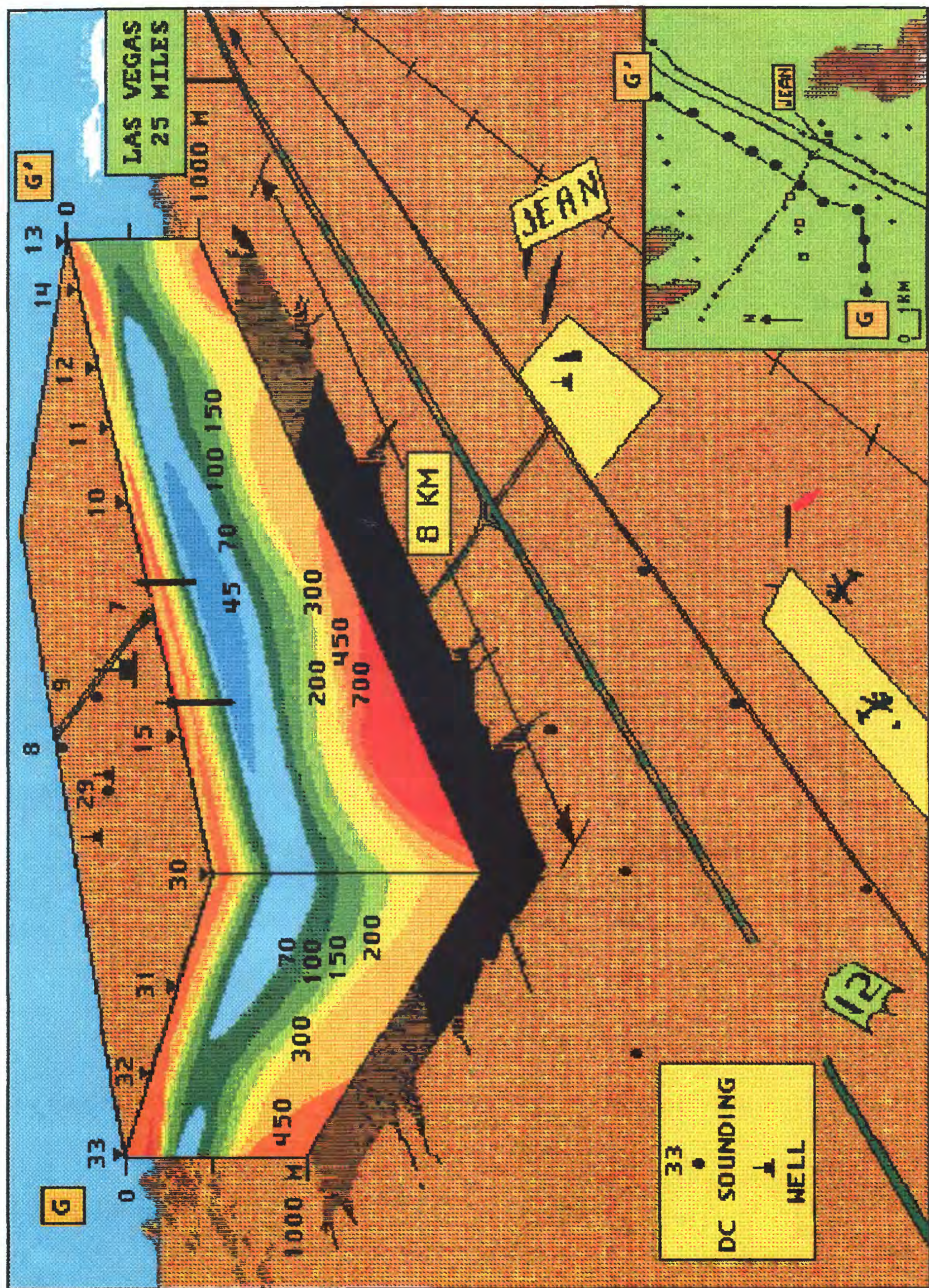


Fig. 12